State of Illinois
Rod. R. Blagojevich, Governor
Illinois Department of Natural Resources
Illinois State Geological Survey

Reservoir Characterization and Three-dimensional Models of Mt. Simon Gas Storage Fields in the Illinois Basin

David G. Morse and Hannes E. Leetaru

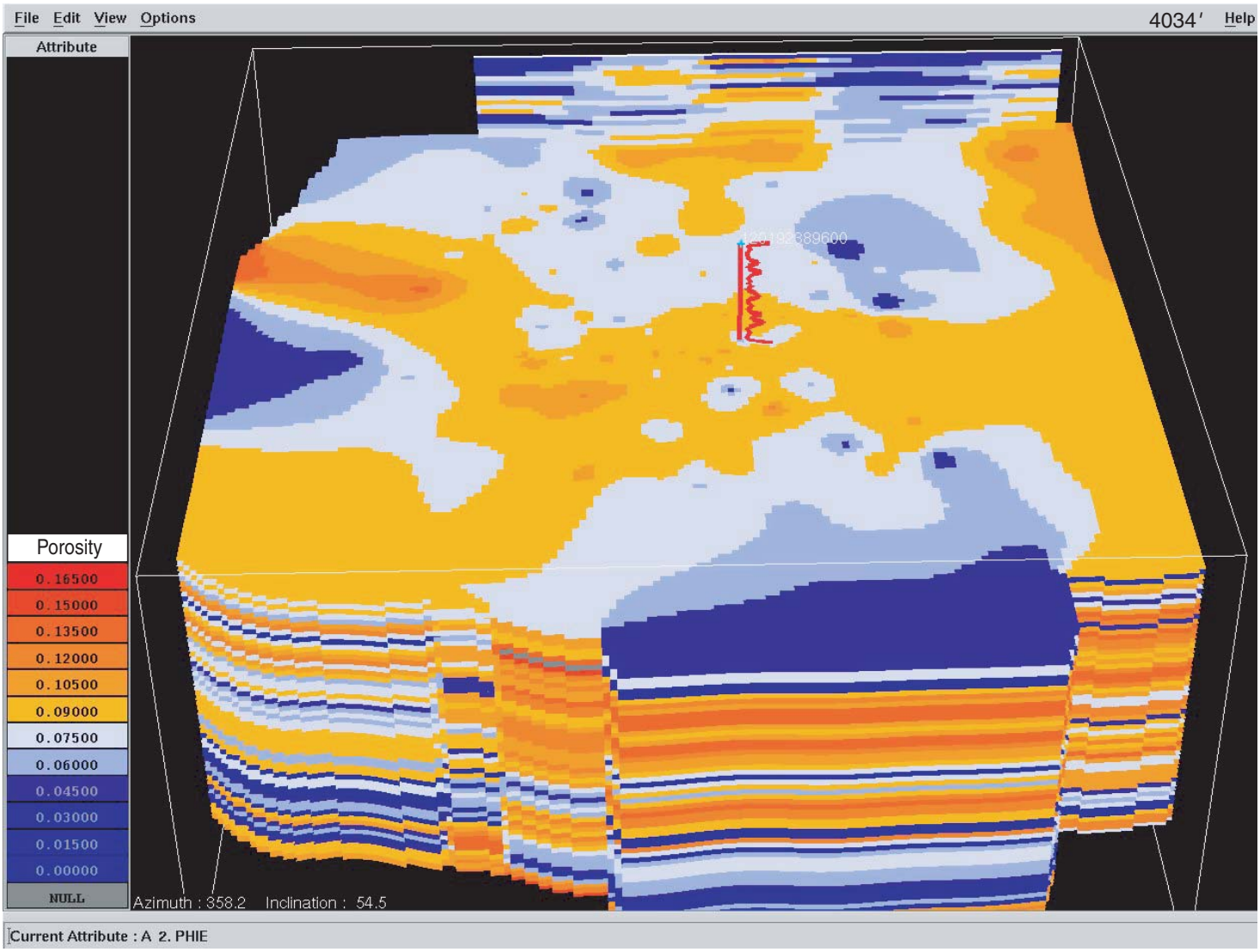

Circular 567 2005

Illinois Department of Natural Resources

1905-2005 ISGS Illinois State Geological Survey

Disclaimer

Front Cover: *Horizontal slice map of Manlove Field porosity model, at a depth of 1,230 m (4,034 ft).*

Released by the authority of the State of Illinois 11/05

Reservoir Characterization and Three-dimensional Models of Mt. Simon Gas Storage Fields in the Illinois Basin

David G. Morse and Hannes E. Leetaru

Circular 567 2005

Illinois Department of Natural Resources
ILLINOIS STATE GEOLOGICAL SURVEY
William W. Shilts, Chief
615 E. Peabody Drive
Champaign, Illinois 61820-6964
217-333-4747
www.isgs.uiuc.edu

Contents

Appendices 57

Table

Figures

Abstract

In northern Illinois, the Upper Cambrian Mt. Simon Sandstone is a permeable and porous formation that is used for natural gas storage by the utilities in the state. This study, sponsored by the U.S. Department of Energy, examined the Mt. Simon Sandstone in the Manlove gas storage field, Champaign County, Illinois, and the Herscher gas storage field, Kankakee County, Illinois, in order to improve knowledge of the reservoir's character and geometry. The top of the reservoir sandstone occurs at 1,190 m (3,900 ft) in Manlove Field and at 670 m (2,200 ft) at Herscher Field. There were significantly more data available for the reservoir characterization study at Manlove Field than for Herscher Field. The three-dimensional (3-D) porosity model of Manlove Field was well constrained by porosity and permeability measurements from 35 cores and calculated porosity values from modern compensated formation density and compensated neutron logs (FDC-CNL) run in half of the 175 wells in the field. The resulting 3-D model indicated a heterogeneous reservoir with channel-confined, vertically discontinuous, high-porosity compartments.

Modeling of Herscher Field was less constrained, but still provided insight into reservoir compartments. At Herscher Field, only 9 wells had reservoir core data, and 2 wells had FDC-CNL; the remaining wells had only 1960s era gamma-ray–neutron logs, many of which were useless for neutron porosity determination because of the "gas effect." An alternative modeling approach was developed using a Vshale-porosity transform. This 3-D model indicated the presence of sand bodies with more lateral continuity than at Manlove Field, although vertical continuity remains fairly poor at both fields. Thus, although well-constrained models are preferable, models built with older, less-constrained data can provide improved understanding of the heterogeneous Mt. Simon reservoir's geometry and potential flow units.

Regional structure maps of the top of the Ordovician Galena Group ("Trenton limestone"), the St. Peter Sandstone, and the Mt. Simon Sandstone delineate present and prospective locations for Mt. Simon gas storage reservoirs. A new regional salinity map of the Mt. Simon waters shows the transition from potable water in northern and northwestern Illinois to a brine-filled formation in the deeper parts of the Illinois Basin.

Introduction

The Illinois State Geological Survey (ISGS) studied the Upper Cambrian Mt. Simon Sandstone and the gas storage reservoirs that occur in this formation in the northern half of Illinois. For this study, regional structure maps and porosity-depth charts were prepared to identify potential new natural gas storage areas. Published regional data on total dissolved solids (TDS) content of water in the upper Mt. Simon was compiled and mapped to characterize the variation in formation water chemistry. Detailed three-dimensional (3-D) models of porosity at two gas storage fields, Manlove and Herscher, were prepared to illustrate the character of the reservoir. These studies improve the geological understanding of reservoir gas injection and production and can be used to prepare reservoir fluid flow simulation studies for optimal field management.

Methods

Regional structure mapping of the top of the Ordovician Galena Group ("Trenton limestone"), the top of the St. Peter Sandstone, and the Mt. Simon Sandstone in northern Illinois was compiled from ISGS well record files. Information from more than 9,100 wells was entered into a spreadsheet and used for this mapping. A conformable mapping technique, described later, was used to project the structure defined from the abundant shallow wells to deeper horizons that have only limited formation penetrations. Chemical analysis data (TDS) for the Mt. Simon covering the northern half of Illinois were very limited and were assembled from the literature, gas storage field operator databases, and ISGS analytical chemistry databases and were used to compile a map that showed the lateral distribution of the salinity in this aquifer.

At Manlove Field, digital log and core analysis data from approximately 330 wells were acquired directly from the operating company; 175 of these wells reached the Mt. Simon Sandstone. Once the well logs were loaded on a workstation, the major formation boundaries and internal correlation markers were picked primarily using the Vshale log, which is based on the gamma-ray trace. Porosity was calculated conventionally from neutron and density logs and calibrated against core data. Wells with only gamma-ray–neutron logs that had gas-affected values were not used in the modeling.

Two cores that passed through the entire gas storage interval at Manlove Field were described in detail, and the sedimentary environments were interpreted. Samples from the different facies in these cores were thin-sectioned and examined with a scanning electron microscope (SEM) as well as with standard transmitted polarized light petrography. The thin sections from these cores were point-counted at 300 points per slide to determine mineralogical percentages in the Mt. Simon Sandstone.

Three-dimensional models of porosity were prepared for the Manlove and Herscher gas storage fields using a suite of Landmark Graphics Corporation (Houston, Texas) software consisting of Openworks™, ZMAP™, Petroworks™, and Stratamodel™.

Wireline logs for 31 wells in Herscher NW Field and 72 wells in Herscher Field that penetrate into the Mt. Simon were digitized and used in the reservoir characterization. Although no whole cores were available for description and petrographic sampling, 9 wells had commercial core descriptions and conventional porosity and permeability data that were used for calibration. Porosity was calculated from a Vshale-porosity transform developed for Herscher using off-structure gamma-ray–neutron logs and core porosity to avoid the anomalous neutron values caused by gas (the "gas effect"). Conventional neutron porosity values

were calculated and calibrated to core porosity. Then, the transform was developed from a gamma-ray–porosity cross plot of these data from off-structure well logs and subsequently was applied to the gamma-ray log values for the gas reservoir wells to obtain their porosity values. All of the wireline log normalization, contouring, and volume modeling were performed with the Landmark Graphics software.

Results and Discussion

Background on Mt. Simon Sandstone Geology

In Illinois, the Mt. Simon Sandstone (fig. 1) is Upper Cambrian in age and lies unconformably on the Precambrian basement rocks composed of granite or granodiorite in the north (Atekwana 1996) and granite or rhyolite in the south (Bradbury and Atherton 1965). In all of Illinois, only about 20 wells have penetrated through the entire Mt. Simon Sandstone interval to the Precambrian basement. Much of the Precambrian basement formed between 1.48 and 1.38 billion years ago and is part of the eastern granite-rhyolite province (Bickford et al. 1986). In east-central Illinois, the Mt. Simon may be resting on a unit with up to 3,600 m (12,000 ft) of rocks called the Centralia Sequence (not shown). In seismic lines, these sub-Mt. Simon rocks display "well-defined stratiform reflectivity" in east-central Illinois. The upper part of the Centralia, called the Enterprise Sequence, has sedimentary characteristics such as prominent dipping and truncated reflector clinoforms suggestive of a prograding shelf-margin-type sedimentary succession (McBride et al. 2003). The contact between the basement igneous rocks and the overlying Mt. Simon Sandstone is a major unconformity of unknown duration, perhaps as long as 500 million years (Willman et al. 1975).

The Mt. Simon Sandstone was named by Ulrich (in Walcott 1914, p. 354) for outcrops of Mt. Simon near Eau Claire, Wisconsin. In general, the Mt. Simon is present throughout Illinois, ranging in thickness from less than 150 m (500 ft) in southwestern Illinois to over 780 m (2,600 ft); the greatest thickness in Illinois occurs in the east-central part of the state (Buschbach 1964, 1975; McBride et al. 2003). In some areas of west-central Illinois, such as in Pike County (Nelson 1995), and in several wells in southwestern Illinois, the Mt. Simon is very thin or absent. Presumably, this reflects non-deposition over Precambrian topographic highs with up to 240 m (800 ft) of relief in a distance of less than 12.7 km (8 mi) at the time the regional blanket of Mt. Simon was being deposited elsewhere (Workman and Bell 1948, p. 2043; Atherton 1971, p. 31).

The Mt. Simon is overlain conformably by the Cambrian Eau Claire Formation, a unit composed of fine to medium-grained, dolomitic sandstone, siltstone, and shale that may contain fossils of inarticulate brachiopods and dismembered trilobites (Twenhofel et al. 1935, p. 1695). The base of the Eau Claire is characterized by gray sandstone with some "sooty" quartz grains that are coated with a fine black powder that consists of disseminated pyrite (Workman and Bell 1948). This basal sandstone is called the Elmhurst Sandstone Member by Buschbach (1964, p. 32); this sandstone is sufficiently porous at Herscher NW Field to be used as a reservoir. Shales above the Elmhurst provide seals for the many Mt. Simon gas storage fields in Illinois. Compared with the Elmhurst, the Mt. Simon is coarser-grained, may include quartz granules, generally lacks "sooty" grains, exhibits a marked decrease in the amount of siltstone and shale, and lacks fossils, glauconite, dolomite, and calcite (Bell et al. 1964, p. 26)

The Mt. Simon does not crop out in Illinois, but correlative units are exposed in southern Wisconsin, southeastern Minnesota, and Missouri. The Mt. Simon is known in the subsurface throughout Indiana, Iowa, Michigan, and western Kentucky (fig. 2). Equivalent Cambrian sandstones are present as far east as Ohio. To the southwest, the Mt. Simon has been correlated with the Lamotte Sandstone of Missouri (Workman and Bell 1948, p. 2043; Houseknecht and Ethridge 1978). The Mt. Simon may include equivalents in the Bayfield Sandstone of northern Wisconsin, the Jacobsonville Sandstone of northern Michigan, and the Fond du Lac Sandstone of Minnesota (Buschbach 1964). The Mt. Simon comprises the lower part of the Sauk Sequence of Sloss (1963). The regional relationships of the lower Sauk were summarized by Sargent (1991). The Mt. Simon is the basal sandstone of the Potsdam Sandstone Megagroup of Swann and Willman (1961) and Willman et al. (1975).

The Mt. Simon consists primarily of medium to coarse quartzose sandstone with local granule-rich sandstone beds. Thin beds of red, green, or gray micaceous shale are sparsely interbedded with the sandstone, especially toward the top of the Mt. Simon. Also interbedded are thin beds of fine to medium feldspathic sandstone. The Mt. Simon varies from fair to very well sorted. Typically, the coarse-grained beds are better sorted and have higher porosity than the fine-grained sandstone beds.

Although the Mt. Simon in northern Illinois has been divided into seven members based on alternation of relatively coarse sand and granule-rich intervals with relatively fine-grained intervals (Templeton 1950), these seven have not been traced to northeastern Illinois where Buschbach (1964) has recognized only the upper three members. From the base upward, these three consist of the Lacey, Gunn, and Charter Members (not shown). Gas storage is typically in the upper 65 m (200 ft) of the formation, presumably in the Charter Member, although this study made no attempt to recognize the members.

The Mt. Simon, where it occurs at depths of less than approximately 1,500 m (5,000 ft), is a porous sandstone. It is overlain nearly everywhere by a thick, impervious shale, the Eau Claire Formation. On anticlinal structures, this combination creates potential storage reservoirs for natural gas that have been recognized and utilized by most of the utilities for gas storage in Illinois. Twelve Mt. Simon gas storage fields were developed in Illinois in the 1950s and 1960s; two of these, the Manlove and the Herscher Fields, were examined in detail for this study. The Mt. Simon fields are called "aquifer gas storage reservoirs" because the Mt.

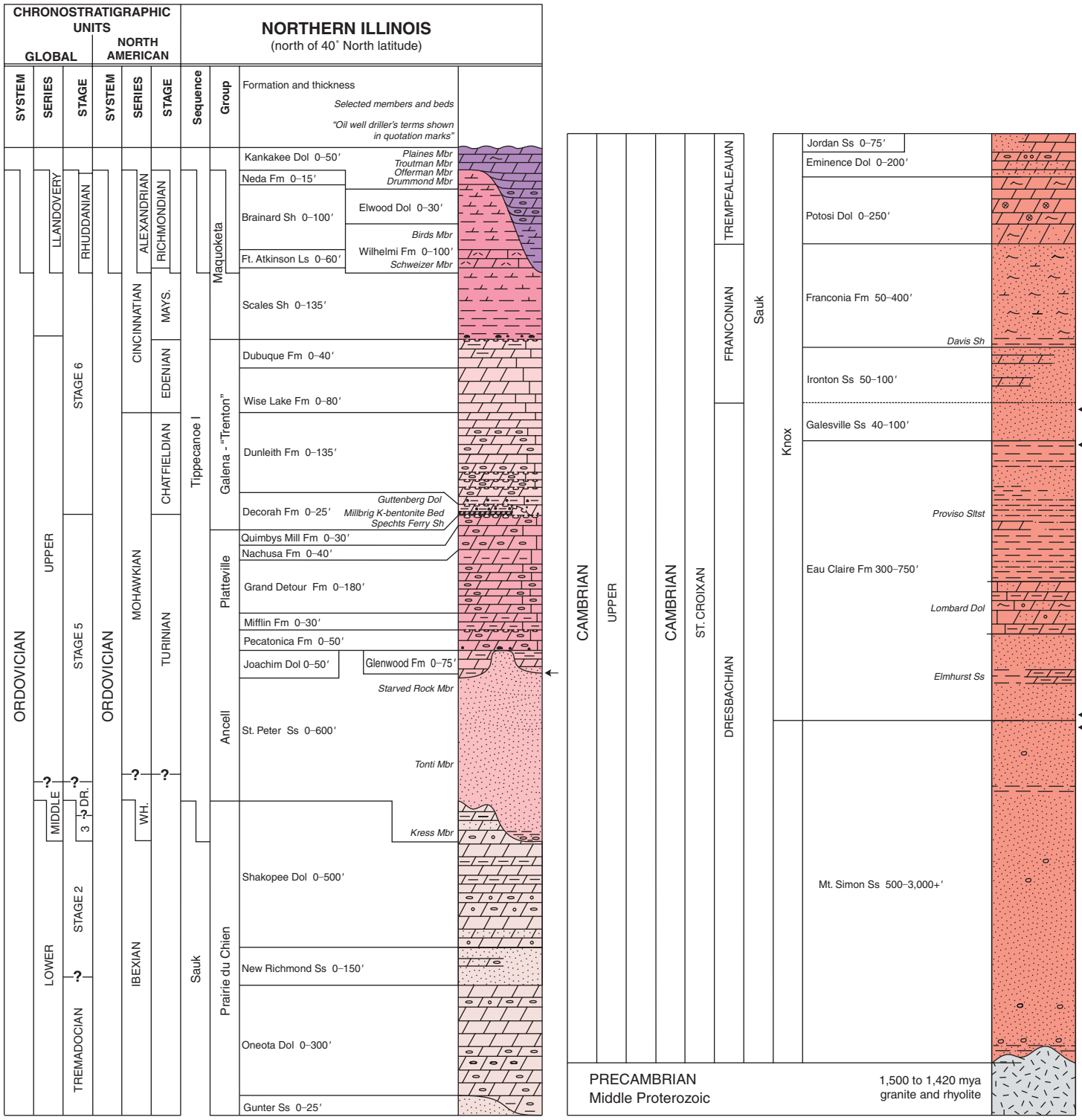

Figure 1 Stratigraphic column of Ordovician through Precambrian rocks in northern Illinois. Arrows point to the formations discussed in this report (from Kolata et al. 2005). DR., Darriwillian; Dol, dolomite; Fm, formation; Ls, limestone; MAYS., Maysvillian; Mbr, Member; Sh, shale; WH., Whiterockian; mya, million years ago.

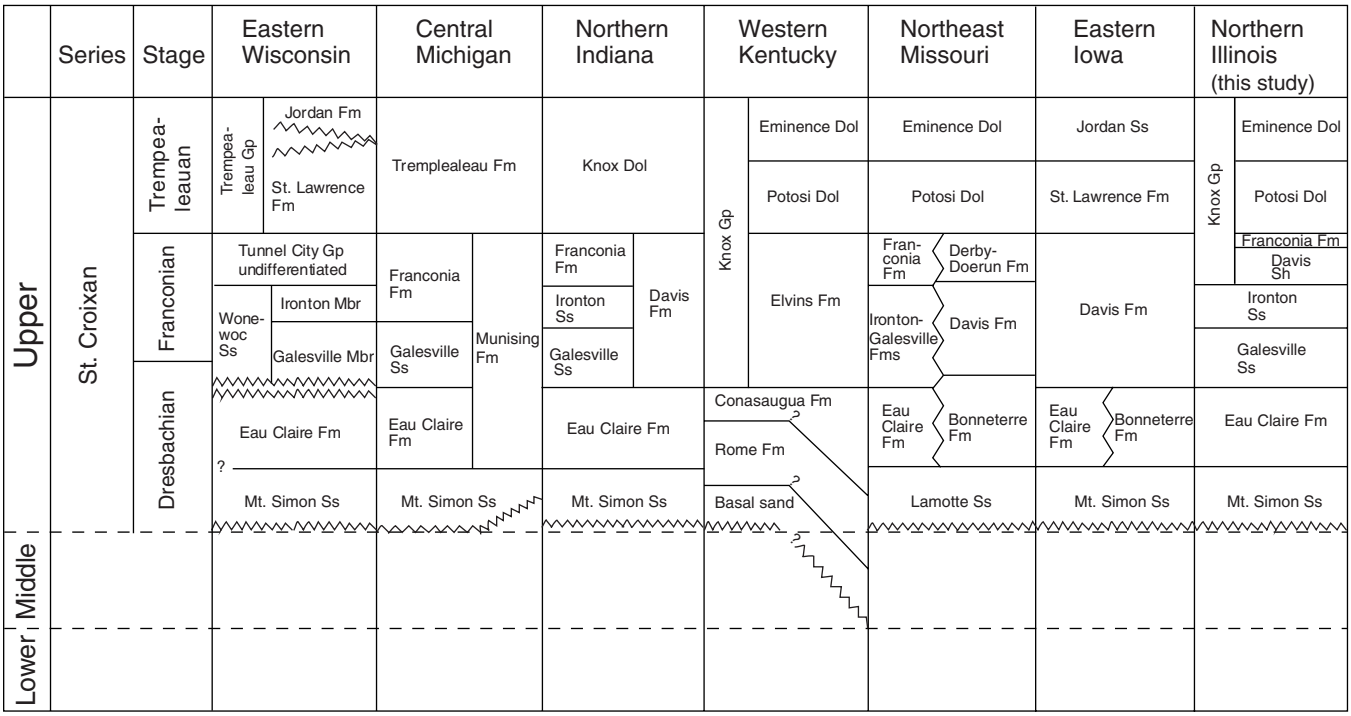

Figure 2 Cambrian correlation chart for midwestern states adjacent to Illinois (Shaver 1985, Adler 1987).

Simon was generally water-bearing prior to the injection of natural gas that was brought to the site by pipeline. Once injected, part of the gas volume, called, "working gas," is withdrawn and delivered to market to meet peak use requirements. Gas remaining in the reservoir provides pressure and is called "cushion gas" or "base gas." Storage typically occurs in the upper 30 m to 60 m (100 ft to 200 ft) of the Mt. Simon, following the limits of structural closure at the reservoir.

Regional Geology: Depositional Environment The Mt. Simon Sandstone is commonly interpreted as forming in shallow, subtidal marine environments (Droste and Shaver 1983). Based on southern Wisconsin outcrop studies, Driese et al. (1981) interpreted the Mt. Simon as a stacked, largely progradational, shoaling- and fining-upward tidal sequence that contains marine trace fossils in many intervals. In core from central Illinois, Sargent and Lasemi (1993) have interpreted the fining-upward cycles in the upper part of the Mt. Simon as peritidal deposits. Cores from the upper part of the Mt. Simon Sandstone at Manlove Field show sedimentary structures that support a similar tidal to shallow subtidal depositional environment for the rocks in east-central Illinois. See the Depositional Systems section for a more detailed description and interpretation. In general, the paleogeography of Illinois at the time of uppermost Mt. Simon deposition was one of a low relief coastal setting in a subsiding basin open to the ocean to the south (Kolata 1991, p. 197).

Regional Structure Data from all significant wells drilled in the northern half of Illinois were compiled to create regional structure contour maps of the tops of the Ordovician Galena Group ("Trenton limestone") (fig. 3), the Ordovician St. Peter Sandstone (fig. 4), and the Upper Cambrian Mt. Simon Sandstone (fig. 5). The region covered by the database comprises the prime potential area for developing new natural gas storage sites in Illinois that could reasonably provide gas to the Chicago market. A pallistering technique that adds isopachs to shallow structure maps was used to create deeper structure maps. Thus, the isopach from the top of a shallow, well-controlled marker bed, such as the Galena Group ("Trenton limestone"), to the top of the next underlying interval, the St. Peter Sandstone (fig. 6), was added to the structure map of the top of the Galena (fig. 3) to create a structure map of the St. Peter Sandstone. This process was then repeated from the St. Peter to the Mt. Simon to create the Mt. Simon structure map (fig. 5). This technique is also called, "conformable mapping."

Up to eight regional formation tops in all wells of northern Illinois have been compiled, but the number of deeper formation penetrations decreases sharply below the Galena Group ("Trenton limestone"). The database containing these log tops comprises over 9,100 wells. The formation tops data were reviewed for accuracy using contoured isopach and structure maps of the units. This quality check procedure permitted the identification and correction of wells where contour bull's-eyes occurred.

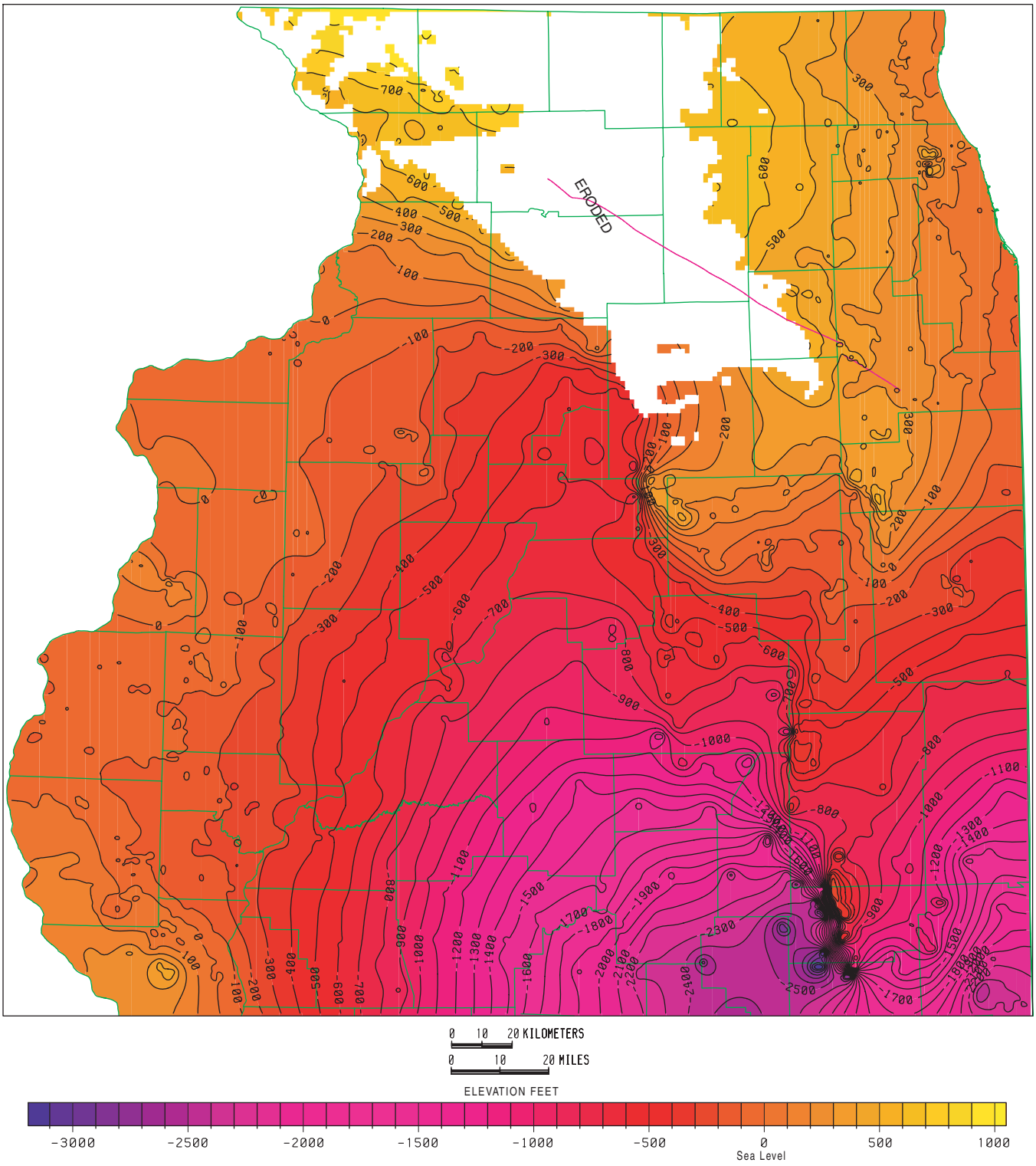

Figure 3 Regional structure map of the top of the Galena Group in the north half of Illinois. Contour interval is 100 ft (33.3 m).

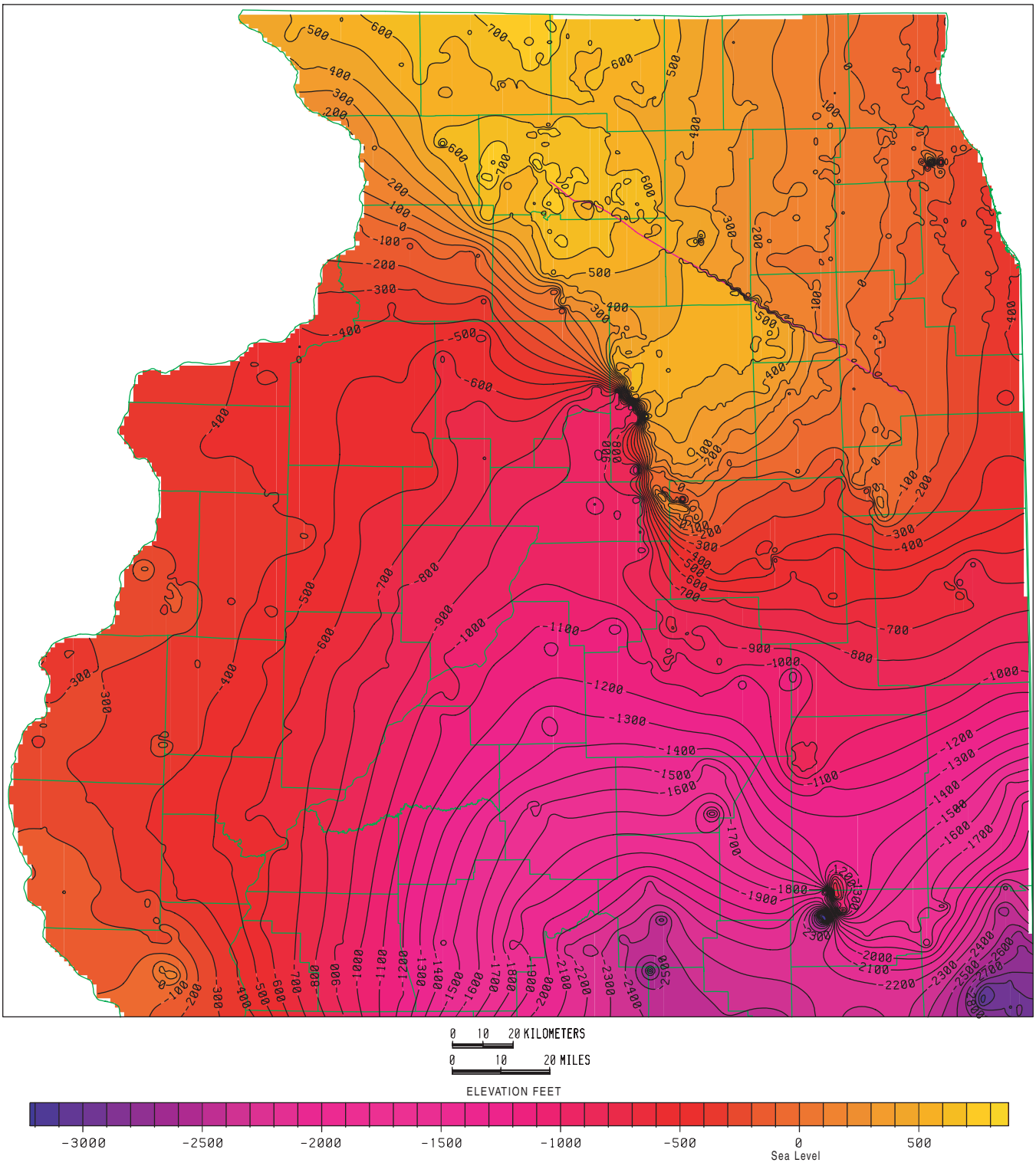

Figure 4 Regional structure map of the top of the St. Peter Sandstone in the north half of Illinois. Contour interval is 100 ft (33.3 m).

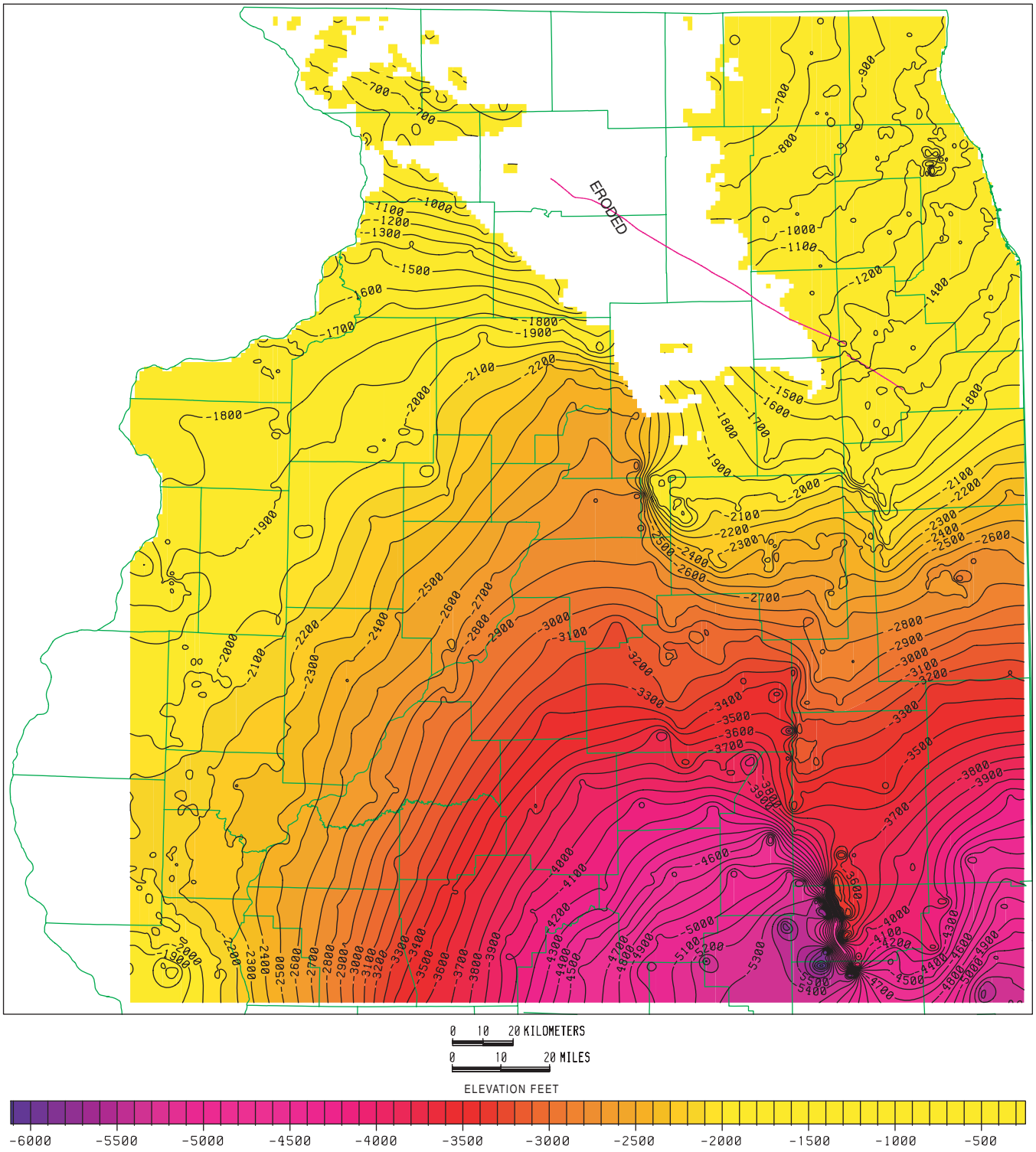

Figure 5 Regional structure map of the top of the Mt. Simon Sandstone in the north half of Illinois. The contour interval is 100 ft (33.3 m).

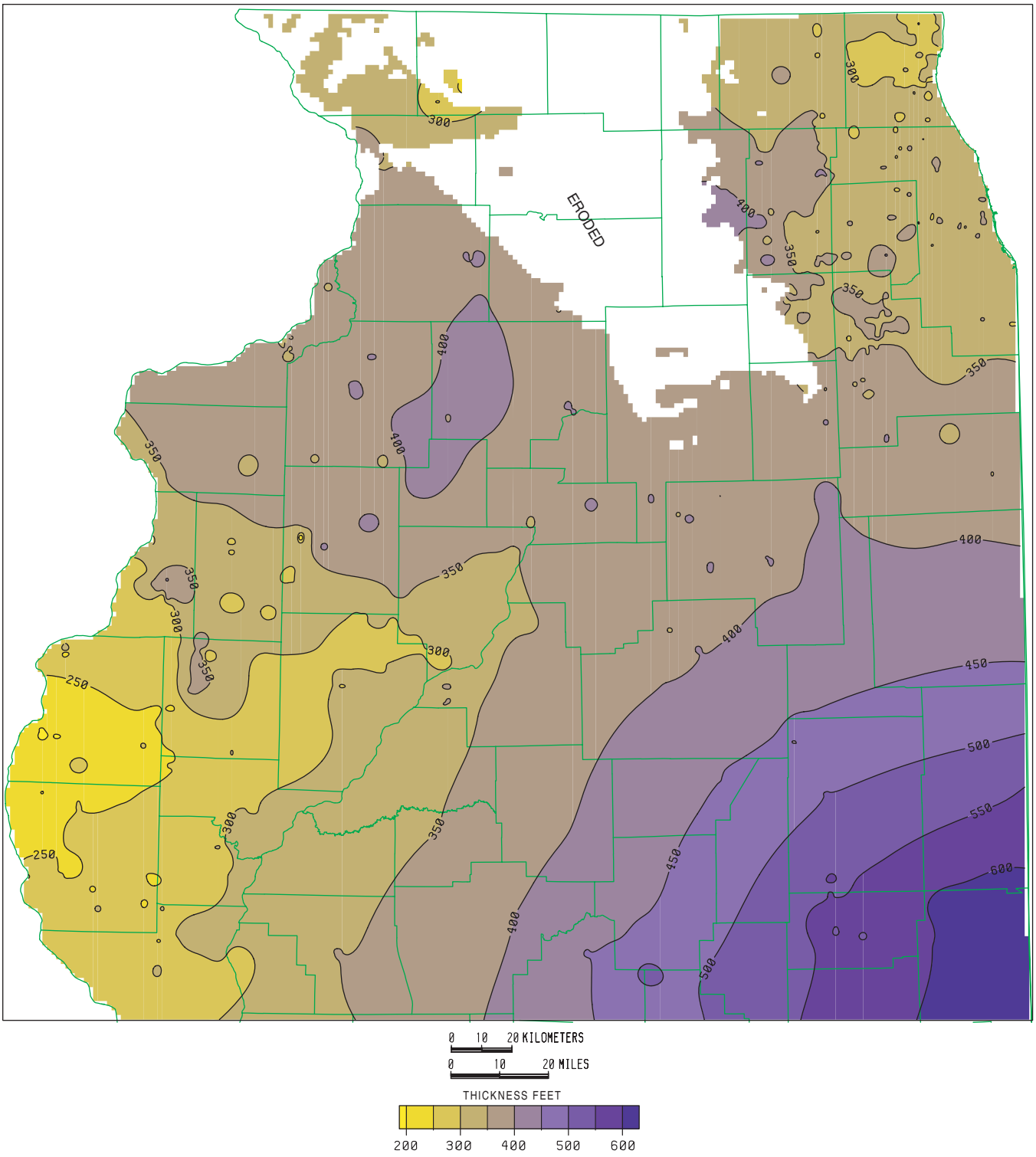

Figure 6 Regional isopach from the top of the Galena Group carbonates to the top of the St. Peter Sandstone in the north half of Illinois. The contour interval is 50 ft (16.75 m).

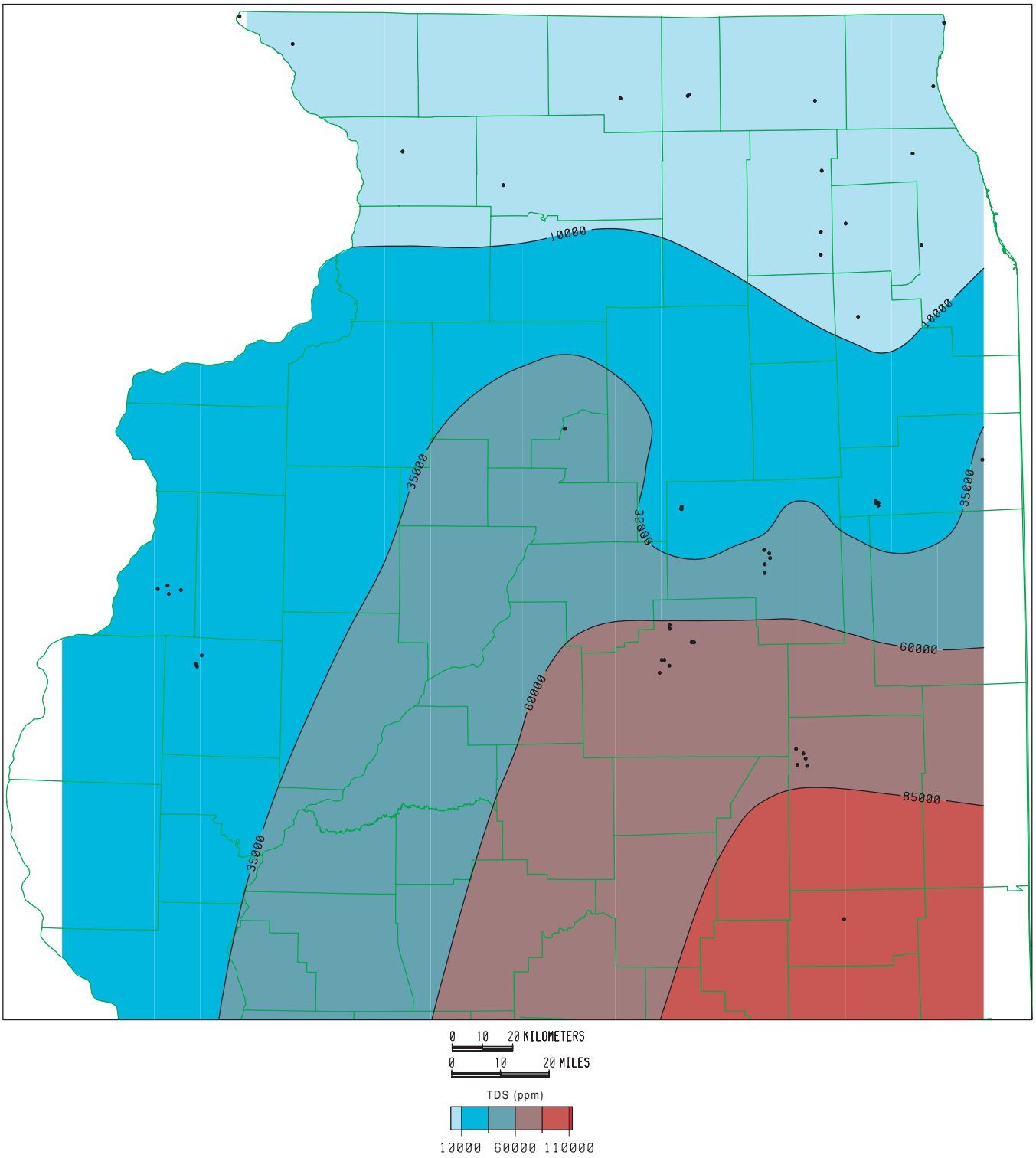

Figure 7 Regional Mt. Simon Sandstone salinity map in the north half of Illinois. The contour interval is 25,000 ppm. TDS, total dissolved solids.

The existing gas storage fields are clearly identified by the closed contours that have abundant well spots. Additional areas of closure that may have potential for gas storage are delineated by the closed contours.

Salinity Chemistry data are sparse for the water in the Mt. Simon Sandstone formation in the northern half of Illinois, especially in areas other than the natural gas storage fields that utilize the Mt. Simon Sandstone as a reservoir. The U.S. Geological Survey drilled several test holes and analyzed water from several different aquifers in northeastern Illinois. A map of the variations in salinity (TDS) of the water in the upper Mt. Simon Sandstone formation is shown in figure 7. The raw data for this map are found in Appendix 1. The salinity of the water in the Mt. Simon Sandstone increases from north or northwest to south or southeast and with depth. Total dissolved solids increase from 235 mg/L to as much as 100,000 mg/L along this trend. The Mt. Simon is a potential aquifer for potable water in northern and northwestern Illinois, near its recharge area, which lies to the north in Wisconsin where the formation outcrops. However, in the deeper parts of the Illinois Basin, the water is a brine.

Generalized Porosity versus Depth Relationships Core analysis data were compiled from reports and well data donated to the ISGS, primarily by the gas storage operators. The core data came from 56 wells and included about 8,400 values from tested samples that ranged in depth from 661 m (2,168 ft) to 1,799 m (5,900 ft). These data were supplemented with 610 porosity values calculated from geophysical logs (density or density-neutron cross plot) of deep, clean, Mt. Simon Sandstone intervals that ranged in depth from 1372 m (4,500 ft) to 3,505 m (11,492 ft) from 5 deep Illinois wells. A summary cross plot of porosity versus depth was prepared by computing and plotting the mean porosity of each of the wells with core and log data, the mean porosity plus one standard deviation, and the mean plus two standard deviations. Logarithmic regression lines were drawn for each of these sets of data. Well summary data points and the respective regression curves are shown on figure 8.

Typical reservoir intervals are anticipated to have greater porosities than the mean computed from random core analysis points. The best reservoir sandstones have porosity values close to two standard deviations above the mean, whereas the more typical reservoir rocks have porosity values close to the mean plus one standard deviation. Thus, the Mt. Simon Sandstone is likely to have a reservoir porosity of about 3% at 3,660 m (12,000 ft), 8% at 1,830 m (6,000 ft), 13% at 1,220 m (4,000 ft), and 18% at 610 m (2,000 ft).

Manlove Field

Introduction Manlove Field, a 153 billion cubic feet (BCF) aquifer gas storage field, including cushion gas, is located in Champaign County, Illinois,

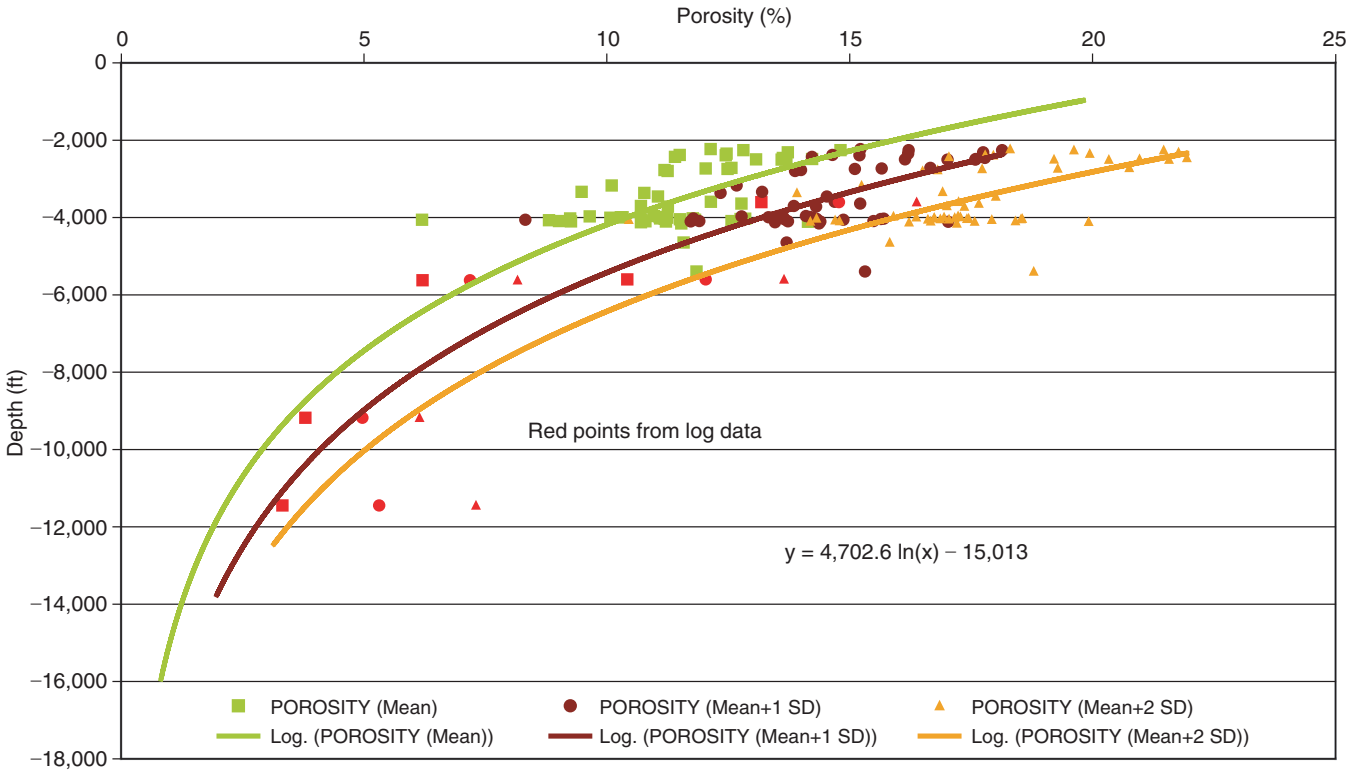

Figure 8 Regional variation of Mt. Simon porosity with depth from core and log data.

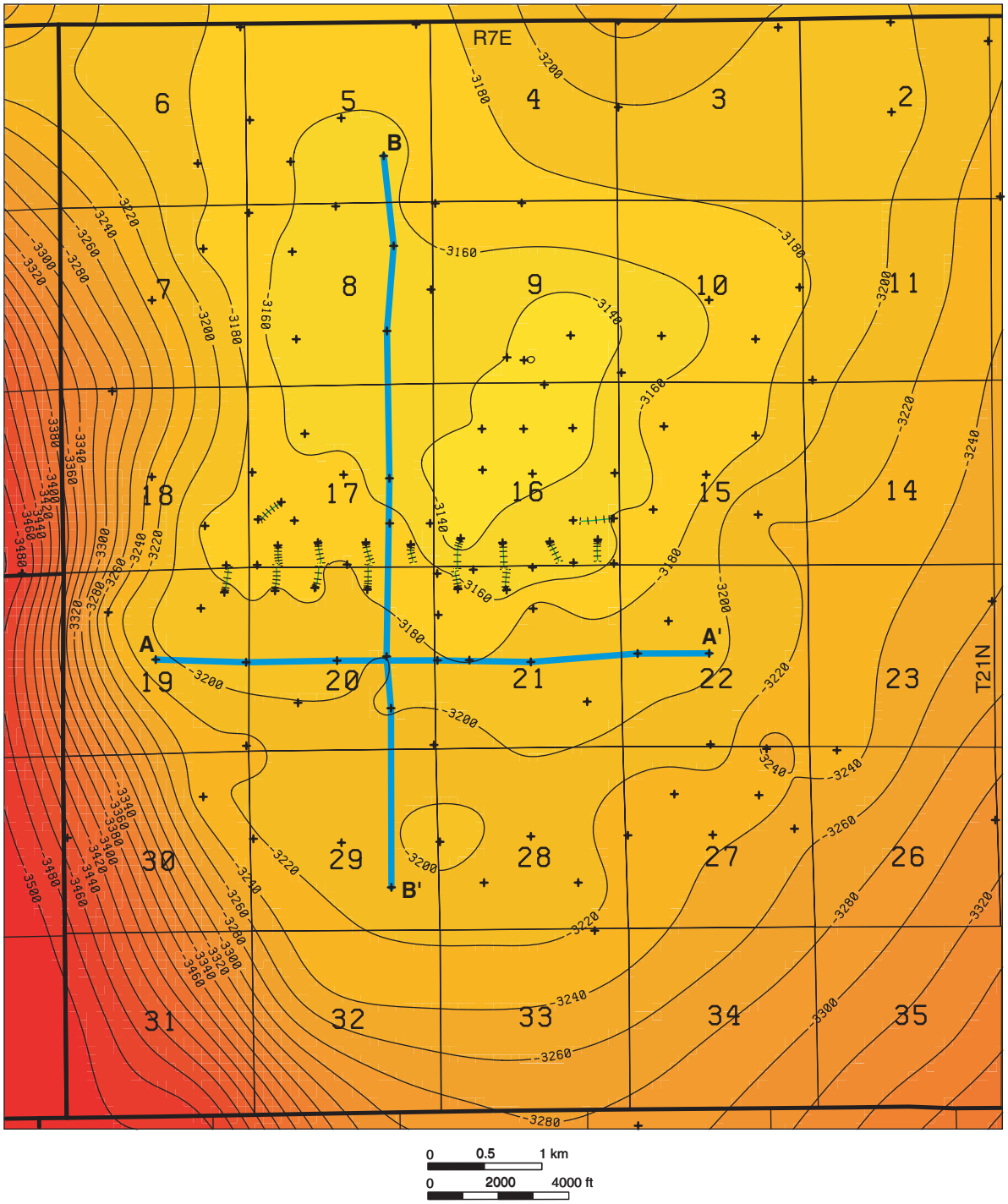

Figure 9 The top of the Mt. Simon Sandstone structure map, Manlove Field. The locations of all Mt. Simon wells used in the 3-D model are indicated. Wells with a ladder-like symbol show the traces of deviated wells. The plus mark indicates the well location at total depth. The structure conforms to the shape developed from the Galena level. Cross section locations A–A′ (see figs. 11 and 28) and B–B′ (see figs. 20 and 29) are shown in blue. The contour interval is 20 ft (6.1 m).

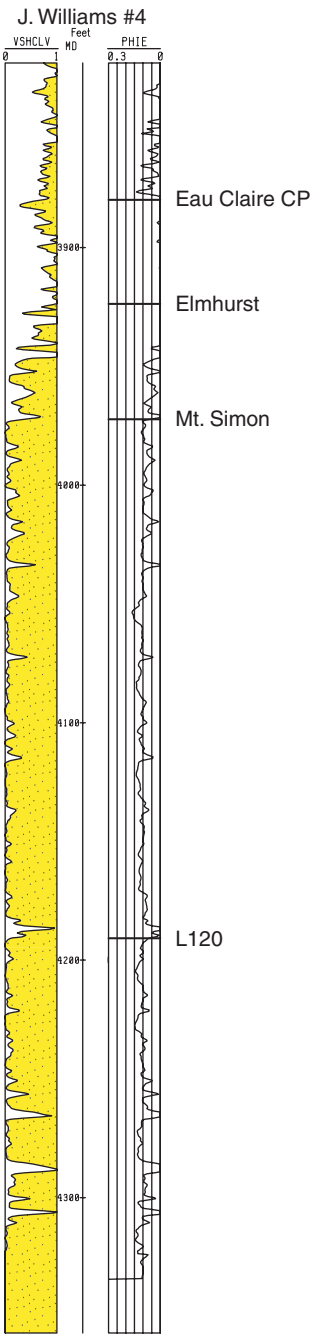

Figure 10 Manlove Field, J. Williams #4 well type log. Correlation marker beds used for the Mt. Simon reservoir characterization include a laterally continuous shale (L120), the top of the Mt. Simon Sandstone, the top of the Elmhurst Sandstone Member of the Eau Claire Formation, and a laterally correlative point in the Eau Claire. Gas is stored at Manlove Field in the more massive sandstones above the L120 marker. VSHCLV, Clavier shale volume; PHIE, shale-corrected neutron prorosity.

and is operated by Peoples Energy Corp. The field is formed by a north-south–trending, closed anticline 11.3 km (7 mi) long and 9.7 km (6 mi) wide with about 45 m (150 ft) of structural closure in T21N and R7E. The reservoir is in the Upper Cambrian Mt. Simon Sandstone, with a sealing caprock formed by about 31 m (100 ft) of dense shale in the overlying Cambrian Eau Claire Formation. The field has a steep west flank and a gentle east flank (fig. 9). The spill point lies in the northeastern part of the field. The field covers approximately 73 km^2 (28 mi^2). The Mt. Simon is about 1,220 m (4,000 ft) deep in this field and has an average porosity of 12% and an average permeability of 100 millidarcies (mD).

The field, located about 209 km (130 mi) south of Chicago, began withdrawals in 1966. Maximum daily withdrawal capacity is approximately 1 BCF; maximum annual withdrawal (maximum working gas) is about 44 BCF (Anonymous 1994, p. 47). Gas is transported to the Chicago market via two large-diameter, company-owned pipelines.

The field was originally drilled as a St. Peter Sandstone gas storage field, but after initial injection in 1961, gas was discovered in the glacial drift above the field. Injection was halted in August 1961, but the source of the leak could not be determined. Gas was then injected into the underlying Galesville Sandstone in 1963, which also appeared to leak. Later tests of the even deeper Mt. Simon Sandstone indicated that the Eau Claire Formation provided a proper seal and that porosity and permeability in the reservoir were sufficient to store and deliver gas effectively. Gas was initially injected into the Mt. Simon aquifer in 1964, and the project became operational in 1966.

The Mt. Simon Sandstone at Manlove Field is not a homogeneous reservoir. Gamma-ray logs indicate that many thin shaley interbeds separate sandstones in the Mt. Simon (fig. 10), but most of these shaley strata cannot be correlated widely (fig. 11). Examination of core from the J. Williams #4 well in the field indicated that the shale beds that caused these spikes in the gamma-ray logs are very thin, ranging from a few millimeters to a few centimeters in thickness, but with natural radioactivity sufficient to generate high gamma-ray values. The Mt. Simon Sandstone consists of stacked clean sandstone units capped with thin interbeds of fine sandstone, siltstone, and shale. These interbeds produce the indents observed in the Vshale log curves. Correlating the interbeds between neighboring wells just 200 m (660 ft) apart was difficult, however, and the interbeds could not be used to finely subdivide the reservoir. The only good correlative marker within the Mt. Simon was the L120 located approximately 67 m (220 ft) below the top of the Mt. Simon Sandstone (fig. 11).

Structure In order to define the structure of the field with the greatest detail, shallower formation tops, such as the Galena Group (fig. 10), were mapped in addition to those of the Mt. Simon Sandstone. The field had numerous shallow wells that had been used to define the configuration of the reservoir. Log tops from all of the wells were compiled, and structure maps for the top of the Galena Group (Ordovician) (fig. 12) and the top of the Mt. Simon Sandstone (fig. 9) were prepared with the structure of the deeper maps conforming to the details of the shallower structure. This structure map of the top of the Mt. Simon and a 3-D porosity model of the area (fig. 13) illustrate the north-south–oriented, asymmetrical, doubly plunging anticline. Gas is stored to a depth of about –994 m (–3,260 ft) filling a vertical closure of approximately 45 m (150 ft). At this depth, the area under closure is approximately 73 km^2 (28 mi^2) (Buschbach and Bond 1974, p. 51).

Depositional Systems Five lithofacies were identified and described in cores from the Peoples Gas, J. Williams #4 and Hazen #5 wells. The detailed core descriptions of these cores are presented in Appendices 2–5 of this report. These cores are from the upper 76 m (250 ft) of the Mt. Simon Sandstone and encompass the intervals used for gas storage.

The type well, the J. Williams #4, was drilled in July 1992, late in the field's development. The well was cored through the upper Mt. Simon and has modern compensated formation density-compensated neutron logs

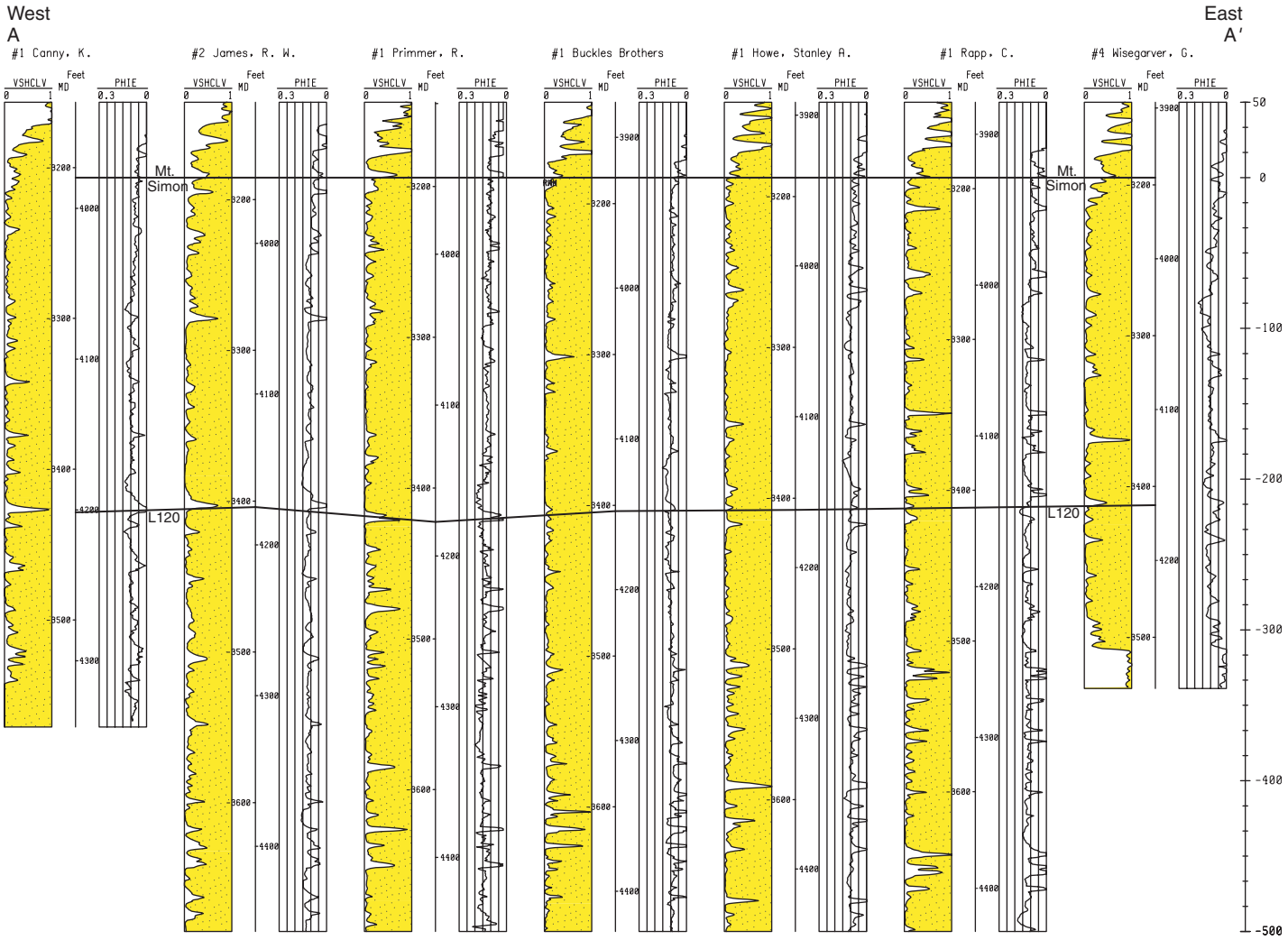

Figure 11 West-east stratigraphic log cross section, Manlove Field. Clavier shale volume (VSCHCLV) and shale-corrected neutron porosity (PHIE) for each well are shown with the lateral correlation of the top of the Mt. Simon (datum) and the L120 marker shale.

(FDC-CNL). The upper 23 m (75 ft) of Mt. Simon Sandstone is not used for gas storage at Manlove. This interval is more shaley and contains sandstones that are thinner, finer-grained, and with lower porosity than the sandstones that lie below. The deeper strata that constitute the active Mt. Simon gas storage reservoir consist of thick-bedded, coarse-grained, cross-bedded sandstone beds separated by thin intervals consisting of impermeable beds with high gamma-ray spikes composed of very fine sandstone, siltstone, and shale.

The lithofacies seen in the two primary cores consist of the following: (1) cross-bedded sandstone, (2) bioturbated sandstone, (3) deformed sandstone, (4) interstratified fine sandstone and shale, and (5) laminated shale.

Cross-bedded sandstone The cross-bedded sandstone is primarily composed of moderately well-sorted, medium- to coarse-grained, cross-bedded sandstone strata, some of which may have very thin, poorly sorted, granule conglomerate beds at their bases (fig. 14). This facies is the main reservoir type in the Illinois gas storage fields. The sandstone is commonly porous and permeable. Cross-bedding consists primarily of thin trough-shaped sets (5 to 15 cm high) and less abundant, thicker, tabular-shaped sets (30 to 100 cm high). Reactivation surfaces, rarely marked by a fine dark gray shale drape a few millimeters thick, occur locally. The rock is typically pale buff-colored, but, at the top and base of the J. Williams #4 core, the sandstone has a pale reddish (hematitic) color. Quartz granules up to 4 mm in diameter may also occur within the sandstone along the bases of some of the trough sets; granules 2 mm in diameter may be scattered within the sandstone. Some of the trough strata may contain asymmetrical ripples within the cross-bed planes. Trough cross-bed sets are stacked, forming co-sets up to 4 m

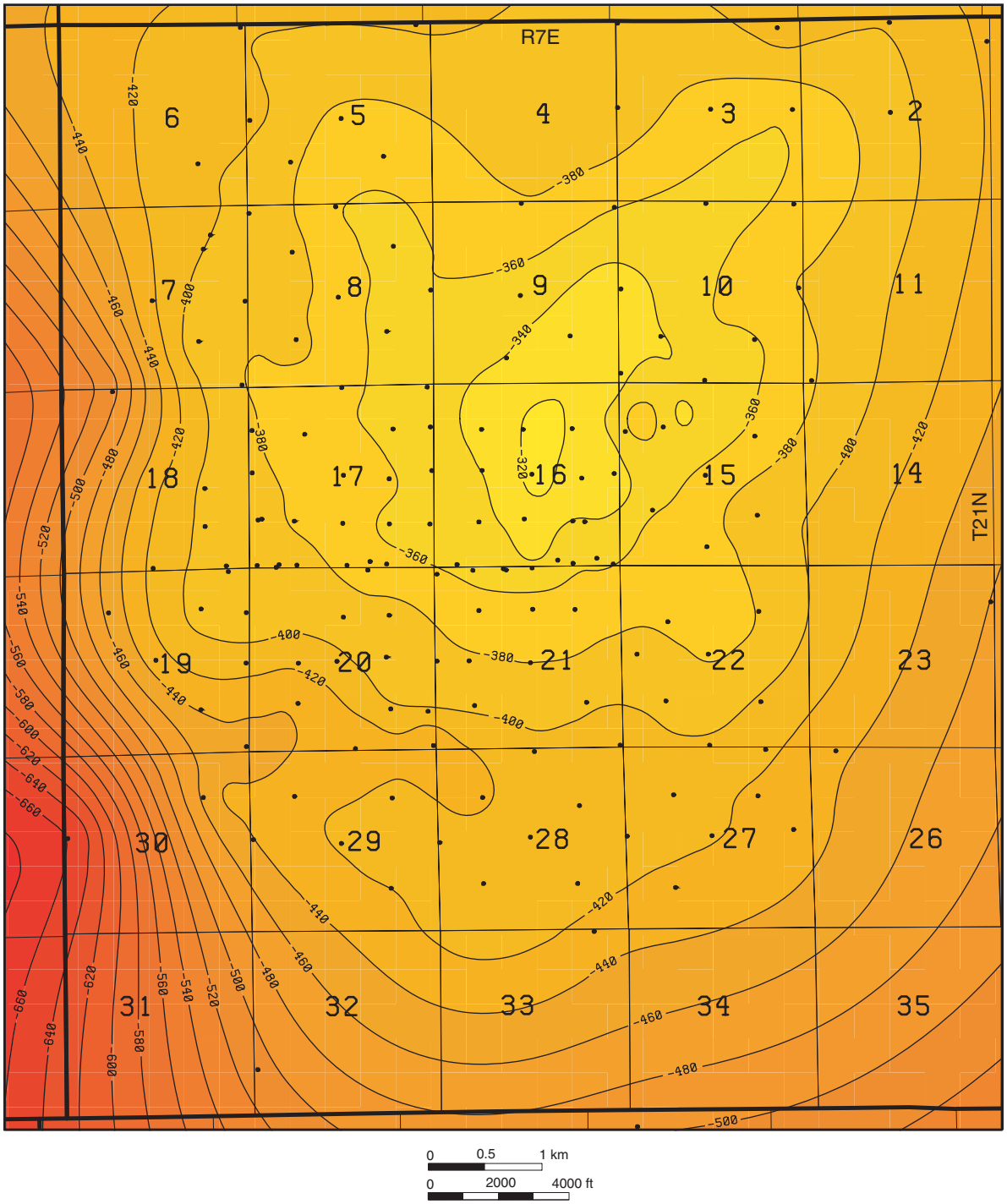

Figure 12 Top of the Galena Group (“Trenton limestone”) structure map, Manlove Field. Wells reaching the Galena include all the Mt. Simon wells in addition to a number of shallower test holes that were specifically drilled to delineate the nature of the structural closure. The contour interval is 20 ft (6.1 m).

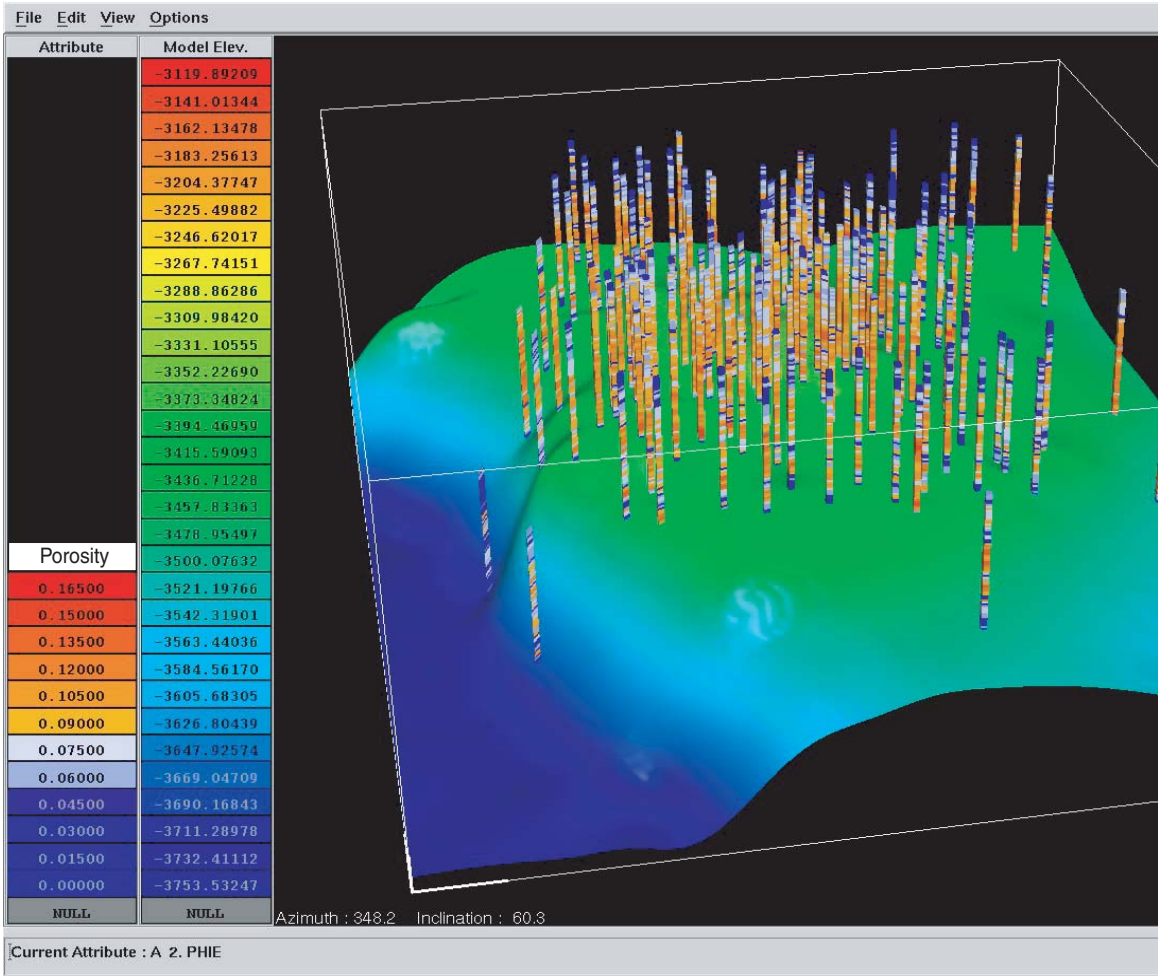

Figure 13 Three-dimensional view of Mt. Simon well control, Manlove Field. Data from the 121 wells were used to construct the 3-D porosity model. The surface shown is the L120 marker.

(13 ft) thick. These co-sets have sharp bases and are typically overlain by thin sequences of the finer-grained, bioturbated sandstone or by the interstratified sandstone and shale facies. The cross-bedded sandstone strata commonly have a blocky or fining-upward gamma-ray log motif.

Bioturbated sandstone The bioturbated sandstone consists of fine to coarse, poorly to moderately well-sorted sandstone (fig. 15). The bioturbated sandstone includes strata with clusters of sand-filled, vertical burrows, each approximately 3 to 5 mm in diameter and up to 5 cm in length, as well as structureless or mottled sandstone beds. The burrow filling may have a darker gray hue than the surrounding sandstone. The vertical, tube-like burrows are identified as *Skolithos*. The degree of burrowing ranges from slight to complete destruction of any sedimentary layering. Multiple beds of the bioturbated sandstone may stack up to 3 m (9.8 ft) thick. Faint bedding of the cross-bedded sandstone may be preserved between these burrows or between stacked beds of the bioturbated sandstone. This facies may or may not be porous, depending on the original facies prior to bioturbation.

Deformed sandstone The deformed sandstone consists of medium to coarse sandstone with swirly, convoluted, or discontinuous bedding (fig. 16). It is relatively rare, occurring within thick co-sets of cross-bedded sandstone. The deformed intervals range from 30 to 130 cm thick and are bounded by normal, horizontal, or cross-bedded strata. A dewatering or flame structure was observed within this facies.

Interstratified sandstone and shale The interstratified sandstone and shale, one of the fine-grained, non-reservoir facies seen in the Mt. Simon, consists of interstratified thin beds and laminae of very fine to fine sandstone and fine-grained siltstone or shale (fig. 17). Rhythmic alternations of millimeter-thick laminae of these lithologies occur in beds up to 30 cm thick. Shale laminae range from less than 0.5 mm to 1 or 2 cm in thickness. Horizontal, tubular, very fine, sandstone-filled, *Planolites* burrows occur within many of the shaley laminae. The sandstone-shale laminae may be planar, wavy, lenticular, or flaser-bedded. Mud cracks filled with fine sandstone (fig. 17B) were

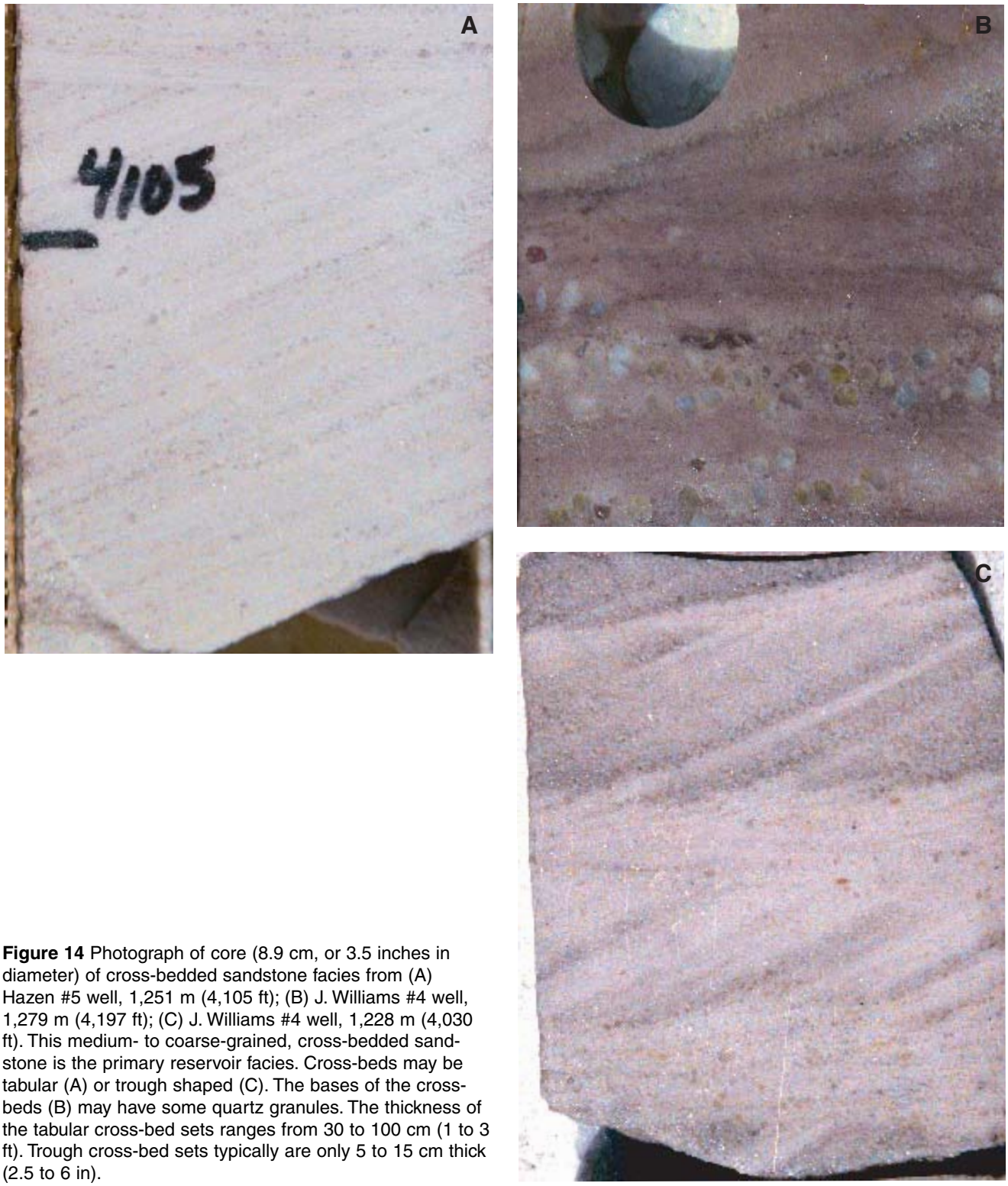

Figure 14 Photograph of core (8.9 cm, or 3.5 inches in diameter) of cross-bedded sandstone facies from (A) Hazen #5 well, 1,251 m (4,105 ft); (B) J. Williams #4 well, 1,279 m (4,197 ft); (C) J. Williams #4 well, 1,228 m (4,030 ft). This medium- to coarse-grained, cross-bedded sandstone is the primary reservoir facies. Cross-beds may be tabular (A) or trough shaped (C). The bases of the cross-beds (B) may have some quartz granules. The thickness of the tabular cross-bed sets ranges from 30 to 100 cm (1 to 3 ft). Trough cross-bed sets typically are only 5 to 15 cm thick (2.5 to 6 in).

Figure 15 Photograph of core (8.9 cm, or 3.5 inches in diameter) of bioturbated sandstone facies from (A) J. Williams #4 well, 1,274 m (4,180 ft) and (B) Hazen #5 well, 1,221 m (4,005 ft). Vertical *Skolithos* burrows in medium to coarse sandstone may obliterate most of the original stratification. These burrows are formed from filter feeders that live in a high-energy substrate and intercept food from the moving water that lies above.

observed within these strata in both cores. Intervals of this facies commonly are interbedded with beds of the bioturbated sandstone or may be sharply overlain by beds of the cross-bedded sandstone. This fine-grained facies forms vertical and lateral barriers to gas flow in Manlove Field, although, except for at the L120 marker, intervals of the facies could not be readily correlated from well to well.

Laminated shale The laminated shale occurs as part of the L120 marker bed. Shale is the predominant lithology, although thin interlaminae of siltstone or shale with fine-sand–filled *Planolites* burrows can be seen. This non-reservoir facies (fig. 18) is rarely more than 10 cm thick. It may grade into the interlaminated sandstone and shale facies, but is recognized when the lithology is predominantly shale. The L120 marker, which consists of both the laminated shale and the interstratified sandstone and shale facies, contains the thickest layers of the laminated shale facies

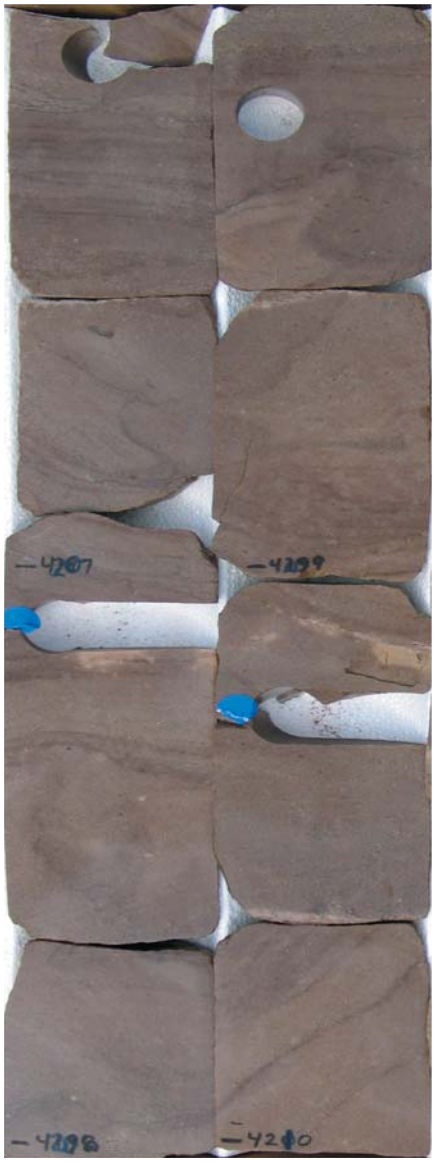

Figure 16 Photograph of core (8.4 cm, or 3.5 inches in diameter) of deformed sandstone facies from the Hazen #5 well, 1,282 to 1,283 m (4,206 to 4,210 ft). Structureless to swirly bedded sandstone strata formed from liquefied sand and subsequent fluid escape.

seen at Manlove Field and can be correlated across the field. Elsewhere, thinner unnamed shale strata can be identified by their high-value spikes on the gamma-ray log, but these strata are discontinuous from well to well.

Facies interrelationships These Mt. Simon lithofacies are packaged into units 2 to 5 m (6.6 to 16.4 ft) thick that can be identified on gamma-ray logs (fig. 19). They are composed predominantly of cross-bedded sandstone capped by beds of bioturbated sandstone and overlain by interlaminated sandstone and shale, thus forming a fining-upward package. These packages, or simply the interlaminated sandstone and shale beds, can rarely be recognized by their gamma-ray log signatures farther than one well location away (201 m or 660 ft) (figs. 11 and 20). One shaley interval located below the gas storage zone, named the L120 marker, was correlated field-wide, a requirement for the 3-D porosity modeling, but many of the correlation picks for this horizon were extended through sandstone intervals at the level where the shales occurred in adjacent wells.

Depositional environments of sediments The Mt. Simon is commonly interpreted as having been laid down in a shallow, subtidal marine environment (Droste and Shaver 1983). Based on their southern Wisconsin outcrop studies, Driese et al. (1981) interpreted the Mt. Simon to be a stacked succession of largely progradational, shoaling- and fining-upward tidal deposits containing widespread marine trace fossils. In general, the paleogeography of Illinois at Mt. Simon deposition was one of a low relief, subsiding basin that was open to the ocean to the south (Kolata 1991, p. 197).

The depositional environment for the upper part of the Mt. Simon Sandstone interpreted from the cores at Manlove Field was probably a coastal setting comprising fine-grained tidal flat sediments and cross-bedded, meandering tidal channel and tidal bar deposits (fig. 21). Sand body geometries, described later, suggest there may have been barrier bars as well. The presence of *Skolithos* and *Planolites* burrows in these deposits indicates marine influence. The cross-bedded sandstone facies is interpreted as a shallow subtidal deposit formed by meandering tidal channels and subaqueous tidal-delta bars. Clay-drape laminae on some of the cross-bedded sandstone beds are characteristic of a tidal regime in which clay settles out of suspension during slack water periods of a tidal cycle or during neap tides of the lunar cycle. Clay intraclast lags indicate reworking of previously deposited thin shale beds and their transportation for short distances in laterally migrating channels. The bioturbated sandstone facies with *Skolithos* burrows was formed in high-energy settings, such as tidal-delta bars or tidal channels, with coarse-grained substrates that are constantly being reworked by tidal currents and suspension-feeding infauna (Seilacher 1967). The deformed sandstone strata are interpreted as slump deposits that formed during the collapse of undercut banks of meandering tidal channels.

The finer-grained, laminated shale and the interbedded sandstone and shale facies sediments probably were deposited on tidal sand and mud flats. Mud cracks indicate subaerial exposure. Locally, the interlaminated sandstone and shale beds have fine rhythmic spacing, an indicator of tidal deposition. Very fine sandstone is deposited by tidal currents, and the mud is deposited from suspended sediment during slack tides. *Planolites* burrows are common, indicating a marine influence. The laminated shale may form in a subtidal lagoon or bay.

Similar tidal sedimentary environments have been interpreted for the overlying Eau Claire Formation (Huber 1975, Byers 1978). Thus, it appears that essentially the same sedimentation and depositional environments continued across the Mt. Simon-Eau Claire boundary, forming a conformable contact.

Petrography The Mt. Simon Sandstone contains a wide range of grain sizes and minerals. The reservoir sandstones examined in the cores from the J. Williams #4 and Hazen #5 wells consist of clean, well-sorted, medium- to very-coarse grains of quartz cemented by quartz overgrowths (fig. 22, A and B). Pores are large and smoothly lined by this cement (fig. 23). Fine- to very fine-grained sandstones and less well-sorted sandstones (fig. 22C) contain significantly more relatively unaltered K-feldspar grains than do the coarser sandstones (see table 1). K-feldspar in the Mt. Simon occurs only as fine

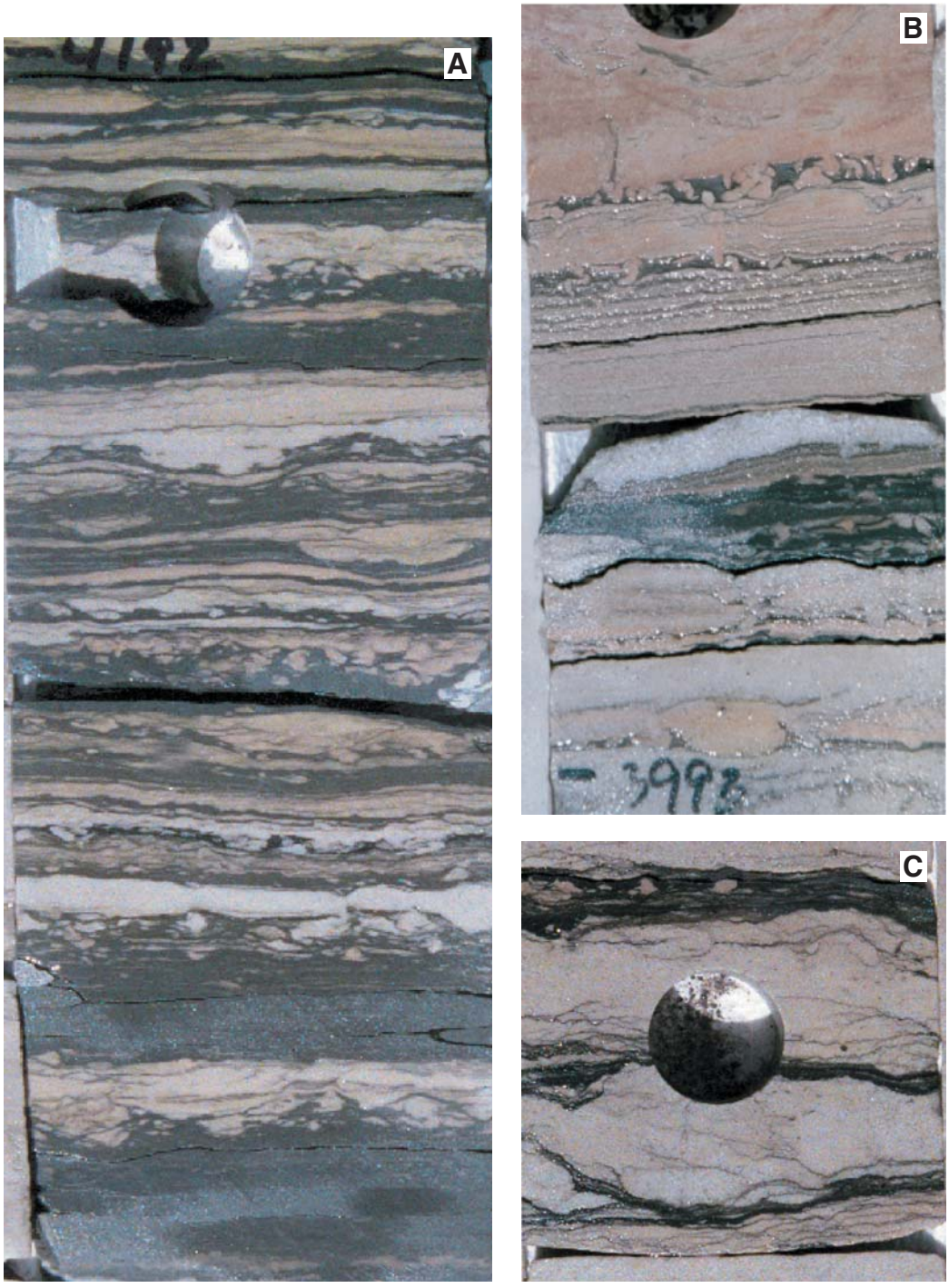

Figure 17 Photograph of core (8.9 cm, or 3.5 inches in diameter) of interstratified fine sandstone and shale facies from the J. Williams #4 well at (A) 1,278 m (4,192 ft), (B) 1,218 m (3,996 ft), and (C) 1,218 m (3,997 ft). Heterolithic low-energy sediments were deposited on the tidal flats. Small round horizontal burrows of *Planolites* are filled with fine sandstone. The shale content varies from very high (A) to very thin laminae (B and C). Sand-filled mud cracks are seen in photograph B. Clusters of very thin shale laminae alternating with laminae and thin beds of very fine sandstone (C) are typical of tidal rhythmites.

Figure 18 Photograph of core (8.9 cm, or 3.5 inches in diameter) of laminated shale facies from the Hazen #5 well at 1,276 m (4,187 ft). Laminated, dark gray shale with thin laminae of siltstone and local very fine sandstone or siltstone-filled *Planolites* burrows.

to very fine grains. These grains have angular, euhedral outlines indicative of diagenetic feldspar overgrowths. No plagioclase feldspar was seen. Modal analyses of 31 thin-sections from the J. Williams #4 well are listed in Appendix 6. The SEM images of coarse-grained reservoir sands (fig. 24) illustrate the euhedral quartz overgrowths and the open pore system. Diagenetic clay minerals are sparse and, based on the SEM images, appear to be composed mostly of illite (fig. 25).

Petrophysics A major goal of this research project was to create an accurate porosity model of the Manlove Field gas storage reservoir that could be used both in volumetric analysis and in reservoir simulations. This goal, however, was constrained by the fact that many of the wells had a wireline log suite that included only a gamma-ray log and an older-style neutron log. The older neutron logs were commonly calibrated in counts per second and had to be converted to porosity units.

Gamma-ray logs cannot be directly compared with one another in the field because well-bore conditions and incorrect calibrations result in variable scales for the curves. In order to compare gamma-ray logs from well to well, Vshale values were calculated, using the Clavier equation method. This normalization technique scales the gamma-ray from 0% in pure sandstone to 100% in pure shale. The resulting values allow well-to-well comparison. The Clavier equation is recommended for use in older strata, whereas the linear gamma-ray Vshale equation is better in Tertiary age strata (Clavier et al. 1977).

Neutron porosity was calculated for all of the wells using standard methods described for the older types of neutron logs (Brown and Bowers 1957, Swulius 1986, Dull 1991). There is a linear relationship between the neutron tool count rate and the logarithm of the porosity value. Therefore, the count rate of each log can be converted to porosity using the following equation:

$$\text{Log Phi}_N = -mN + k, \qquad [1]$$

where m is slope, N equals varying neutron value of the log, k is y intercept, and Phi_N is resulting porosity. For each well, using the gamma-ray log to guide the choice, neutron values were determined for pure shale in the Eau Claire Formation, assumed to equal 30% porosity, and for a clean sandstone in the Mt. Simon, assumed from core data to have an average of 14% porosity. Then, using a cross-plot of log porosity versus the neutron counts for these two extremes, the linear equation of the line connecting these points was determined. The m and k were then calculated for neutron logs in each well using this method and applied to the equation. Porosity then could be calculated for any neutron value. A shale correction to porosity was made with the Vshale values from the Clavier equation.

Table 1 Feldspar variation with sandstone grain size.

Sandstone grain size[1]	Average feldspar content (%)
Coarse	2.35
Medium-coarse	6.00
Medium	7.23
Medium-fine	15.67
Fine with shale interlaminae	21.33

[1]Based on thin section point counts, J. Williams #4 well, 300 points per thin section.

Vshale linear:

$$\text{Vsh\_linear} = (\text{GR} - \text{GRmin})/(\text{GRmax} - \text{GRmin}) \qquad [2]$$

where GR is gamma-ray log, max is maximum, and min is minimum.

Vshale Clavier:

$$\text{VSHCLV} = 1.7 - \sqrt{(3.38 - (\text{Vsh\_linear} + 0.7)^2)} \qquad [3]$$

Shale-corrected porosity:

$$\text{PHIE} = \text{Phi}_N(\text{VSHCLV} * 0.3) \qquad [4]$$

where PHIE is shale-corrected neutron porosity, Phi_N is neutron log porosity, and VSHCLV is Clavier shale volume.

Porosities, calculated by logging companies using standard cross plot methods for most of the modern compensated density-neutron logs, correlated very well to detailed core analysis measurements. These log values were used as standards for further porosity analysis. Determining true log porosity and the amount of porosity that had to be

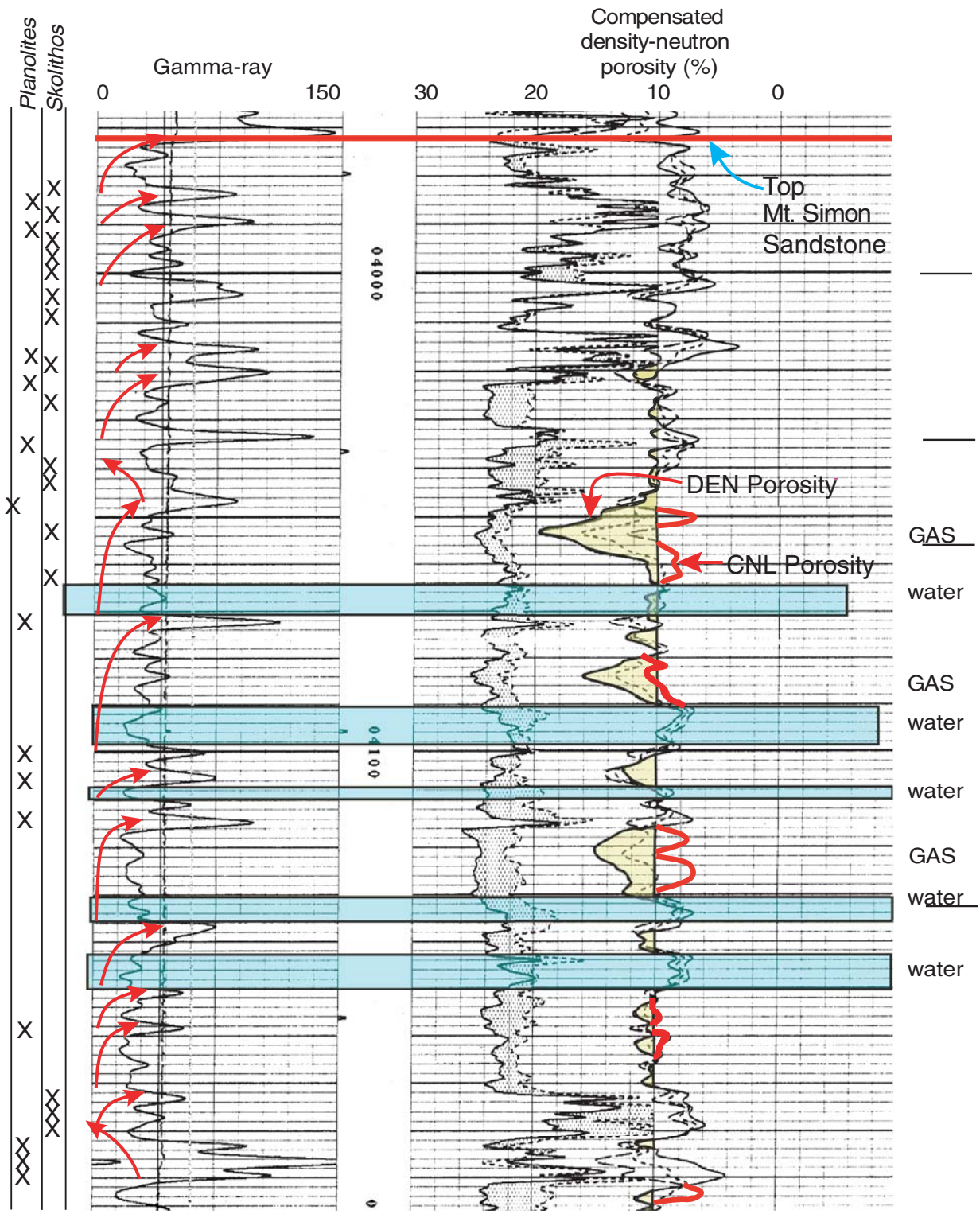

Figure 19 Geophysical log of the Mt. Simon Sandstone, J. Williams #4 well, Manlove Field. Burrow types, grain-size trends, and gas- and water-bearing zones are annotated. Injected gas is identified where density (DEN) porosity and neutron porosity (CNL) values show divergence (yellow). Discrete intervals show "gas effect" density and neutron log separation in several clean sandstones. Individual gas-bearing sandstones appear to have basal water sands (blue) where the density and neutron porosities have similar values, suggesting that individual gas sands may be compartmentalized.

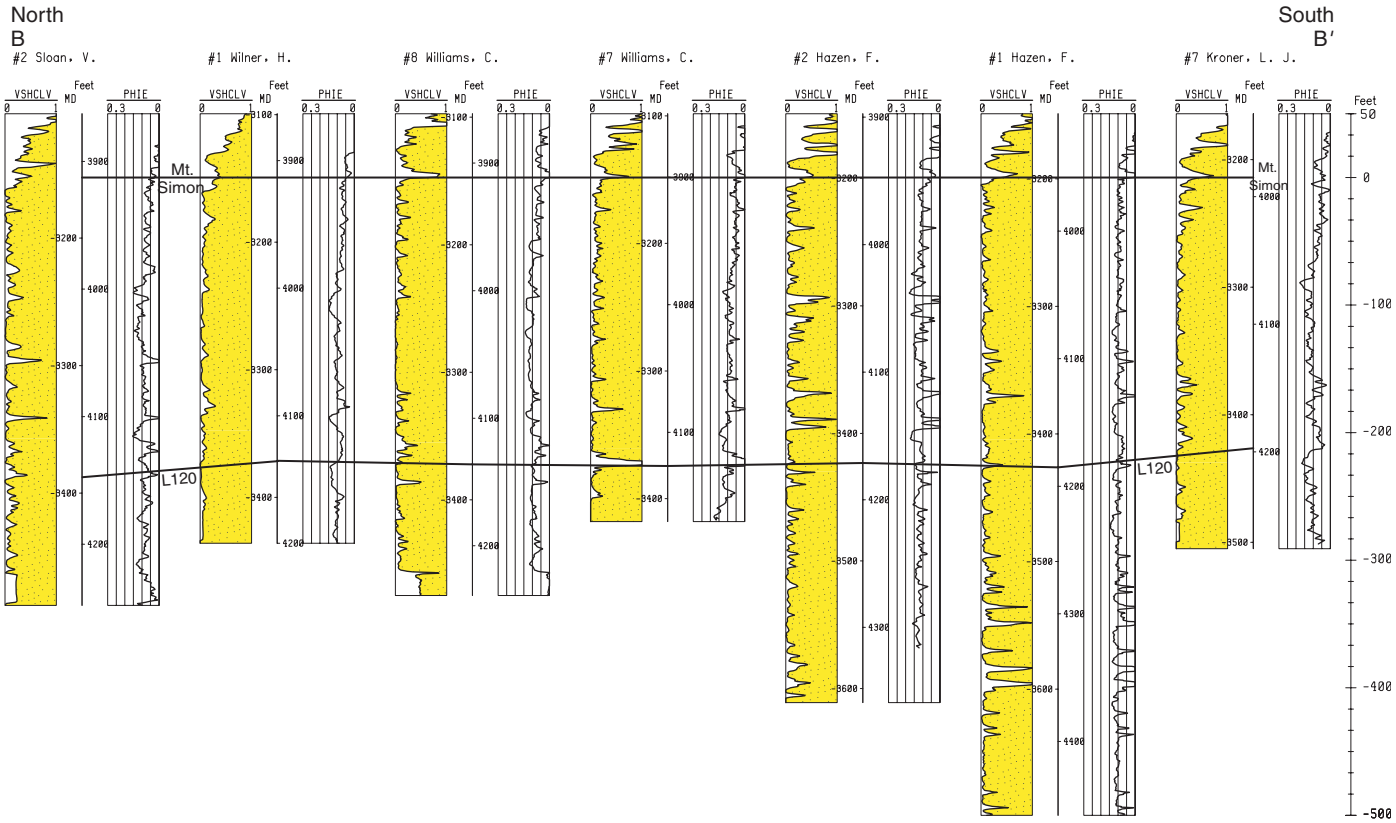

Figure 20 North-south stratigraphic log cross section, Manlove Field. Clavier shale volume (VSCHCLV) and shale-corrected neutron porosity (PHIE) for each well are shown with the lateral correlation of the top of the Mt. Simon and the L120 marker shale.

attributed to "gas effect" and not to true porosity was difficult and caused many of the neutron log porosities to be questioned. Core porosity values in some of these wells provided a basis for calibration, allowing retention of those values. Porosity values in 124 of the total 175 wells in the immediate field area were used to make the 3-D porosity model. These 124 wells included 43 wells with gamma-ray–neutron logs that were drilled prior to gas injection, 35 cored wells that provided a means of calibrating the log porosity, particularly in old gamma-ray–neutron logs, and finally 81 wells with modern FDC-CNL, several of which also had cores for porosity verification.

Typical histograms of cored porosity (shown in red) and density-neutron porosity (shown in green) are shown in fig. 26. Mean core and density-neutron values agree well. Data from 35 cored wells were available for calibration of porosity. Wells with neutron logs that agree with core and uncored wells with neutron logs that showed no "gas effect" were used in the model.

3-D Porosity Model The porosity values calculated from wireline logs were used to generate a 3-D model of the distribution of porosity throughout the Mt. Simon reservoir at Manlove Field. The grid used to generate the model had x and y increments of 76 m (250 ft). The vertical interval was about 0.6 m (2 ft) but varied across the field because the model assumed a proportional thickening and thinning of grid cells in the interval between the top of Mt. Simon and the L120 marker bed.

A 3-D fence diagram view of this model is shown in figure 27. Porosity values have been lumped in 2.5% intervals for color contrast. Key model cross sections have been drawn through this model in north-south and east-west directions. These cross sections can be viewed both structurally or stratigraphically by hanging the section from a datum consisting of the top of the Mt. Simon Sandstone (figs. 28 and 29).

Horizontal slice maps of the porosity model were prepared to determine lateral geometry and continuity of sandstone and shale bodies. A vertical slice from the far northeastern part of the model and a small plot of the gamma-ray log for the J. Williams #4 well are shown in their proper location for reference. These maps plot the average porosity of an approximately 65 to 100 cm (2 to 3 ft) thick grid interval proportionally spaced from the top of Mt. Simon Sandstone at 1,211m (3,972 ft) to the correlated shale located about 65 m (215 ft) below the top of the Mt. Simon. Pertinent samples of these maps, shown in figs. 30 through 35, corresponding to depths in the J. Williams #4 well, reveal

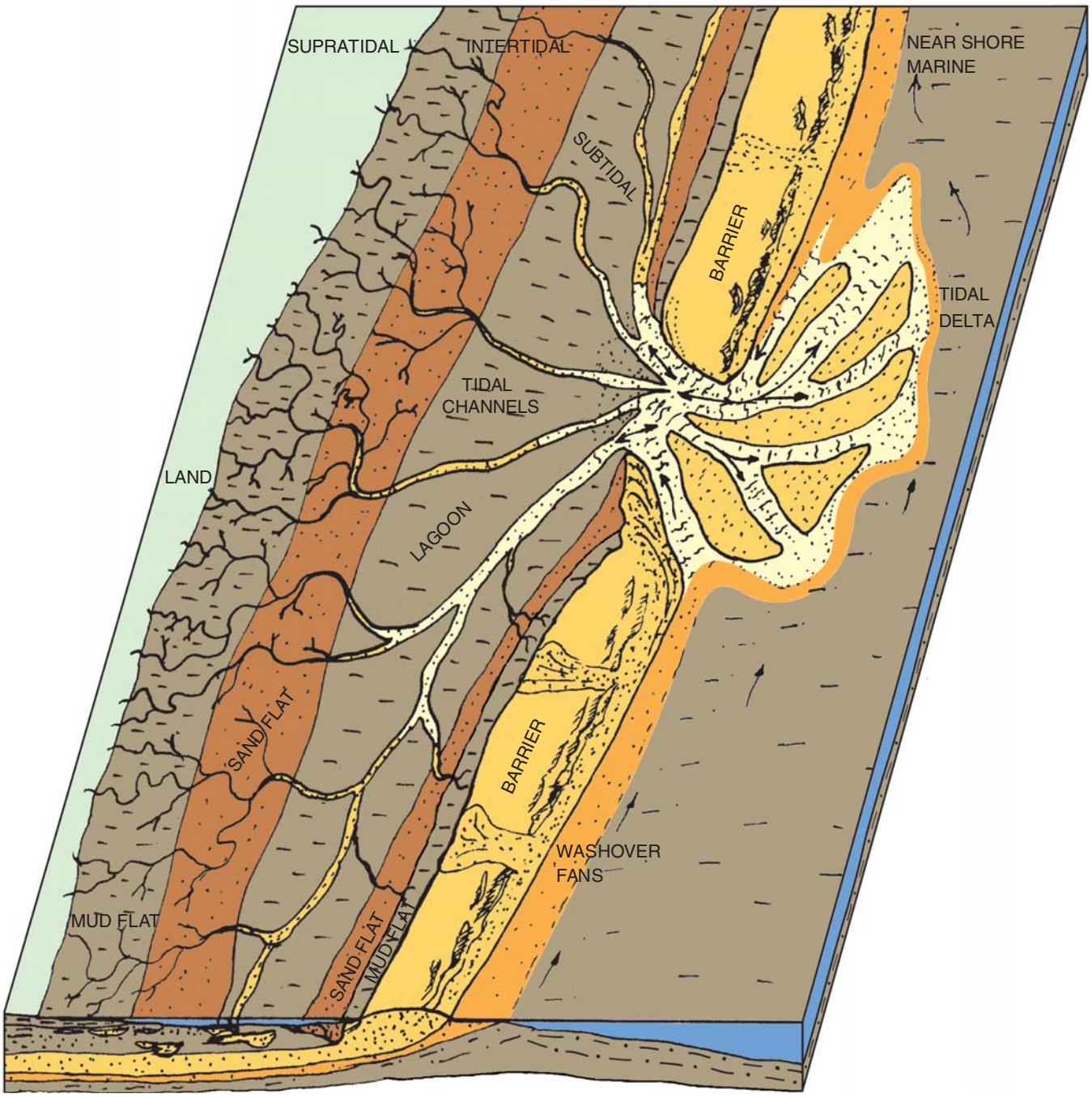

Figure 21 Depositional model block diagram for Manlove Field area. A generalized model showing barrier, lagoon, and tidal flat areas is shown. Exiting from the major tidal channel system separating the barriers is an ebb-tidal delta deposit. Longshore currents from bottom to top in this diagram bring in sediment from an alluvial system outside the model area. Tidal channels cut through the lagoonal area and have sinuous paths. Thin intertidal sand flats and mud flats rim the lagoon. Progradation of the barrier-lagoon-mud flat system creates laterally continuous barrier sands, discontinuous channel sands, and dissected intertidal sand and mud flats.

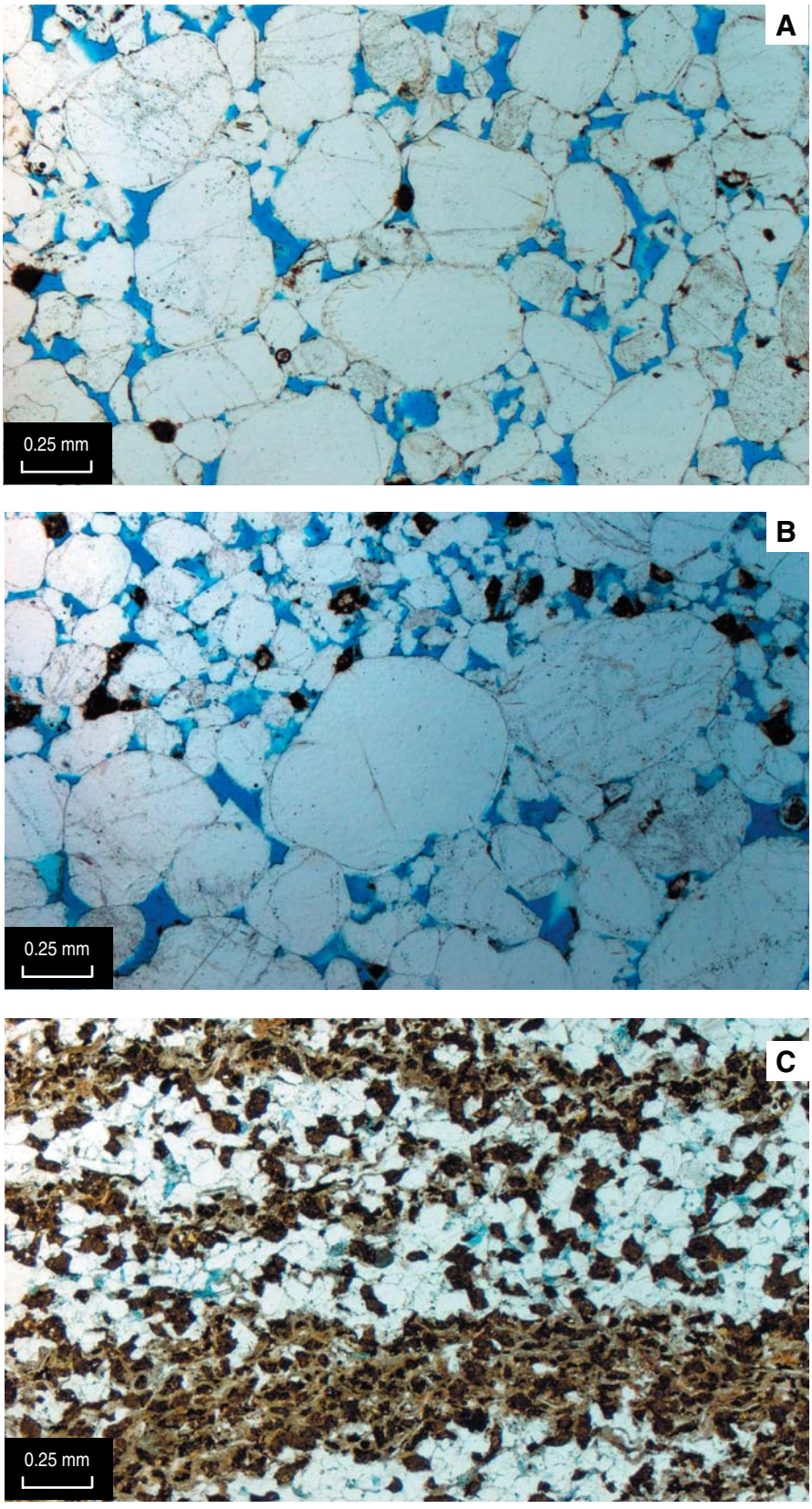

the geometry of reservoir sandstone compartments and shale seals.

The porosity slice at 1,220 m (4,000 ft) in the J. Williams #4 reference well (fig. 30) shows an east-west tidal channel. The core from the reference well indicates that this channel sandstone contains abundant *Skolithos* burrows and a few thin shale intraclasts and is medium- to coarse-grained. Lateral to the reference well, the facies have low porosity and are interpreted to be lagoonal or intertidal mud flats. This interval lies above the gas storage reservoir.

The porosity slice at 1,230 m (4,034 ft) in the reference well (fig. 31) shows a bifurcating, west-to-east–flowing, tidal channel system (high porosity) and surrounding tidal mud flats (low porosity). In the core of the reference well, the sandstone at this depth is coarse- to very coarse-grained and porous and contains thin trough cross-bed sets and a few *Skolithos* burrows. The channel branches to the west of the reference well, and the channel geometry suggests flow from west to east. To the north and south of this well lie lower-porosity tidal flat facies deposits. The FDC-CNL at J. Williams #4 indicates that the channel sand, shown here, lies just above a thin shale and above the main gas reservoir.

The porosity slice at 1,237 m (4,056 ft) in the reference well (fig. 32) shows a

Figure 22 Thin sections of Mt. Simon Sandstone from J. Williams #4 well at (A) 1,283 m (4,209.1 ft)), (B) 1,257 m (4,124.3 ft), and (C) 1,279 m (4,195.2 ft). A, Clean, moderately well-sorted, medium to coarse sandstone cemented with euhedral quartz overgrowths. B, Interlayered medium-coarse sandstone and fine sandstone. The dark grains are stained K-feldspar grains that have been segregated by size into the fine-grain fraction. C, Interlaminated very fine sandstone and clayey siltstone. The dark grains are stained K-feldspar. The light gray to brown, extremely fine-grained material is detrital clay. Porosity is filled with blue-dyed epoxy.

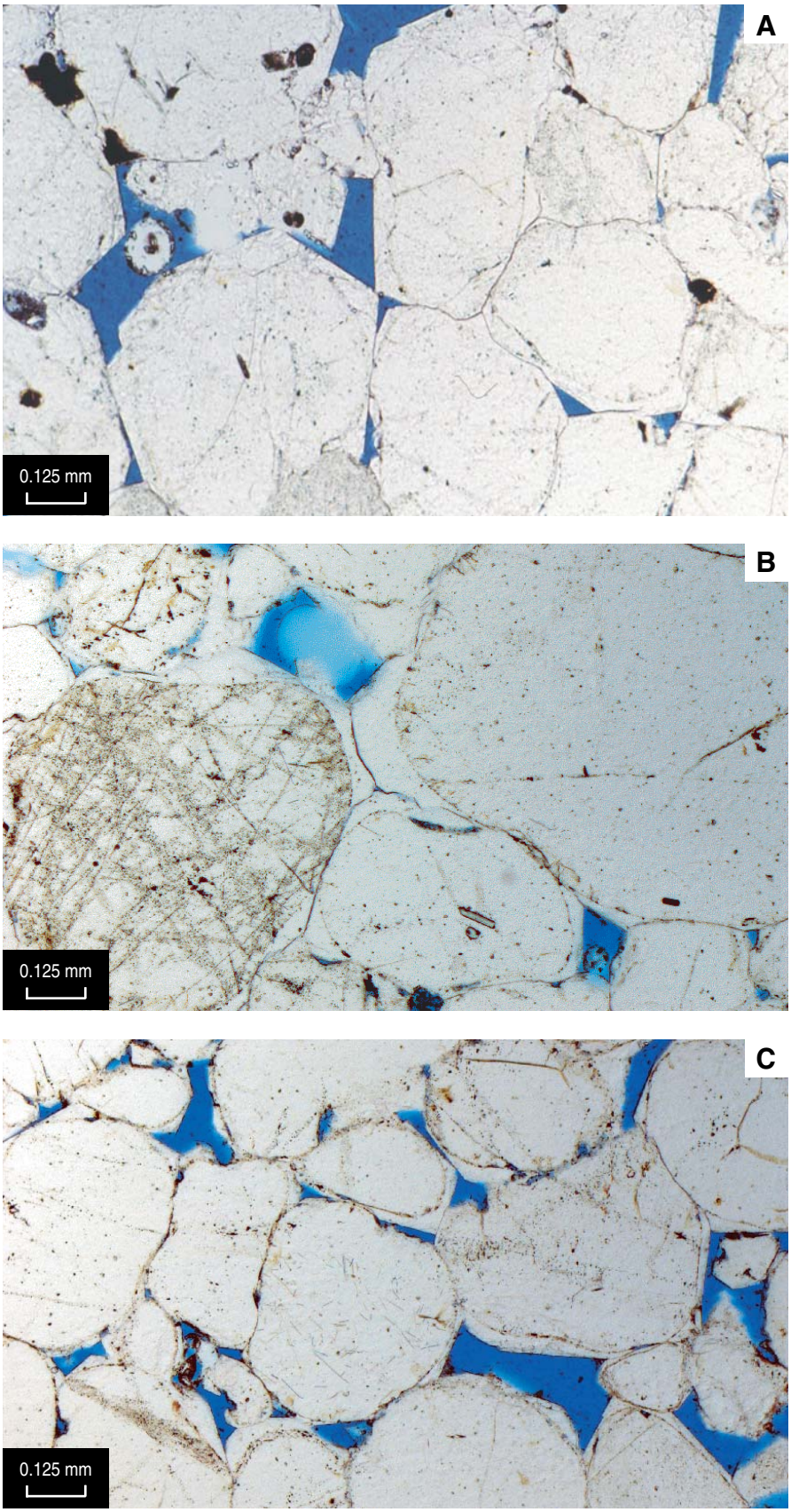

widespread, porous sandstone extending from the reference well in the upper gas storage interval. The sandstone is cross-bedded, coarse- to very coarse-grained and porous. More porous sands occur to the west of the reference well in a band oriented north to south (barrier island or tidal delta?) that is elongate perpendicular to two narrow tidal channels that are further west.

The porosity slice at 1,260 m (4,132 ft) in the reference well (fig. 33) shows another sinuous, high-porosity tidal channel sand oriented east to west. It is joined by a channel or remnant barrier sand from the north. To the east is a possibly younger barrier sand body. The core in this interval in the reference well is coarse- to very coarse-grained and cross-bedded.

The deepest porosity slice at 1,277 m (4,187 ft) in the reference well (fig. 34) shows the distribution of the L120 marker bed, the only high gamma-ray shale that can be readily correlated across the field. In this core the low porosity interval shows interlaminated black and dark greenish black shale and fine- to very fine-grained sandstone. Sand-filled *Planolites* burrows are abundant. Deposition was likely in a back barrier, tidally influenced lagoon, an intertidal mud flat, or a result of a minor marine flooding event.

Herscher Field

Introduction The Herscher and Herscher NW Anticlines (fig. 35), located in the southwest corner of Kankakee County, Illinois, were producing oil from the Galena Group ("Trenton limestone") in the early 1900s. The field was abandoned for more than 40 years until the late 1950s, when it was converted into a natural gas storage

Figure 23 Thin sections of coarse-grained Mt. Simon Sandstone from the J. Williams #4 well at (A) 1,235 m (4,051 ft), (B) 1,220.7 m (4,004.9 ft), and (C) 1,213 m (3,981.1 ft). Quartz grains are cemented by euhedral quartz overgrowth cement. The original grains are well rounded. Primary porosity is filled with blue-dyed epoxy.

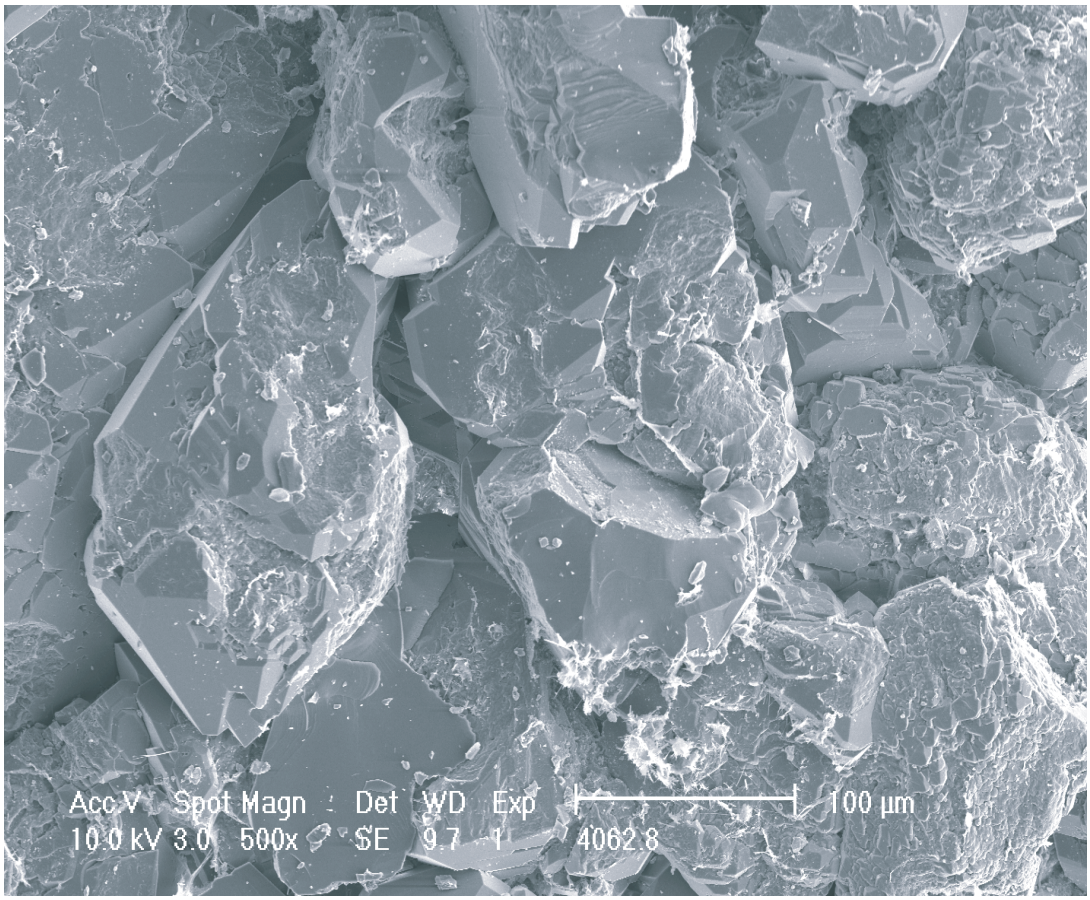

Figure 24 A scanning electron microscopic image of Mt. Simon reservoir sandstone with euhedral quartz overgrowths and an open pore system. Porosity is 12%, and permeability is 414 mD. Sample from the J. Williams #4 well, 1,238 m (4,062.8 ft).

facility for peak demand delivery in the Chicago metropolitan area. Most of this natural gas is stored in the Upper Cambrian Mt. Simon Sandstone (fig. 36), but additional storage occurs in the Cambrian Galesville Sandstone and Elmhurst Sandstone Member of the Eau Claire Formation (Benesh et al. 1956).

The goal of this project was to improve the efficiency of injecting and withdrawing natural gas from the Mt. Simon Sandstone by developing an improved reservoir characterization model for the reservoir. The reservoir characterization project presented a petrophysical problem because there were almost no modern wireline logs (such as the FDC-CNL) through the Mt. Simon and Elmhurst intervals. The only porosity logs were neutron logs that, in many of the wells, were logged after gas storage had begun. These neutron logs consistently measured lower porosity than the actual porosity because of the "gas effect." Petrophysical methodology was developed to circumvent this difficulty, and the method can be used to measure variations in reservoir porosity in other Mt. Simon gas storage reservoirs in Illinois with similar circumstances.

Stratigraphy In the Herscher area, the Mt. Simon is over 762 m (2,500 ft) thick (Buschbach 1975, p. 40). It is composed of fine- to coarse-grained sandstone with localized conglomerates and thin beds of shale and siltstone (Willman et al. 1975). The contact with the overlying Eau Claire Formation is conformable.

The Eau Claire Formation is composed of alternating layers of dolomite, limestone, sandstone, shale, and siltstone. At Herscher Field, the middle of the Eau Claire Formation consists predominantly of shale beds that form an effective seal preventing gas from migrating from the Mt. Simon into the overlying formations, such as the overlying aquifers of the Galesville or St. Peter Sandstones. The basal member of the Eau Claire Formation, the Elmhurst Sandstone, shown on the Herscher Field type log (fig. 36), is also used for gas storage in Herscher NW Field. The Elmhurst Sandstone is less than 30 m (100 ft) thick in the Herscher area and appears to gradationally overlie the Mt. Simon Sandstone, which is the main gas reservoir.

The Eau Claire is conformably overlain by clean, porous, unfossiliferous Galesville Sandstone (Buschbach 1964). The Galesville is used for gas storage at

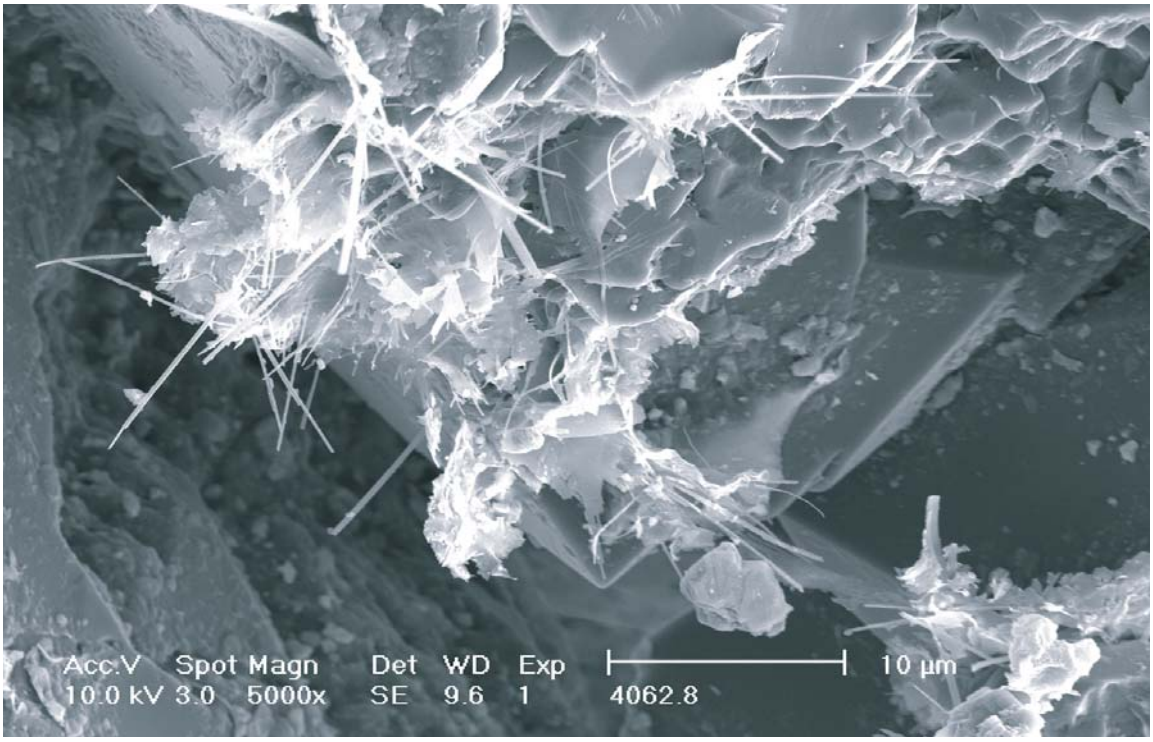

Figure 25 A scanning electron microscopic image of diagenetic clay minerals in Mt. Simon reservoir sandstone. Clay minerals are sparse in the Manlove reservoir sandstones. Very isolated patches of diagenetic illite can be seen coating some quartz overgrowths. This image is from a small area just below the center of figure 24.

Herscher, but, as discussed later, this reservoir does not appear to have an adequate seal separating it from shallower freshwater aquifers.

History of the Field In the early 1900s, the Herscher structure produced oil from the Galena Group ("Trenton limestone") (Bell and Cohee 1939). This early Illinois oil field produced from nine individual wells at an average completion depth of 43 m (140 ft). The best well produced one-half barrel of oil per day and approximately 896 m^3 (32,000 ft^3) of gas per day. The Herscher oil field was uneconomical and was abandoned within a few years.

The first mapping of the Herscher structure was based on the St. Peter Sandstone (Athy 1928). In 1952, the Natural Gas Storage Company of Illinois undertook extensive drilling of more than 100 wells to the Galena Group to further map the structural relief and areal extent of the Herscher anticlines (Buschbach and Bond 1974). After these structure test wells were drilled, the company drilled four additional test wells to the Galesville Sandstone. In April 1953, the company began injecting gas into the Galesville Sandstone for gas storage. However, within 4 months after injection commenced, 33 shallow water wells directly above the Herscher structure began to bubble gas (Benesh et al. 1956). Gas injection into the Galesville Sandstone was immediately stopped. Although the source of the leak was never resolved, Buschbach and Bond (1974) and Benesh et al. (1956) attributed the problem to (1) a possible hole in casing, (2) a possible fault, or (3) a poor seal. It is our interpretation that the lack of an adequate seal above the Galesville was the most probable cause for the leak since there are other fields with similar leaks from these Cambrian sandstone reservoirs (Buschbach and Bond 1974).

In 1956, Natural Gas Pipeline Company of America recommenced injection of gas into the Galesville reservoir, taking some measures to control the gas. They kept the reservoir pressure of the Galesville constant by withdrawing water from the periphery of the gas bubble and re-injecting it into the overlying Potosi Dolomite. They also recycled gas from vent wells in the overlying Galena Limestone and St. Peter Sandstone back into the Galesville. In 1972, the annual withdrawal from the Galesville was over 742 million cubic meters (21 BCF). The base gas volume was more than 1,300 million cubic meters (38 BCF) at the end of the withdrawal season (Buschbach and Bond 1974). These practices are still in use today.

In 1957, after testing showed the Eau Claire Formation to be a good seal, the operator began storing natural gas into the underlying Mt. Simon Sandstone on the Herscher Anticline. Through the early 1960s, the Natural Gas Pipeline Company drilled additional Mt. Simon wells and simultaneously continued gas injection into the Mt. Simon

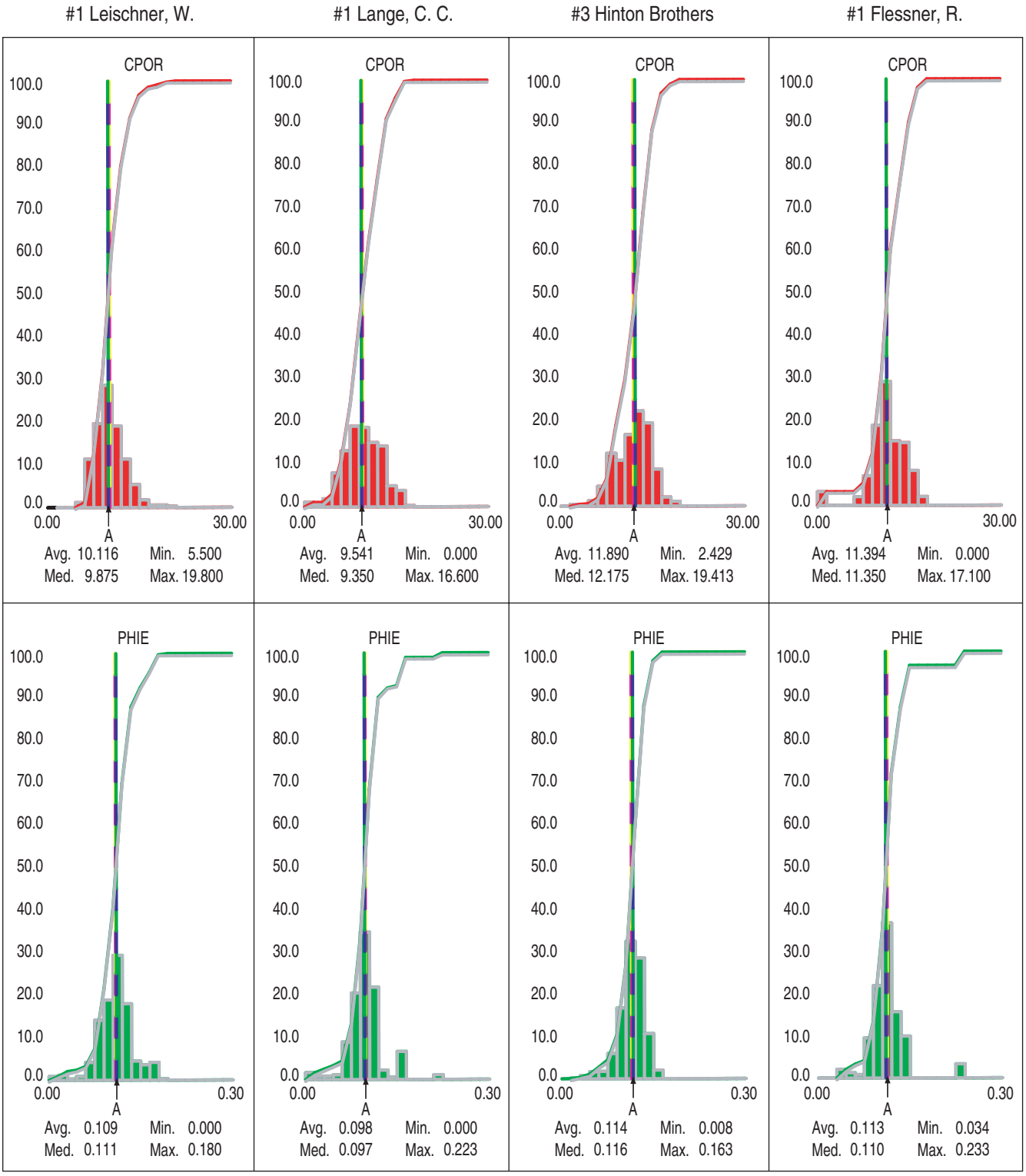

Figure 26 Core and calculated log-derived porosity histograms for selected Manlove Field wells. Mean (dashed vertical line) and distribution of cored porosity (CPOR; red) and density-neutron porosity (PHIE; green) agree well.

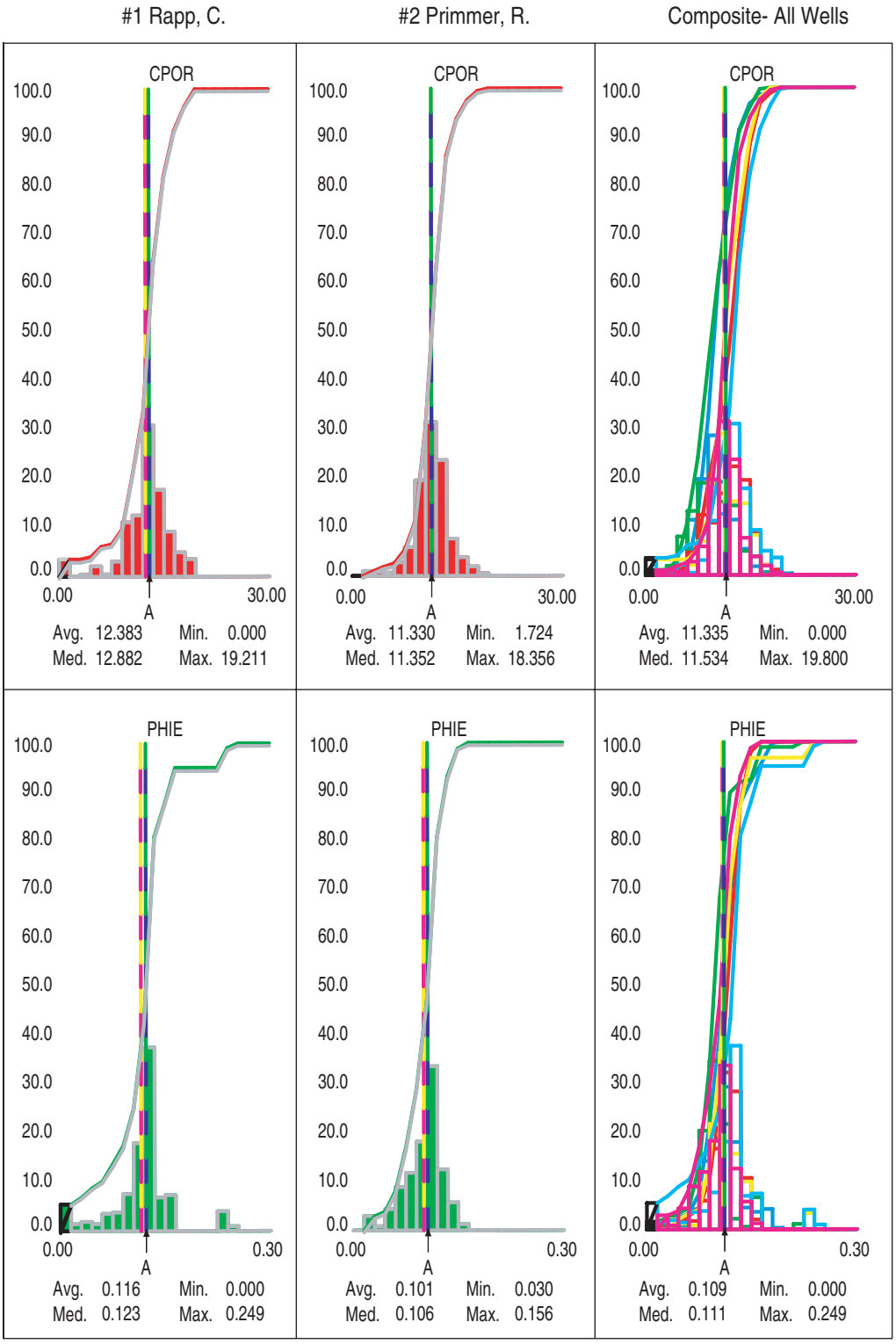
#1 Rapp, C.
#2 Primmer, R.
Composite- All Wells
CPOR
100.0
90.0
80.0
70.0
60.0
50.0
40.0
30.0
20.0
10.0
0.0
0.00
30.00
A
Avg. 12.383 Min. 0.000
Med. 12.882 Max. 19.211
Avg. 11.330 Min. 1.724
Med. 11.352 Max. 18.356
Avg. 11.335 Min. 0.000
Med. 11.534 Max. 19.800
PHIE
0.30
Avg. 0.116 Min. 0.000
Med. 0.123 Max. 0.249
Avg. 0.101 Min. 0.030
Med. 0.106 Max. 0.156
Avg. 0.109 Min. 0.000
Med. 0.111 Max. 0.249

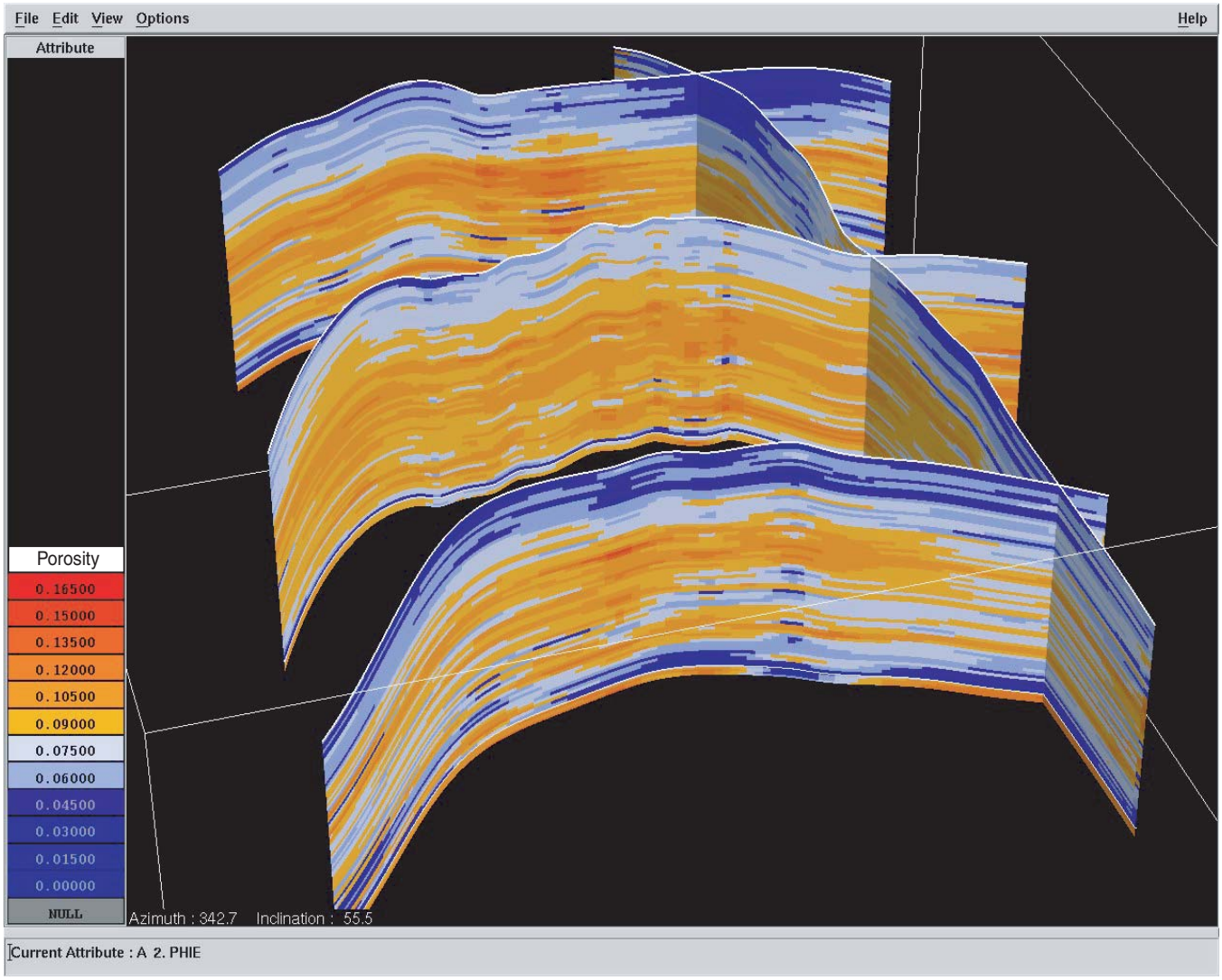

Figure 27 Three-dimensional structural fence diagram of the porosity model for Manlove Field. View is toward the north-northeast and shows the steep west flank and gentle east flank of the doubly plunging anticlinal trap. The spill point lies in the northeastern part of the field.

reservoir. This reservoir provides a second, important storage unit for the field. In 1972, the annual withdrawal from the Mt. Simon was 482 million cubic meters (13.7 BCF). The base gas volume was more than 1,960 million cubic meters (53 BCF) at the end of the withdrawal season (Buschbach and Bond 1974).

In 1959, the Herscher NW gas storage project, located 4 mi northwest of Herscher Field, was begun with the drilling of 32 shallow Galena structure tests. The Herscher NW project is currently inactive because of economic reasons.

The structural closure in the Mt. Simon of 18 m (58 ft) (Buschbach and Bond 1974) and the area under the closure were not as large as the nearby Herscher Anticline located to the south.

Structure Herscher Field and Herscher NW Field are located on an anticlinal feature approximately 24 km (15 mi) long and 3.2 km (2 mi) wide that is parallel to and 48 km (30 mi) northeast of the La Salle Anticlinorium (fig. 37). The fields are on the southwest flank of the Kankakee Arch, a broad northwest-oriented feature separating the Illinois and Michigan basins.

The best marker for structural control in the Herscher area is the top of the Ordovician age Galena Group ("Trenton limestone"), which is a good correlation marker and has 199 wells drilled through it. The Mt. Simon horizon has only 103 well penetrations for structural control. All of the formations from the Galena to the Mt. Simon are assumed to be structurally conformable to the Galena and, therefore, have a similar structural configuration.

The Galena structure map shows two distinct, northwest-aligned anticlinal closures separated by a saddle (fig.

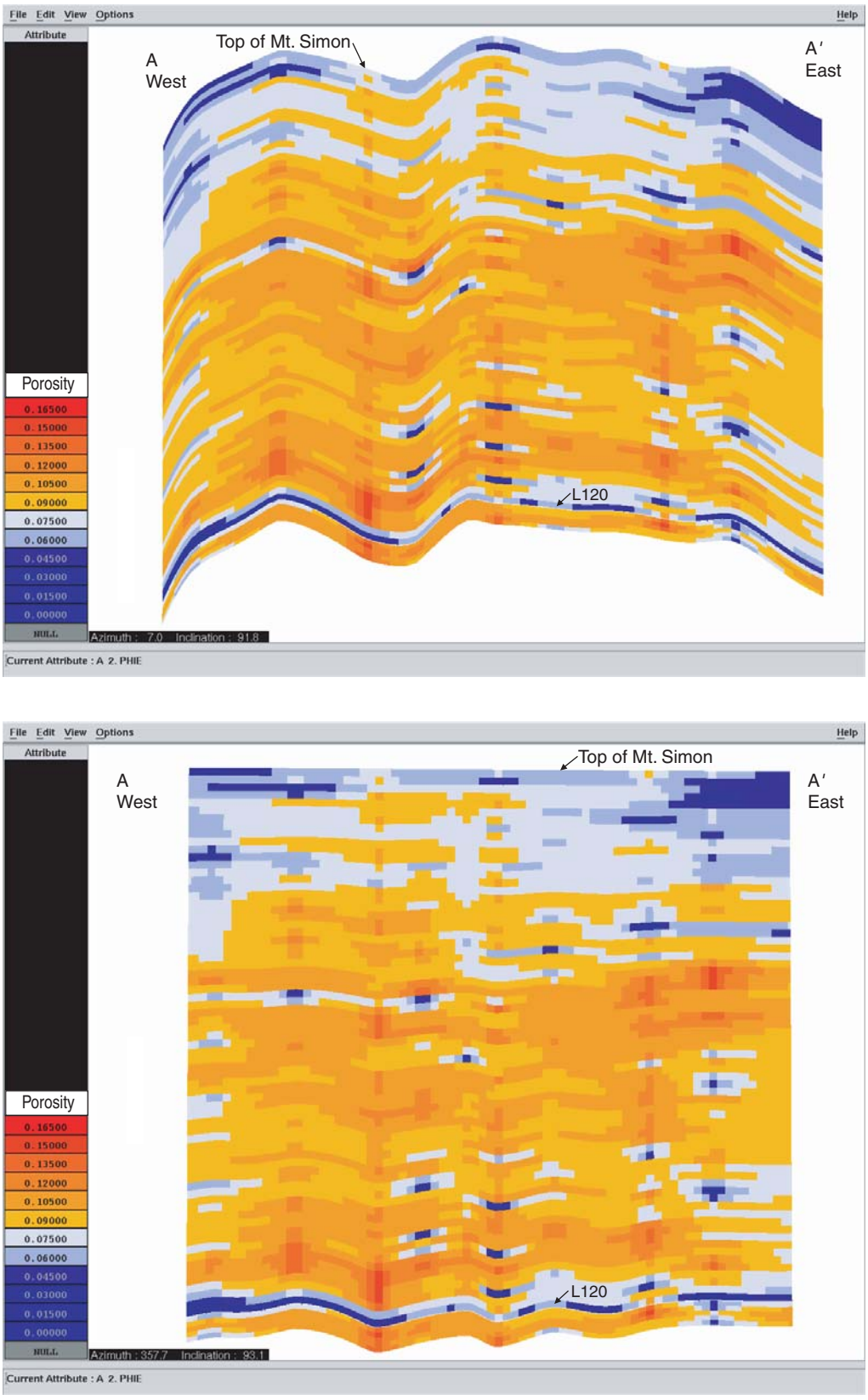

Figure 28 West-east (A–A′) structural (upper) and stratigraphic (lower) cross sections of the porosity model at Manlove Field. See figure 9 for location.

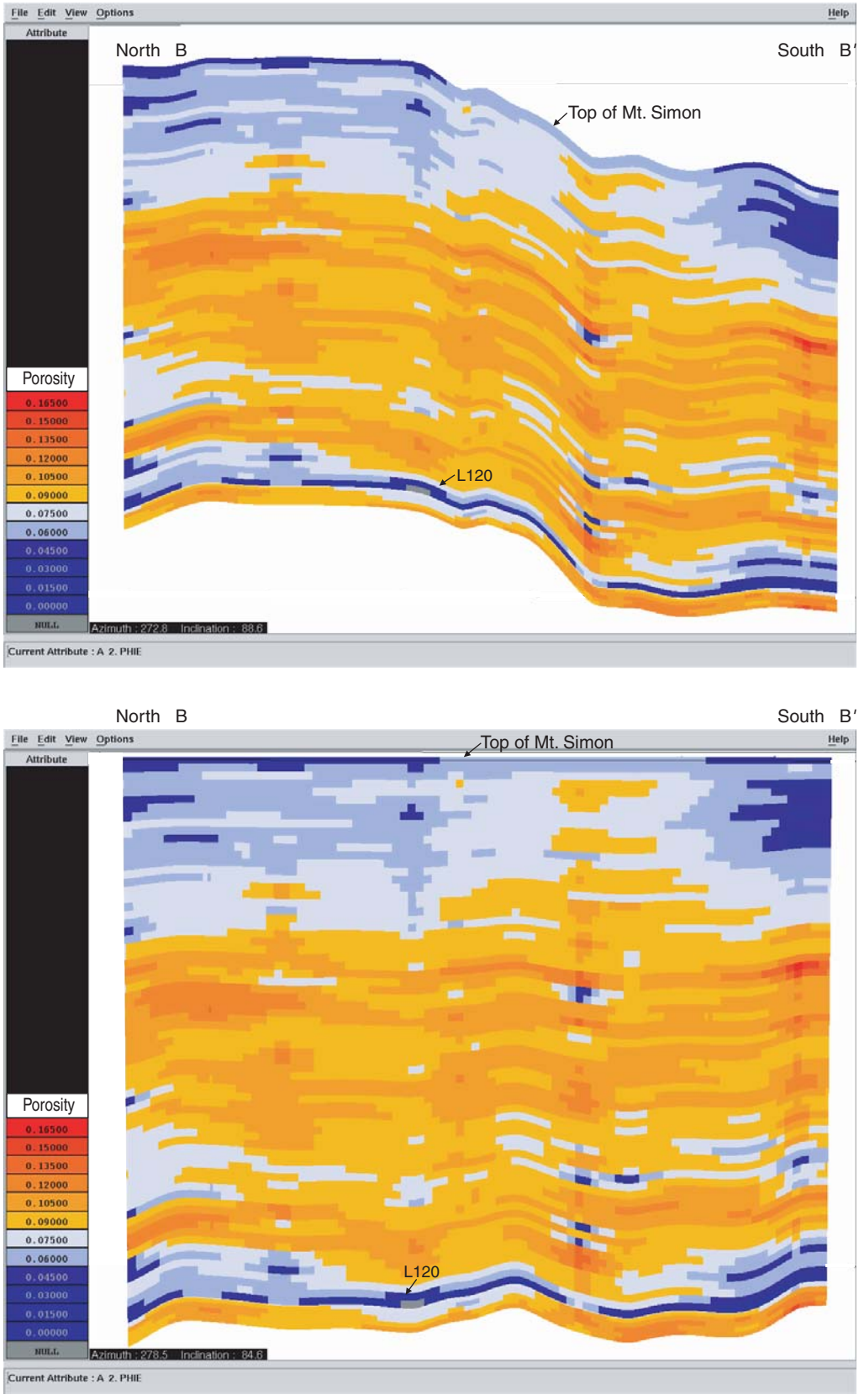

Figure 29 North-south (B–B′) structural (upper) and stratigraphic (lower) cross sections of the porosity model at Manlove Field. See figure 9 for location.

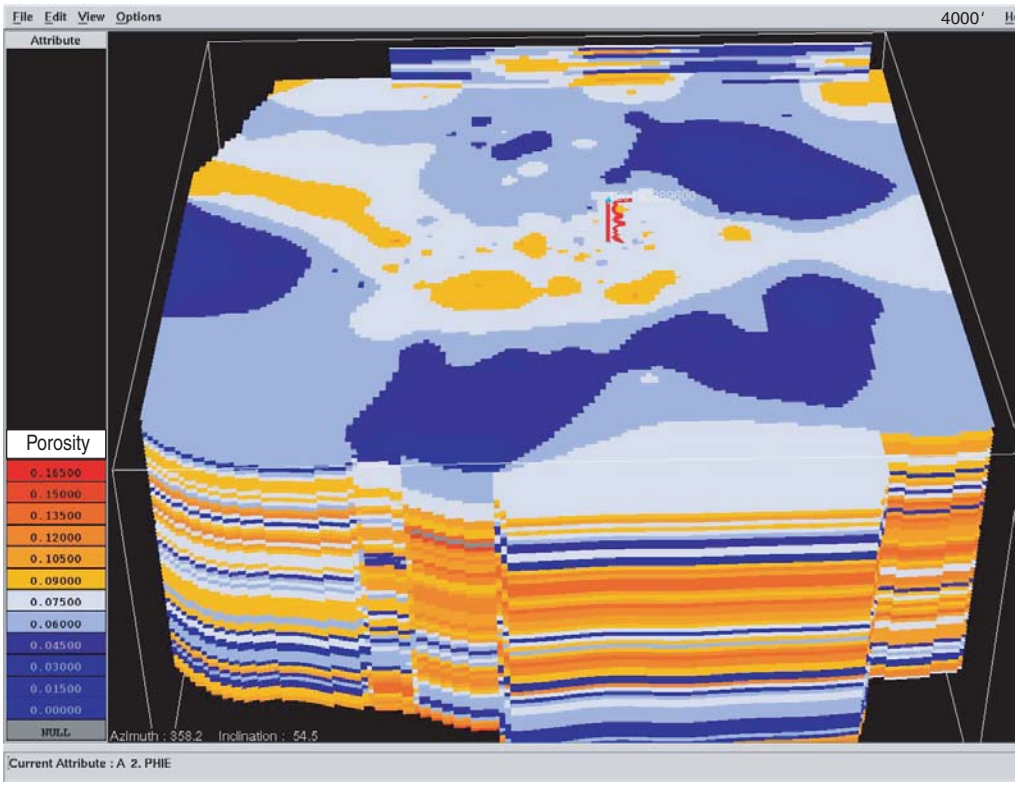

Figure 30 Horizontal slice map of Manlove Field porosity model, 1,220 m (4,000 ft). A high-porosity channel sand crosses the crest of the field. In the J. Williams #4 well core, this sandstone contains abundant *Skolithos* burrows, a few thin shale intraclasts and is medium- to coarse-grained. Lateral to this illustrated reference well, the facies have low porosity and are interpreted to be lagoonal or intertidal mud flats. The interval lies above the gas storage reservoir. View is toward the north.

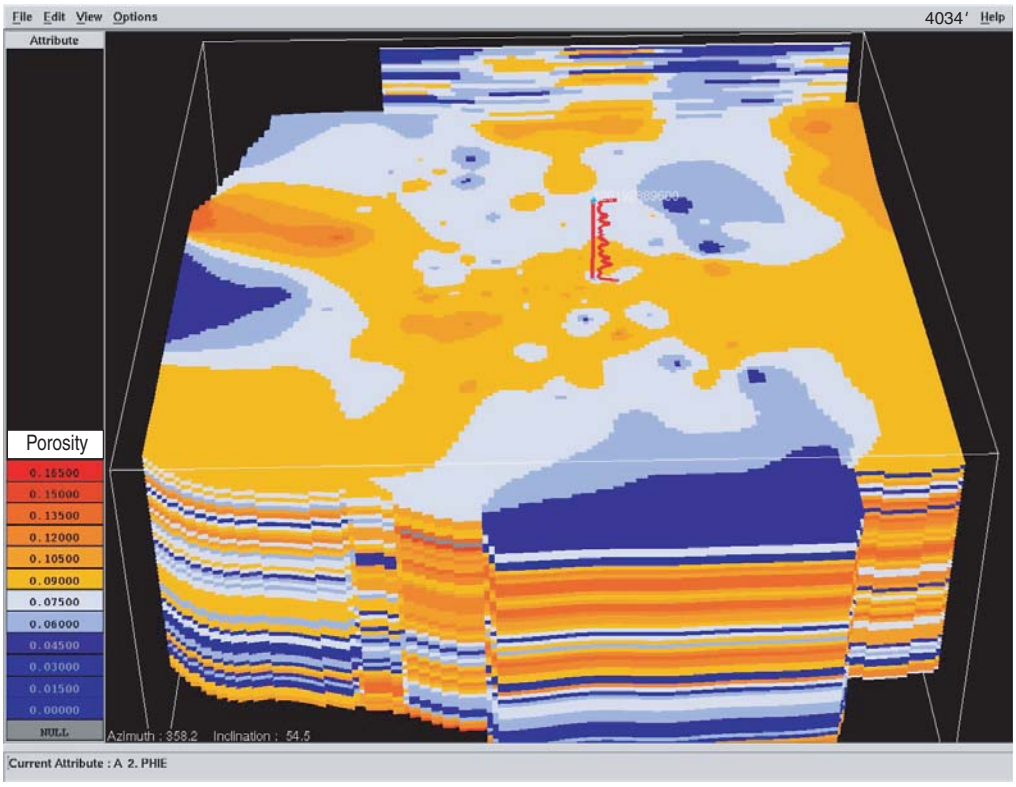

Figure 31 Horizontal slice map of Manlove Field porosity model, 1,230 m (4,034 ft). A bifurcating, high-porosity zone interpreted as a west-to-east–flowing channel system, crosses the center of the field. Core in the J. Williams #4 reference well at this depth contains coarse- to very coarse-grained, porous sandstone with thin cross-bed sets and local *Skolithos* burrows. To the north and south of this well lie lower porosity facies. The compensated density-neutron log indicates that this sand lies just above a thin shale and the main gas reservoir. View is toward the north.

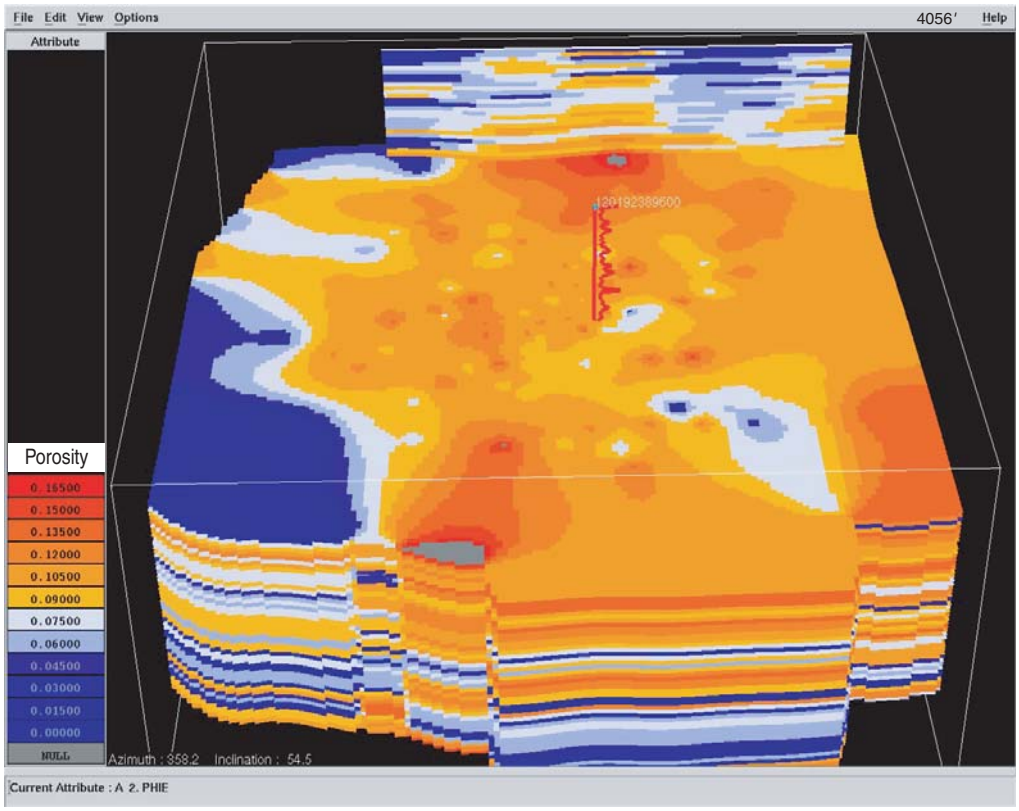

Figure 32 Horizontal slice map of Manlove Field porosity model at 1,237 m (4,056 ft). A widespread, porous sandstone occurs in this upper gas storage interval. The sandstone is cross-bedded and coarse- to very coarse-grained. Just to the west of the reference well log is an area with excellent porosity that trends north-south and is interpreted as a barrier island deposit. Further to the west are two narrow, high-porosity areas that are oriented perpendicular to the barrier and interpreted as tidal channel deposits. View is toward the north.

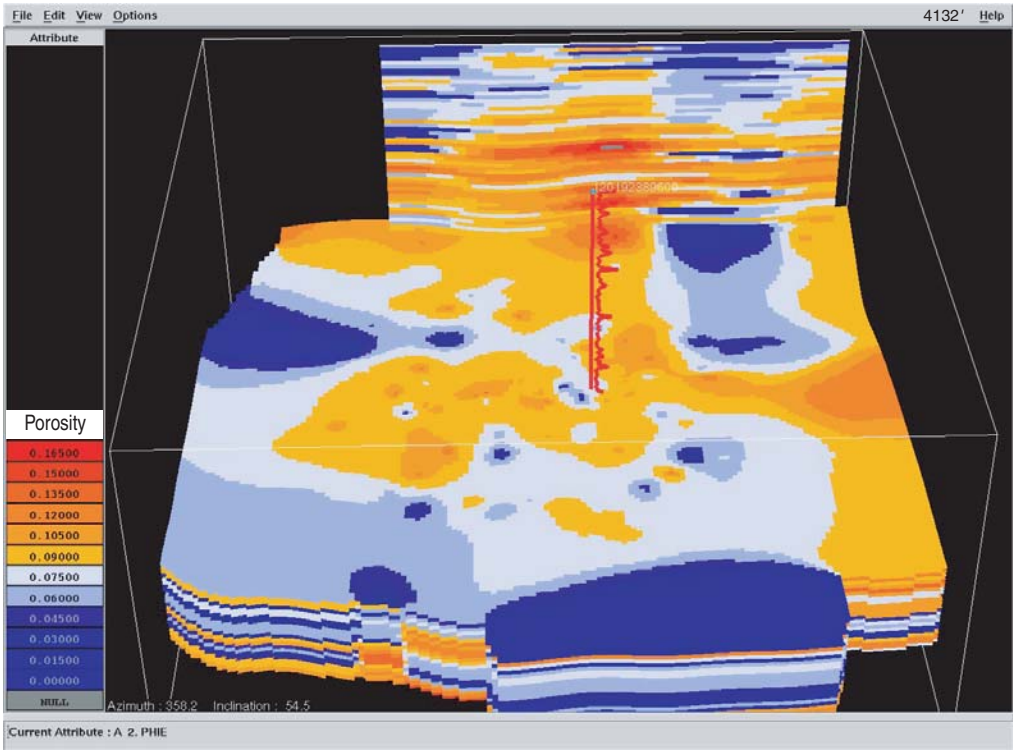

Figure 33 Horizontal slice map of Manlove Field porosity model, 1,260 m (4,132 ft). An east-to-west–oriented, sinuous, high porosity sand body crosses the center of the field just to the south of the reference well and is interpreted to be a tidal channel deposit. This sand body is joined by a channel or remnant barrier island sand from the north. To the east another barrier island may exist. The lithology in this interval in the reference well consists of coarse- to very coarse-grained sandstone that is cross-bedded. View is toward the north.

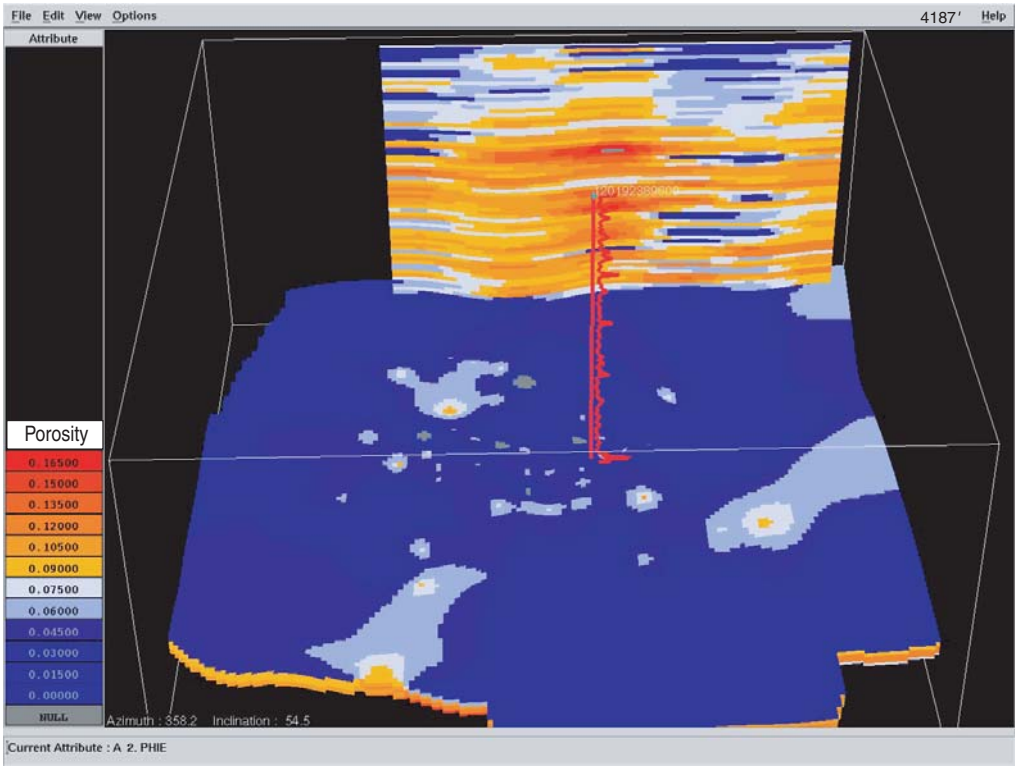

Figure 34 Horizontal slice map of Manlove Field porosity model, 1,277 m (4,187 ft), which occurs at the L120 marker level and shows the continuity of this shale and interbedded shale and fine sandstone, low-porosity interval. Sand-filled *Planolites* burrows are common in core of this interval in the reference well. Deposition was likely in a back-barrier, tidally influenced lagoon or intertidal mud flat. View is toward the north.

38). The southern closure—or Herscher Anticline—has 46 m (150 ft) of structural relief at the top of the Galena Limestone. The Herscher structure is 8 km (5 mi) long and 6.4 km (4 mi) wide at its widest point. There are 4,400 acres of structural closure under the active part of the gas storage project. The entire Herscher structure extends over an area of 17,000 acres. The western flank dips steeply, whereas the eastern flank of the structure dips gently.

The northern—or Herscher Northwest Anticline—is more circular than the elongate Herscher. The Herscher NW structure has slightly more than 15 m (50 ft) of structural closure on the Galena horizon. Similar to the southern lobe, The Herscher Northwest structure has a steeply dipping western flank and a gently dipping eastern flank. The structural closure on the Galena extends for approximately 3,000 acres and has a diameter of 3.2 km (2 mi).

An isopach of the interval from the Eau Claire correlation point (a good marker on wireline logs) to the top of the Galena (fig. 39) shows this interval to be 61 m (200 ft) thicker at Herscher than at Herscher NW. The large variation may be due to different structural histories. Because of the 61 m (200 ft) of thickening of this interval, the top of the Mt. Simon at the Herscher structure is 30 m (100 ft) lower than at Herscher Northwest (figs. 40 and 41), which is a reversal of the structural elevations of the top of the Galena Group. There is 23 m (75 ft) of Mt. Simon structural closure at the Herscher structure, but less than 15 m (50 ft) of Mt. Simon closure at the Herscher Northwest structure.

Petrology The porous part of the Mt. Simon is composed of a medium- to coarse-grained quartz arenite. The quartz grains are cemented with silica; calcite cement has not been observed. The less porous sandstone was fine-grained, silica-cemented, and contained 5% to 10% feldspar.

Based on commercial core analyses from 5 wells, the Mt. Simon Sandstone has an average horizontal permeability (to air) of 70 mD. Eighty percent of the core permeability values fell between 12 mD and 350 mD (fig. 42). The median porosity was 14% and 80% of the measurements fell between 10% and 17% (fig. 43).

Petrophysics A major goal of this research project was to create an accurate porosity model of the reservoir sandstone that could be used both in volumetric analysis and in reservoir simulations. However, this goal was constrained by the fact that the predominant wireline log suite included only the gamma-ray log and an older style neutron log. The older neutron logs were commonly calibrated in counts per second and had to be converted into porosity units. Almost all of the wells were drilled and logged in the late 1950s and early 1960s; therefore, no modern wireline logs measuring porosity were available in the Mt. Simon interval from the field.

A more serious problem was related to the history of the reservoir as a gas storage target. The first wells were drilled in 1957, and almost simultaneously gas injection was started into the Mt. Simon reservoir. The result of

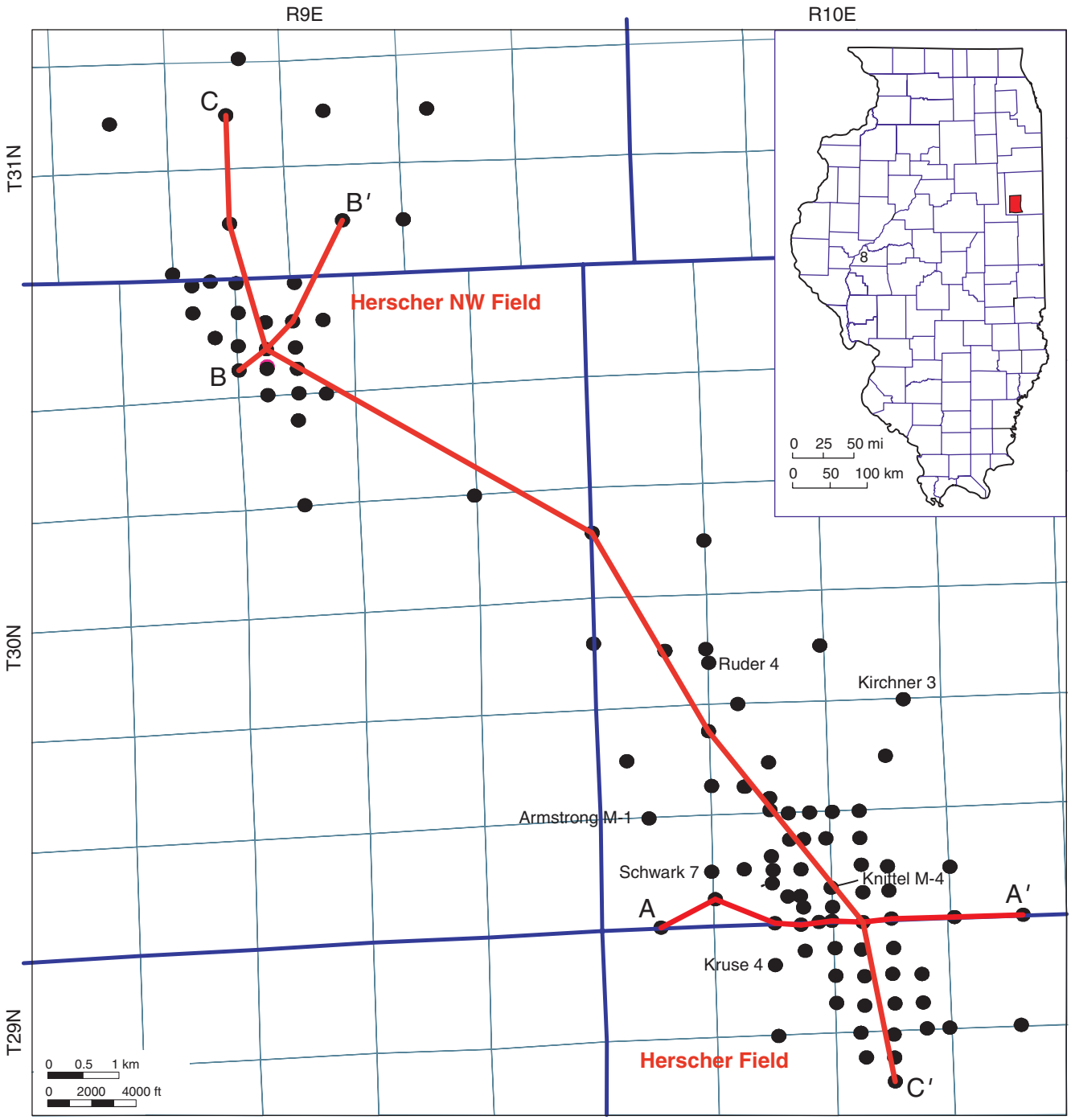

Figure 35 Base map of Herscher and Herscher NW Fields. Geologic cross sections and wells referenced in this report are shown. The insert map shows the location of the Herscher project.

this early gas injection was that the neutron logs were of negligible value in estimating porosity because the neutron tool is strongly affected by natural gas in the reservoir. Calculated porosity in reservoirs filled either with water or with oil accurately measures actual porosity because these fluids have approximately the same density as hydrogen. However, because natural gas has a much lower hydrogen density, calculated neutron porosity values for a gas-filled reservoir are significantly less than the actual porosity. This effect is called the "gas effect."

An alternative method for calculating porosity in Herscher Field was developed using the gamma-ray log. Basic

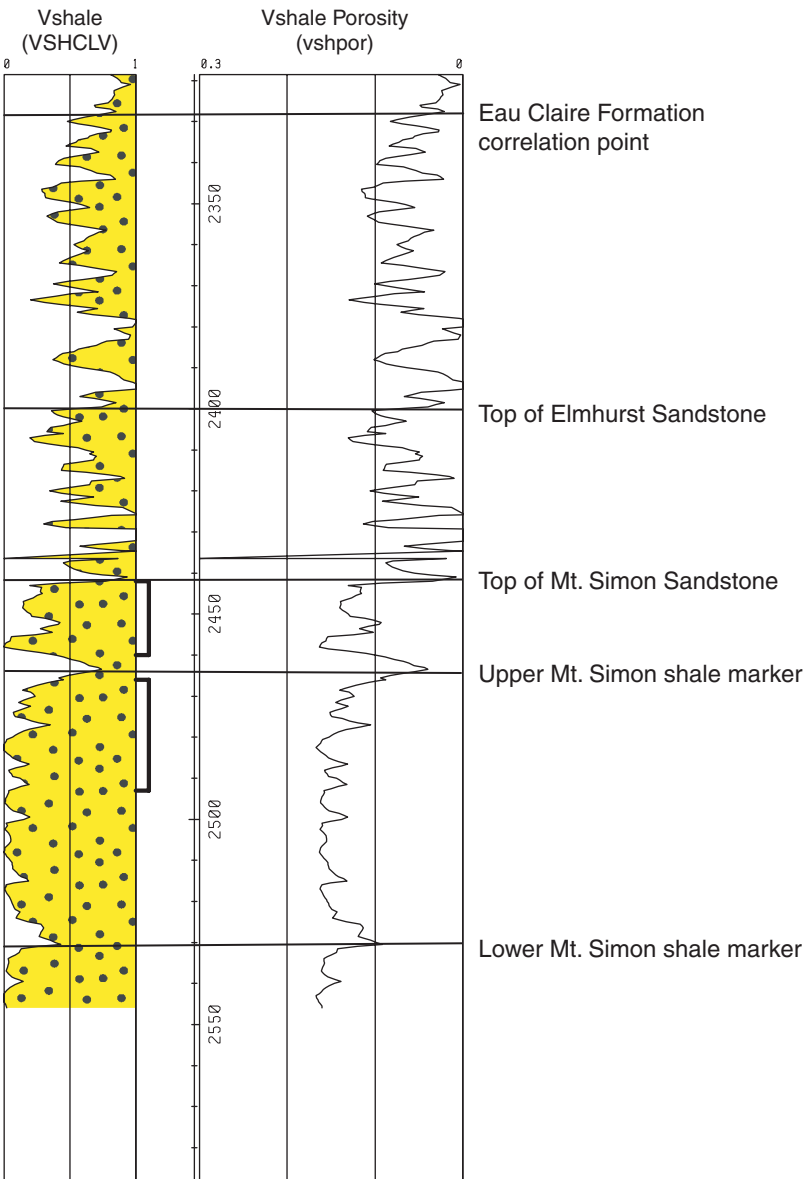

Figure 36 The type log for the Herscher Field showing the important reservoir sandstones used for gas storage. Gas is injected into both the Elmhurst and Mt. Simon Sandstone in the field, but in this well, the Knittel No. 4, only the Mt. Simon Sandstone is an injection target. Brackets indicate perforation intervals. Vshale, shale volume.

gamma-ray logs cannot be directly compared from well to well in the field because of varying well bore conditions and incorrect calibrations. Normalization of these logs can correct this problem. Gamma-ray log values from well to well were converted to Vshale values using the Clavier equation (Clavier et al. 1977). This normalization technique scales the gamma-ray value from 0% in pure sandstone to 100% in a pure shale and allows well-to-well comparison. The Clavier equation [Eq. 3] is recommended for use in older strata. The linear gamma-ray Vshale equation [Eq. 2] is better in Tertiary age strata (Clavier et al. 1977).

Neutron porosity values were calculated for all of the wells using standard methods described earlier [Eq. 1] for the older types of neutron logs (Brown and Bowers 1957, Swulius 1986, Dull 1991). Similar to calculations for Manlove Field, in the neutron porosity calculation [Eq. 1–4], shale porosity is assumed to be 30%, and average porosity in a clean sandstone (small amounts of clay minerals) is estimated from core analyses to be 14%. A shale correction to neutron porosity was made using the Vshale value from the Clavier equation [Eq. 4], resulting in the neutron log-based porosity for the off-structure wells.

Vshale porosity transform:

$$PHIVSH = 0.167VSHCLV + 0.164. \quad [5]$$

Porosity calculated from the Vshale (PHIVSH) compares well to neutron porosity and core porosity in off-structure wells located outside the gas storage zone. The transformation equation [Eq. 5] was then applied to the remaining logs in the two Herscher fields (fig. 44). One limitation to this method is that the porosity appears to be slightly underestimated using the Vshale value. As illustrated in a comparative histogram (fig. 45), the Vshale values reach a maximum and then abruptly stop. They lack the bell-shaped, "normal" distribution of both the neutron log-derived values and the core values. However, the mean core values and the mean Vshale-transformed porosity values in the same interval differ by less than one porosity unit. Comparison of Vshale-derived porosity with neutron porosity is discussed next.

The Knittel #4 well, for example, was drilled through the gas bubble in Herscher Field (fig. 46). In this well, the Vshale porosity minus neutron porosity values are positive (yellow fill "gas effect" is noted) and differ by at least 5%. These intervals occur over much of the Mt. Simon storage reservoir interval above the lower shale marker (fig. 46). These gas-affected values and the unaffected values can be readily differentiated on the cross plot of neutron porosity and Vshale porosity.

In contrast, the neutron porosity and the Vshale-derived porosity in the Armstrong #1, an off-structure Herscher Field well with no gas, show close agreement (fig. 47). Yellow fill, indicating "gas effect" separation between the Vshale porosity and the lower neutron porosity values, is minimal.

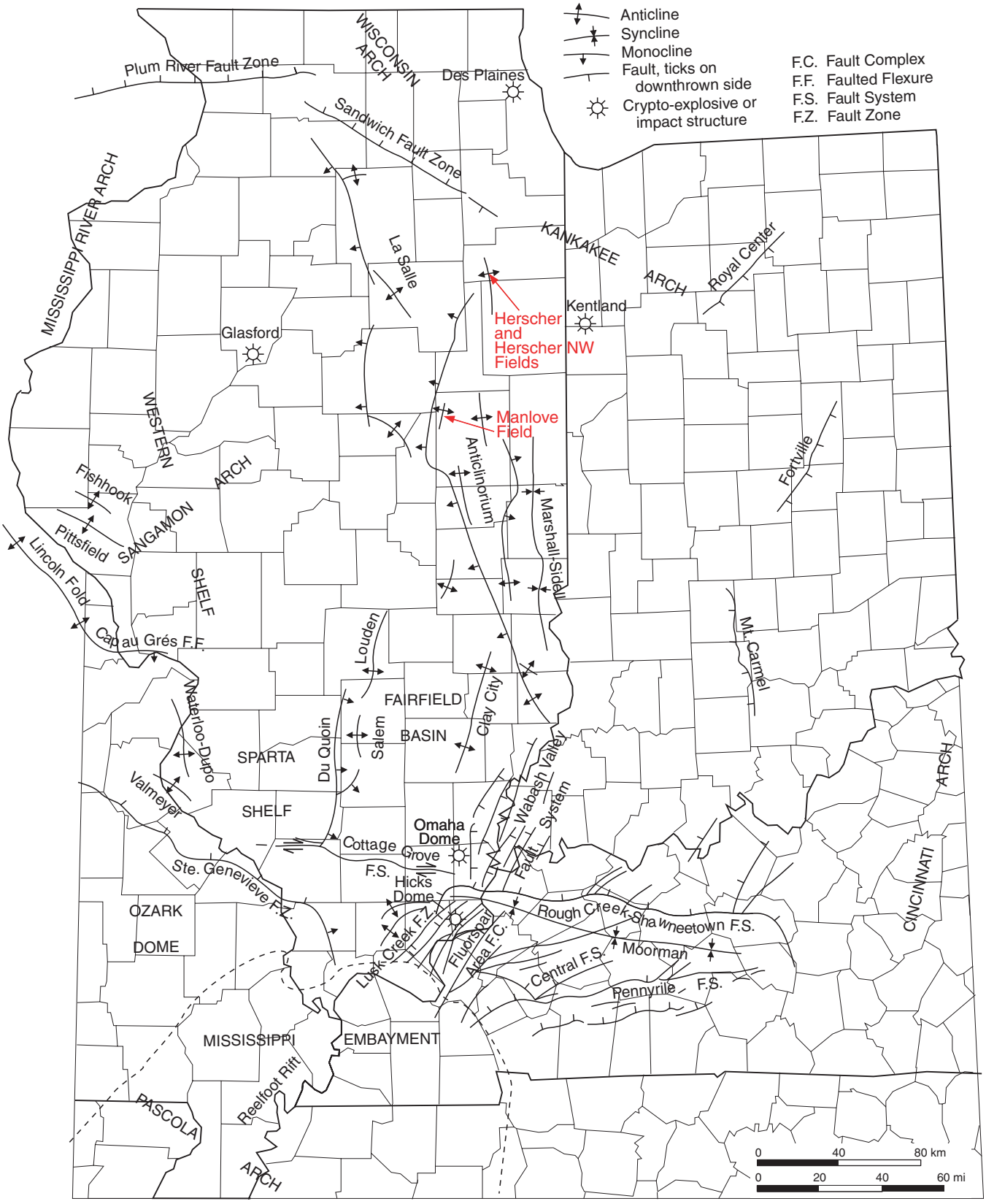

Figure 37 Regional structural features in the Illinois Basin showing the location of Herscher and Herscher NW gas storage fields (modified from Nelson 1995).

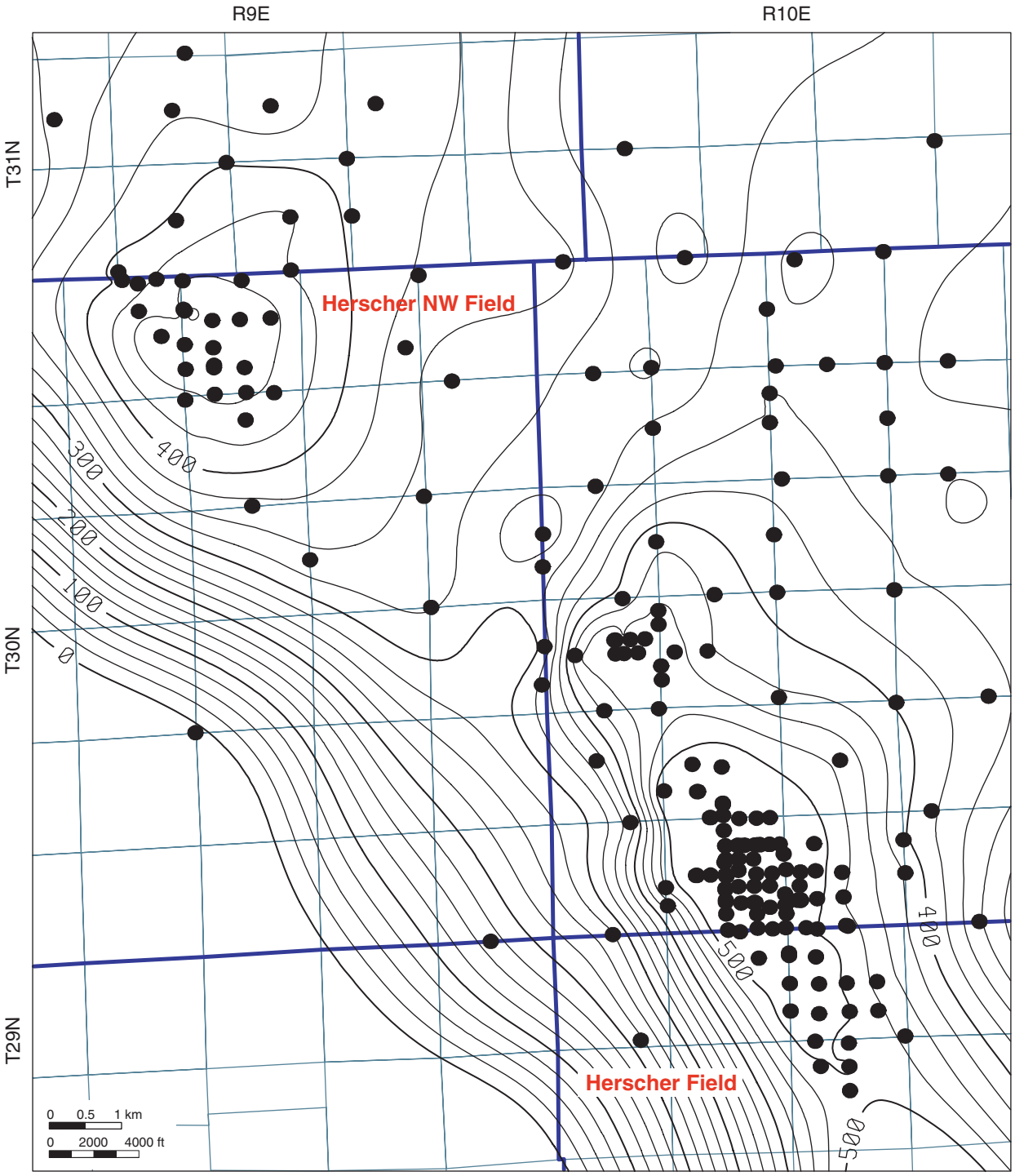

Figure 38 Structure on top of the Galena Group at Herscher and Herscher NW Fields. The well locations shown all have Galena Group surface elevation data and were used in the mapping. Contour interval is 25 ft (7.6 m).

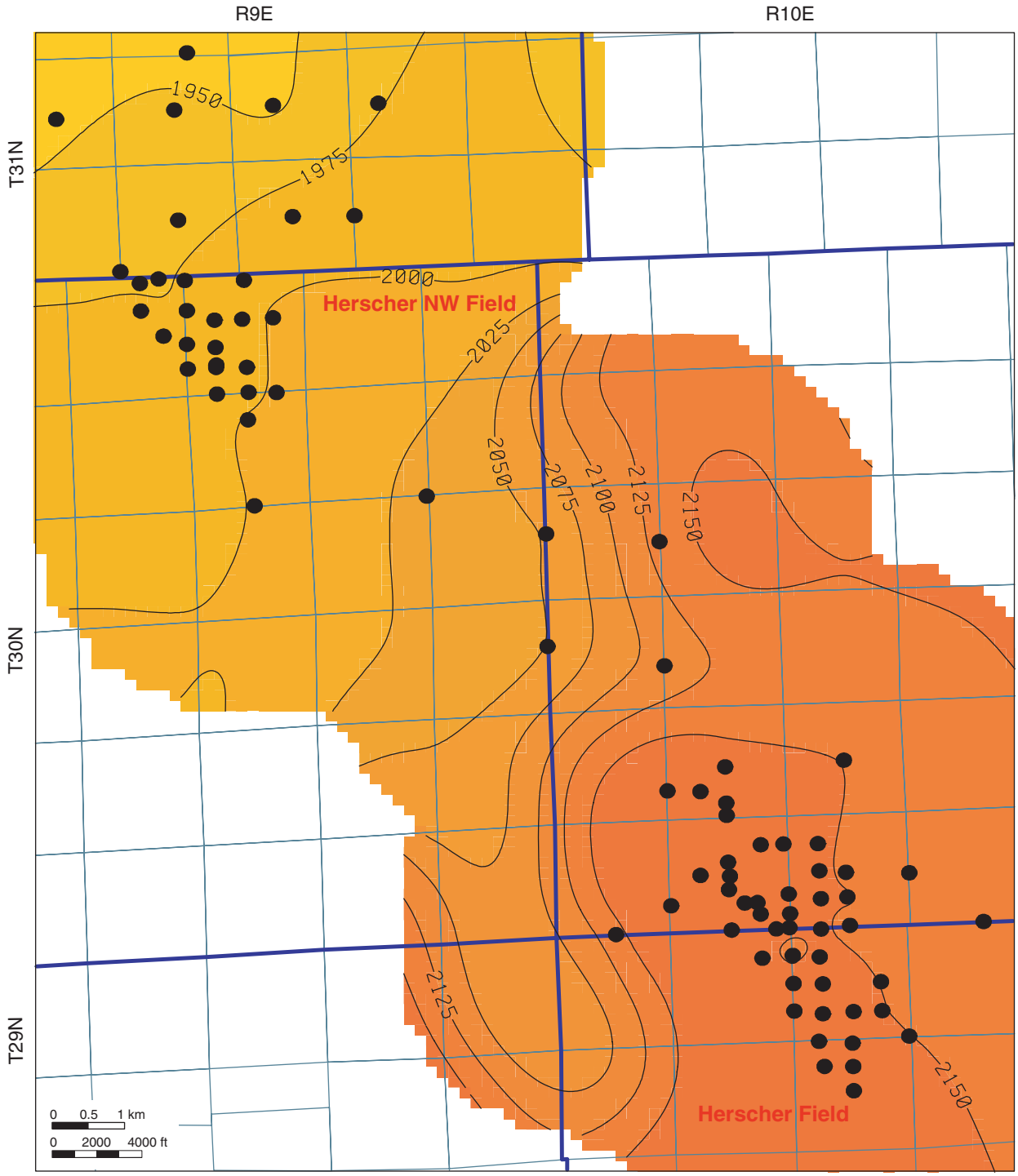

Figure 39 Isopach of the interval between the top of the Galena Group and the Eau Claire Formation correlation point. Only wells with penetration through the entire interval are shown. Contour interval is 25 ft (7.6 m).

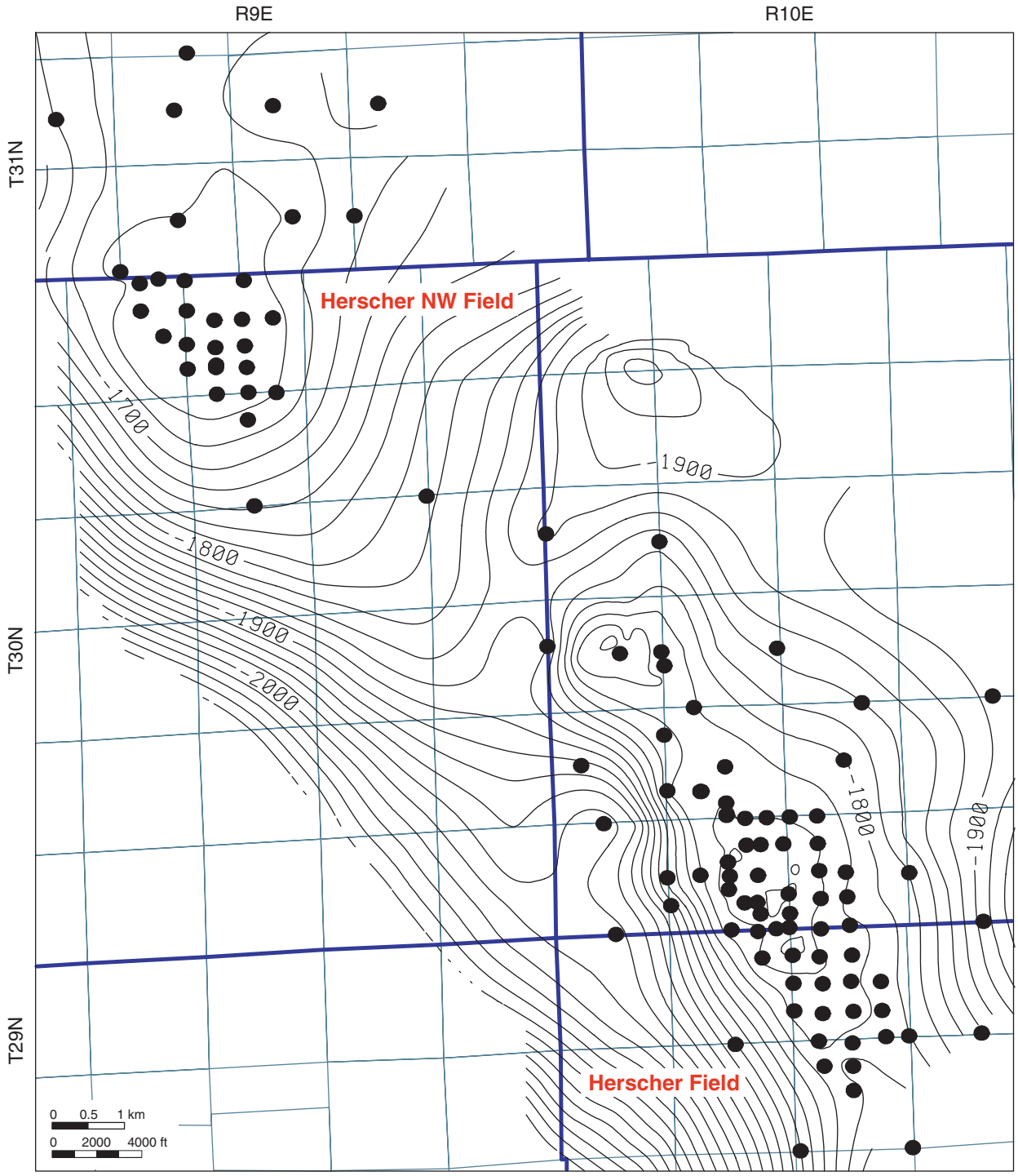

Figure 40 Structure on the top of the Mt. Simon Sandstone at Herscher and Herscher NW Fields. Only wells that penetrated the Mt. Simon surface are shown in this figure. Contour interval is 20 ft (6.1 m).

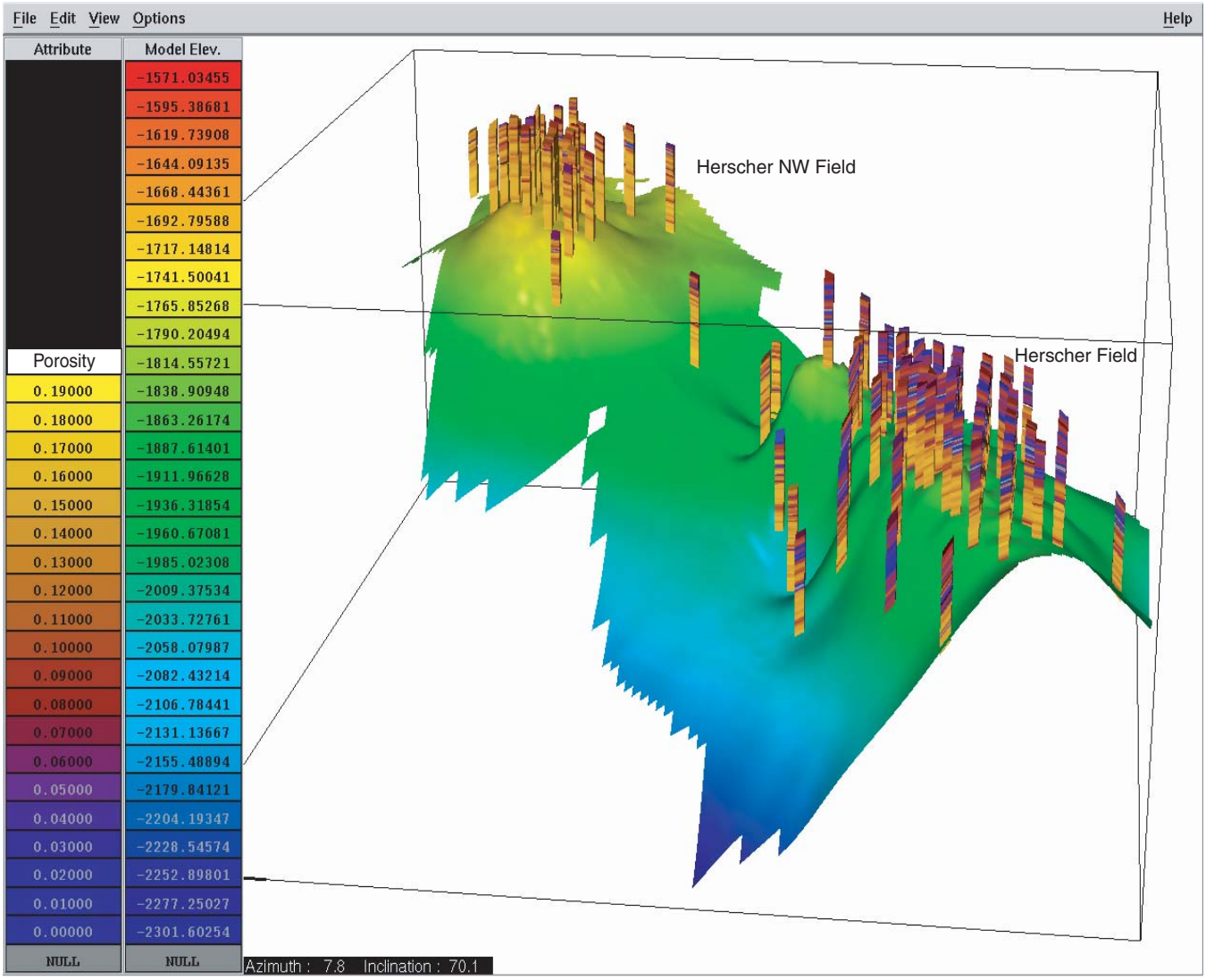

Figure 41 Three-dimensional view of Herscher and Herscher NW Fields illustrating the well control at the reservoir horizon and the configuration of the lower Mt. Simon shale correlation marker. The Mt. Simon reservoir sandstone at Herscher NW Field is structurally about 30 m (100 ft) higher than at Herscher Field. View is toward the north-northeast.

Reservoir Characterization The west-to-east stratigraphic cross section A–A′ of Herscher Field (fig. 48) shows the Mt. Simon to be composed of thick, multiple, stacked sandstone beds. Thin shale beds other than the indicated correlation markers cannot be readily correlated across the field. Thus, the shales appear to form local baffles rather than compartment barriers. A west-to-east stratigraphic cross section of Herscher NW Field (B–B′; fig. 49) shows the reservoir-quality Elmhurst Sandstone bodies to be only 0.6 to 2.4 m (2 to 8 ft) thick and separated by thin shales.

The northwest-to-southeast stratigraphic cross section C–C′ (fig. 50), located approximately along the axes of Herscher NW and Herscher Fields, shows subtle indentations in the gamma-ray log, suggesting that the thick reservoir sandstone beds are composed of stacked, thinner sandstone units. Other than the two shales indicated on these cross sections, marker beds within the upper Mt. Simon cannot be traced across the two anticlines. The Elmhurst Sandstone Member, which contains reservoir sandstone beds in the Herscher NW Field, does not contain significant amounts of sandstone at Herscher Field (fig. 51).

The 3-D models were created by using surface grids of the elevation of the top of Elmhurst Sandstone Member of the Eau Claire Formation, the top of the Mt. Simon Sandstone, and the Mt. Simon shale marker bed. These surface grids were generated with a 152-m (500-ft) grid interval by conformably mapping downward from the top of Galena Group surface. The vertical interval between grid layers is proportional in thickness and is directly related to the isopach interval between the

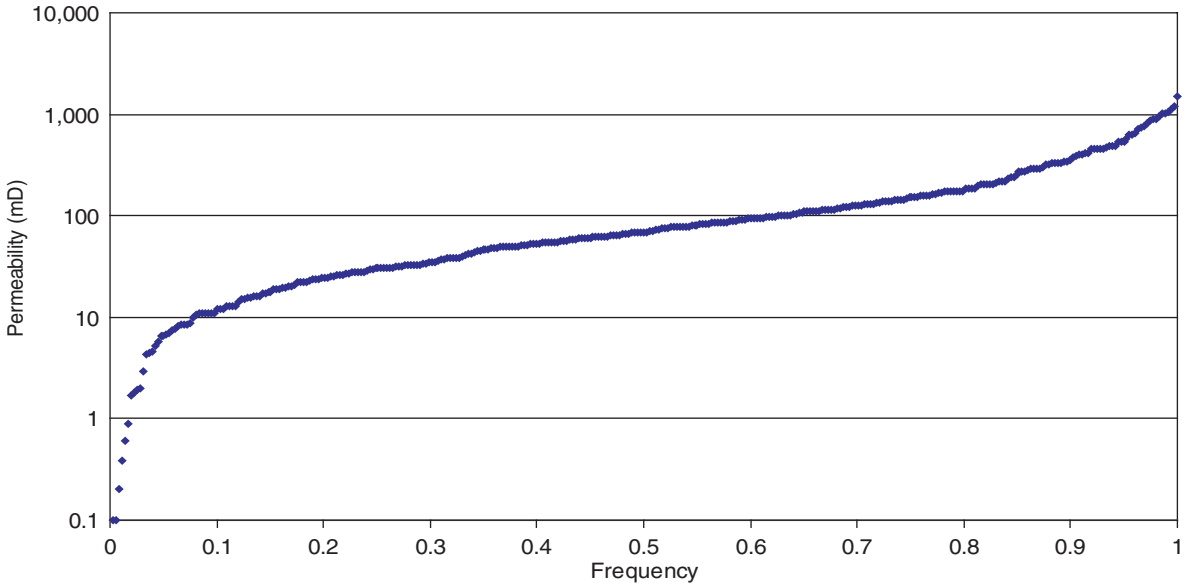

Figure 42 Cumulative distribution of core permeability from the Mt. Simon Sandstone at Herscher Field.

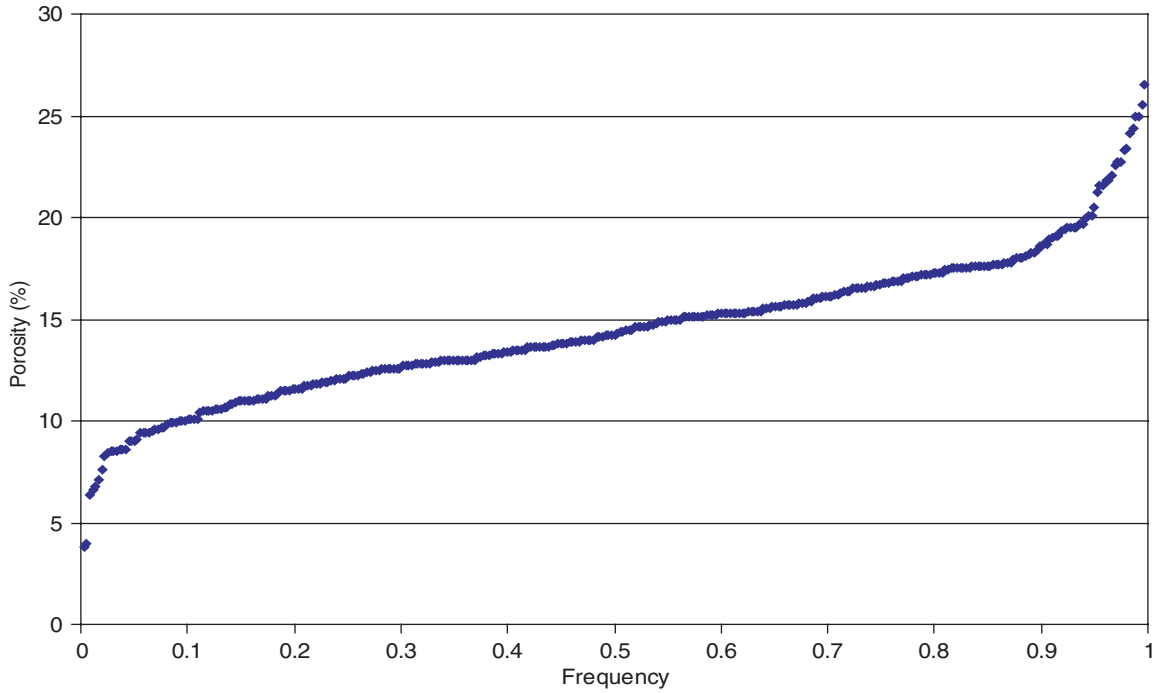

Figure 43 Cumulative distribution of core porosity from the Mt. Simon Sandstone at Herscher Field.

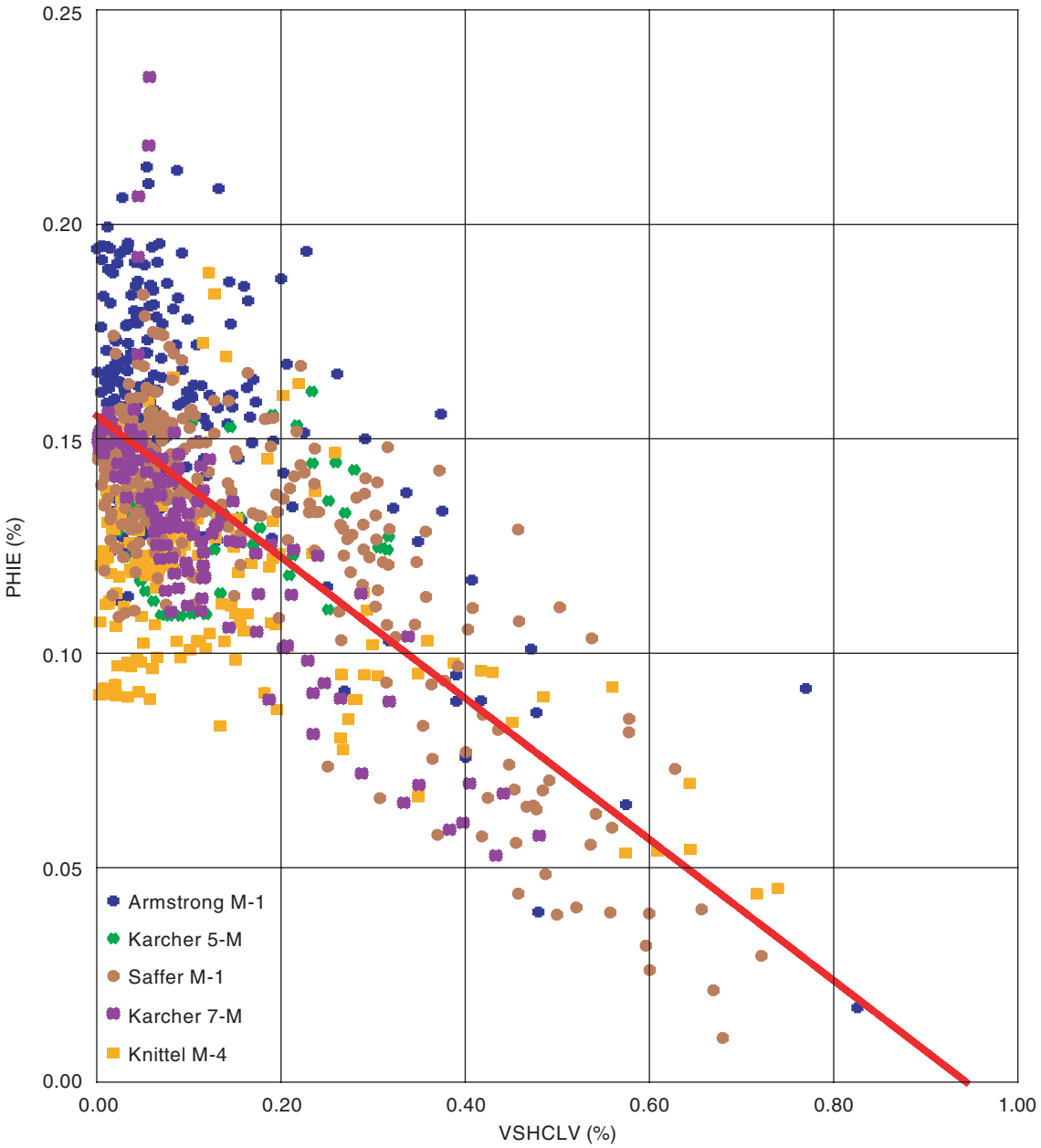

Figure 44 Cross plot of neutron porosity (PHIE) versus Clavier shale volume (VSHCLV) for off-structure, gas-free neutron log values. The linear regression line defines the gamma-ray–porosity transform used to model porosity in Herscher and Herscher NW Fields.

different surfaces. This vertical interval is approximately 1 m (3 ft) thick.

A porosity fence diagram (fig. 52) shows the lateral variation in reservoir sandstones in the Herscher and Herscher NW model area. The top of this diagram is the top of the Elmhurst Sandstone. The Mt. Simon Sandstone top is located at the thin white line by "b." The upper Mt. Simon shale marker bed is located at the white line just below "c." The lower Mt. Simon shale marker is located at the white line just above "f." The levels identified by letters correspond to the slice maps in figure 53.

The deepest porosity slice map, located just below the lower Mt. Simon shale marker bed, horizon f (fig. 53F), shows that widespread high-porosity (15 to 16%) sandstones are common in Herscher NW Field. More laterally variable, 11 to 15% porosity sandstones are seen at Herscher Field. The lower shale marker is discontinuous and forms a potential baffle, not a barrier, to gas flow.

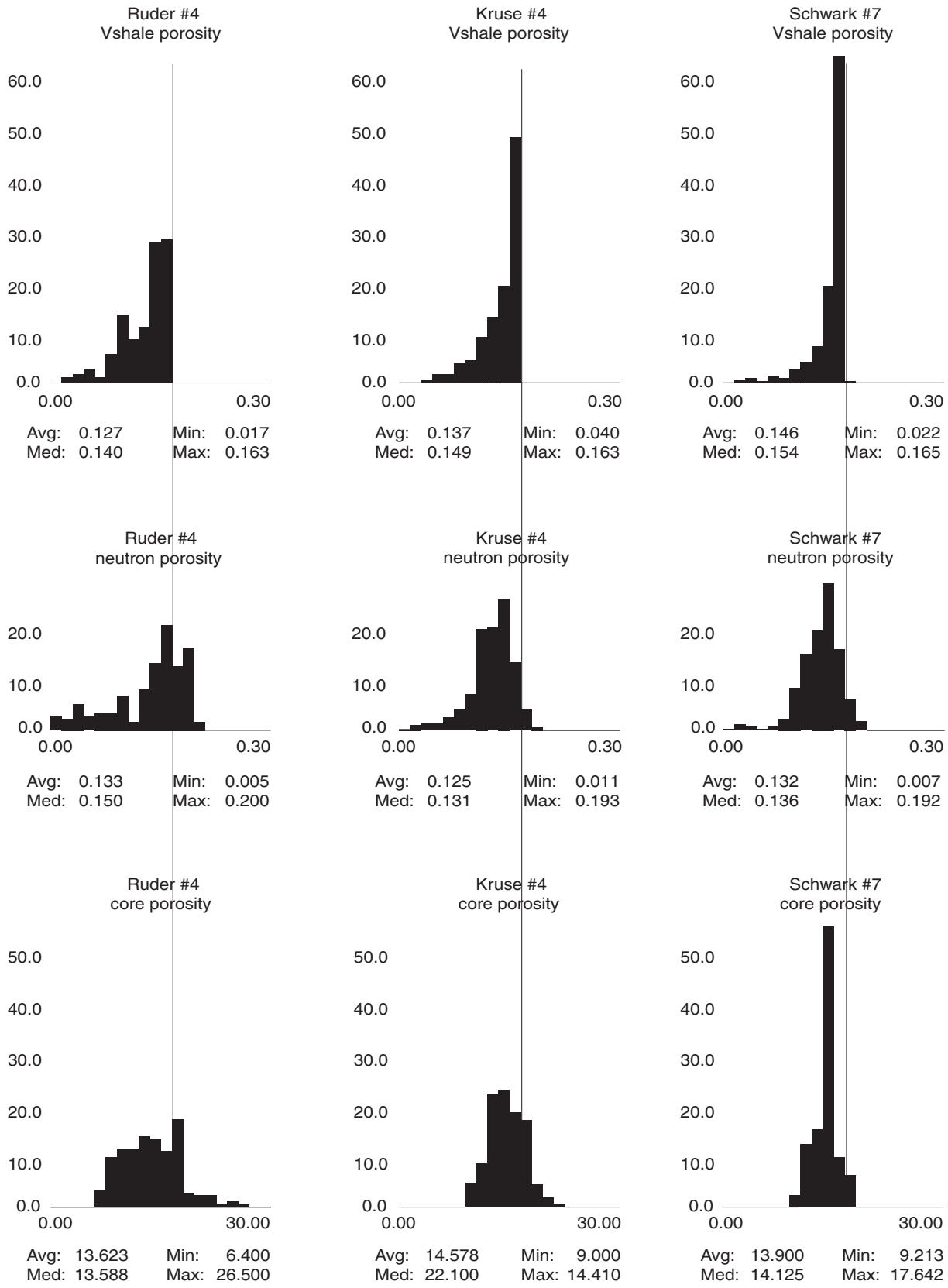

Figure 45 Histograms showing the distribution of porosity using shale volume (Vshale), neutron porosity, and core porosity calculations.

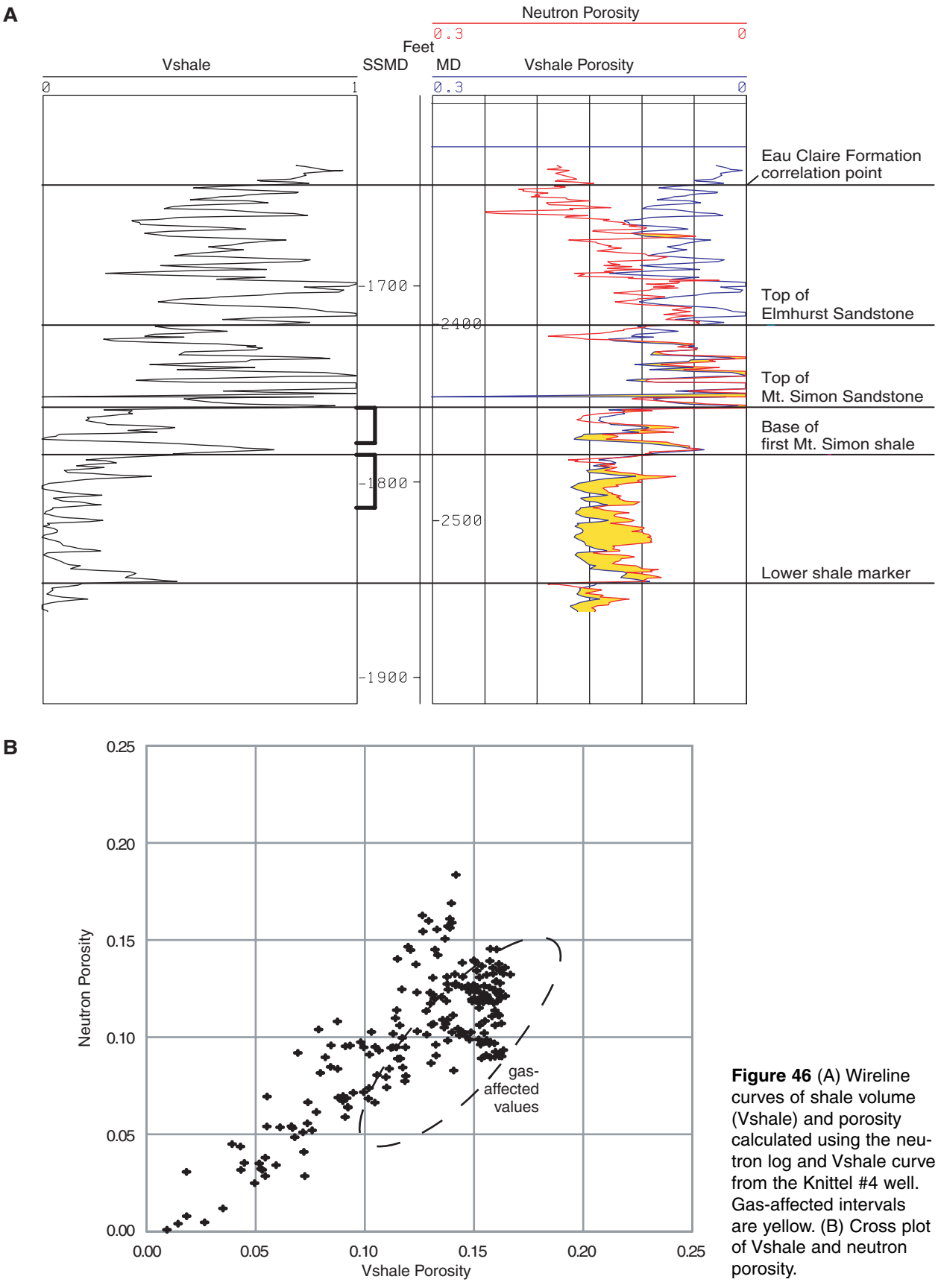

Figure 46 (A) Wireline curves of shale volume (Vshale) and porosity calculated using the neutron log and Vshale curve from the Knittel #4 well. Gas-affected intervals are yellow. (B) Cross plot of Vshale and neutron porosity.

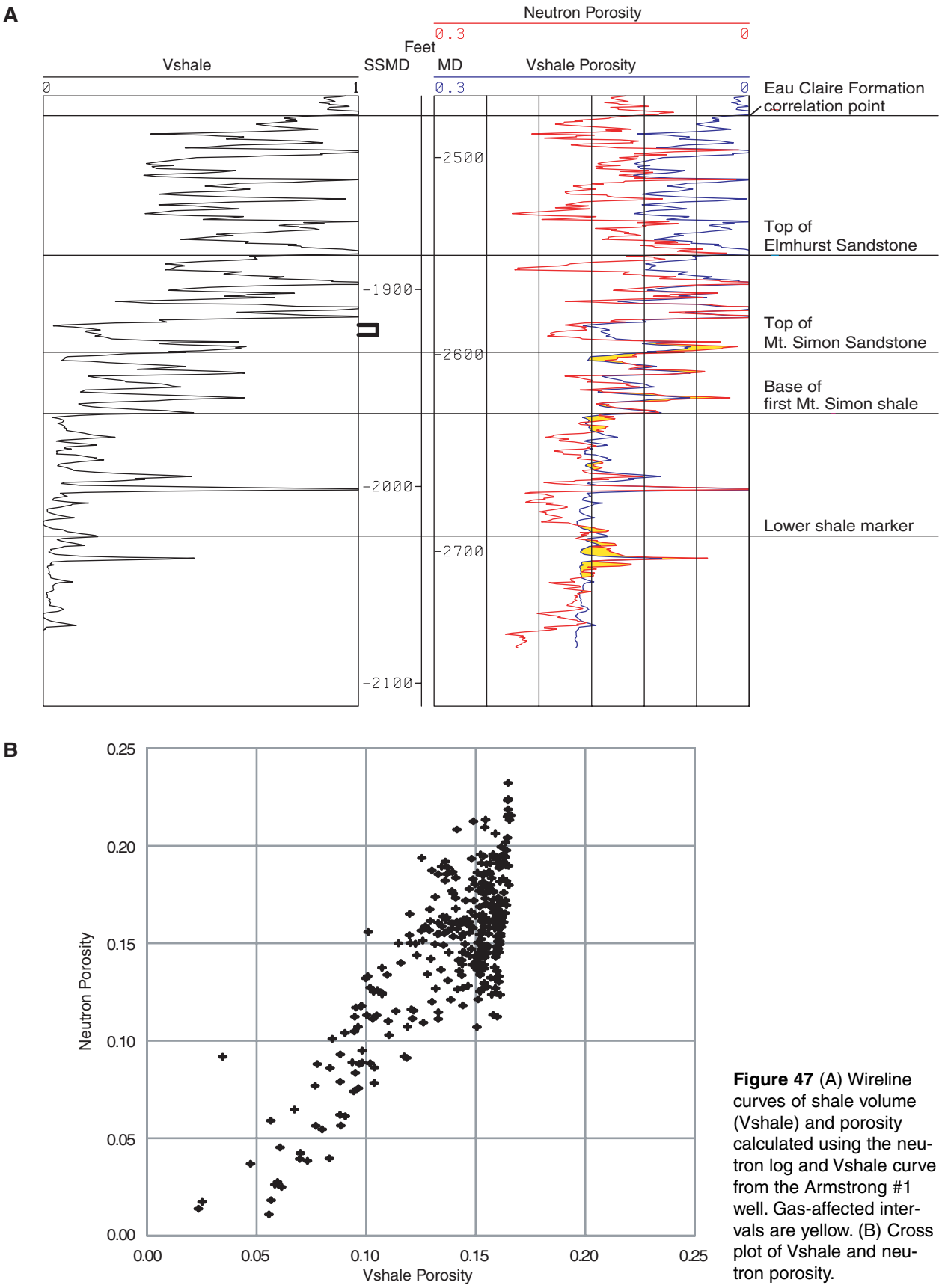

Figure 47 (A) Wireline curves of shale volume (Vshale) and porosity calculated using the neutron log and Vshale curve from the Armstrong #1 well. Gas-affected intervals are yellow. (B) Cross plot of Vshale and neutron porosity.

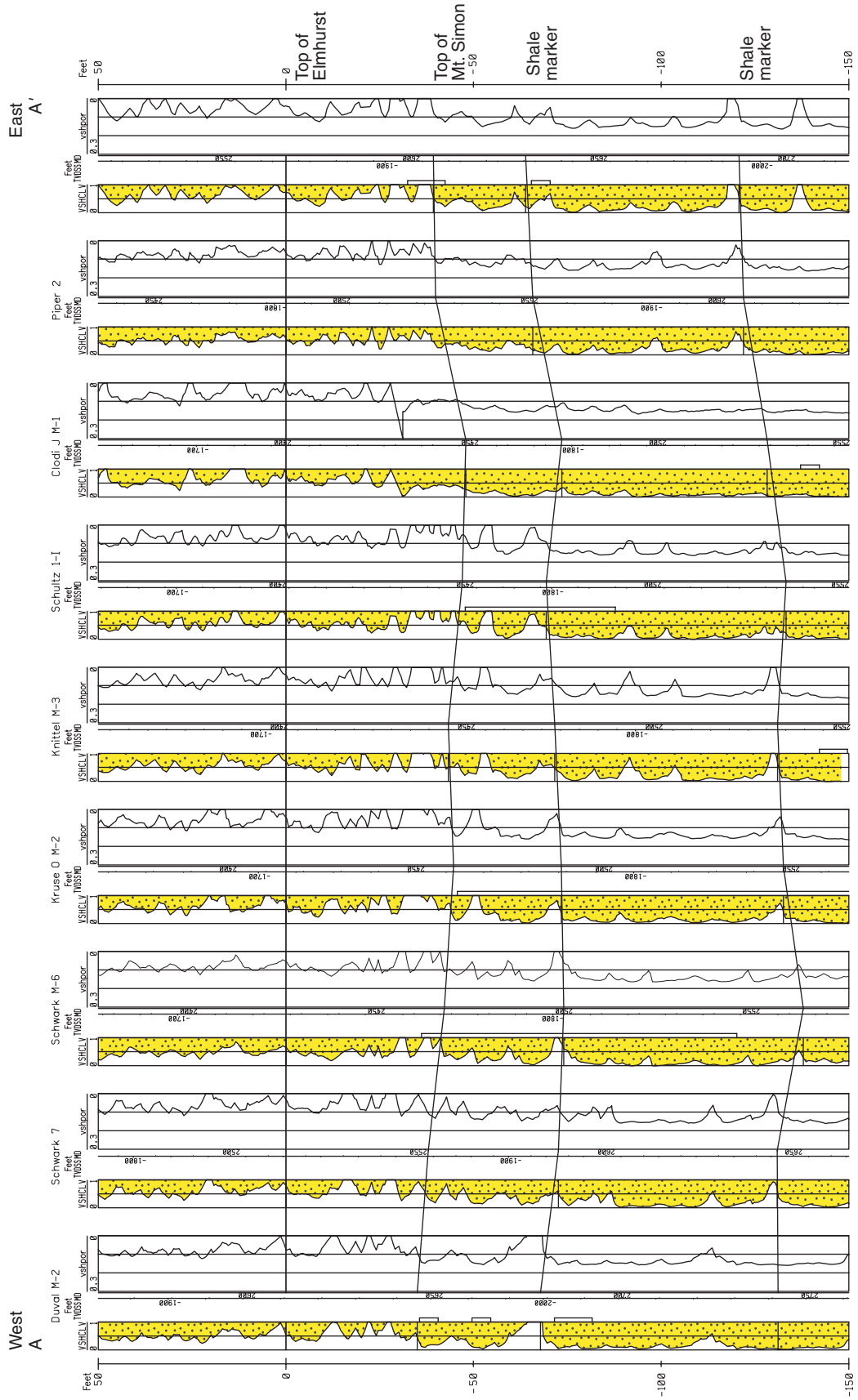

Figure 48 Stratigraphic cross section A–A' through the Herscher Anticline with the top of the Elmhurst Sandstone marker as the datum. Curves show the normalized gamma-ray values and the calculated porosity values and indicate the vertical and lateral variation of the reservoir sandstones. The cross section location is indicated on figure 35. VSCHCLV, Clavier shale volume; vshpor, shale volume porosity.

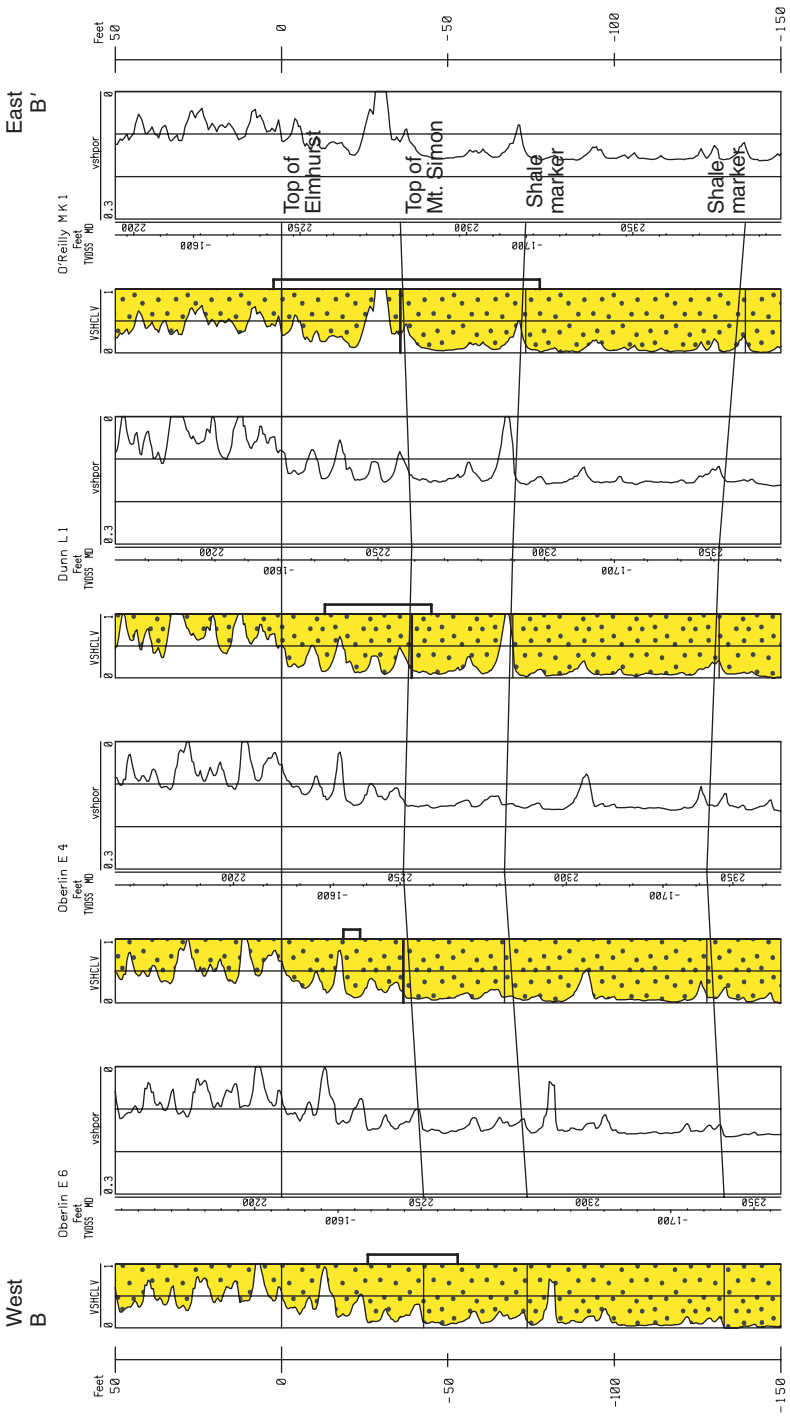

Figure 49 Stratigraphic cross section B–B′ through the Herscher Northwest Anticline with the top of the Elmhurst Sandstone marker as the datum. Curves show the normalized gamma-ray values and the calculated porosity values and indicate the vertical and lateral variation of the reservoir sandstones. The cross section location is indicated on figure 35. VSCHCLV, Clavier shale volume; vshpor, shale volume porosity.

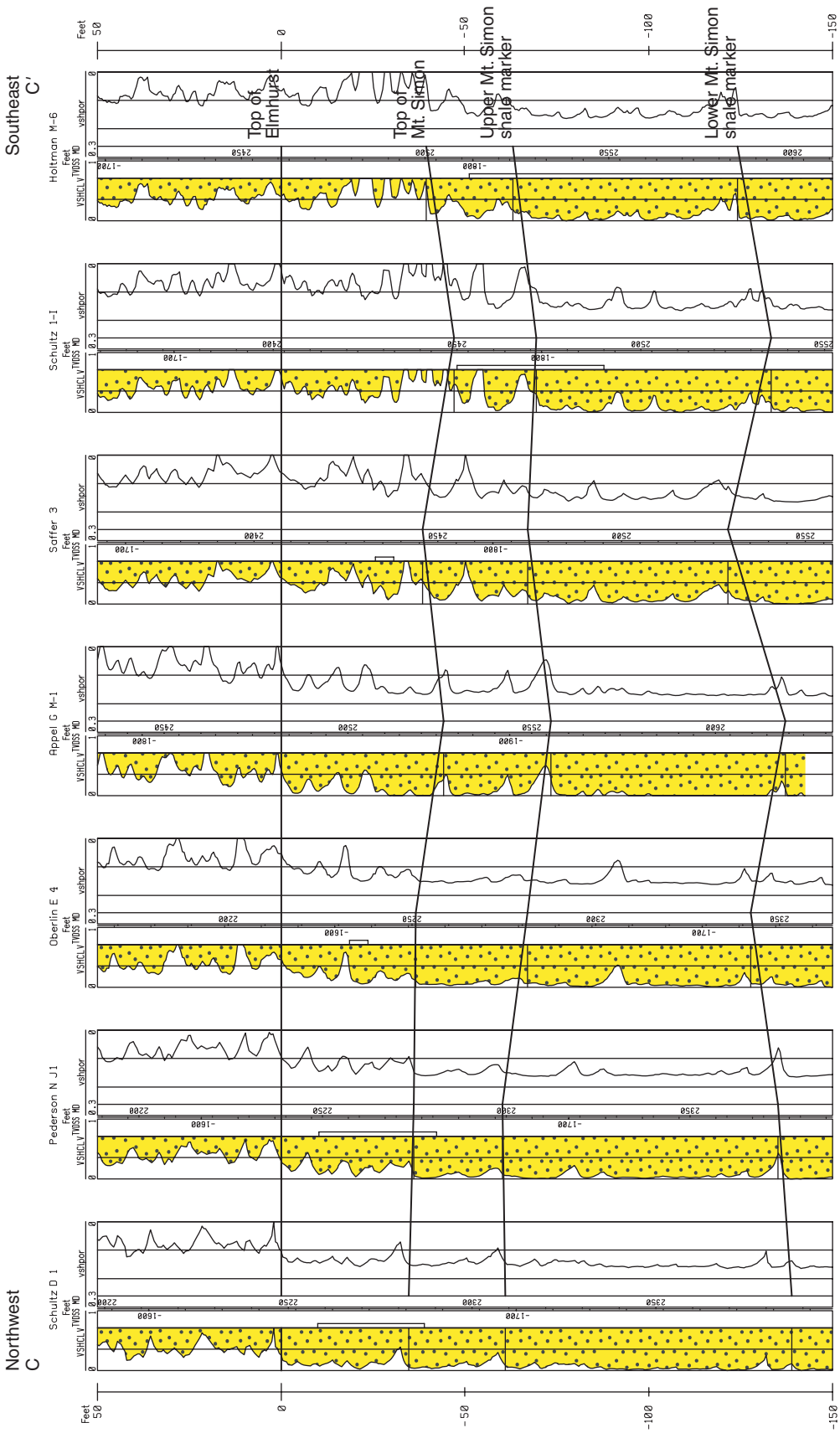

Figure 50 Stratigraphic cross section C–C′ along the axes of both Herscher and Herscher Northwest Anticlines with the top of the Elmhurst Sandstone marker as the datum. Curves show the normalized gamma-ray and the calculated porosity values and indicate the vertical and lateral variation of the reservoir sandstones. The cross section location is indicated on figure 35. VSHCLV, Clavier shale volume; vshpor, shale volume porosity.

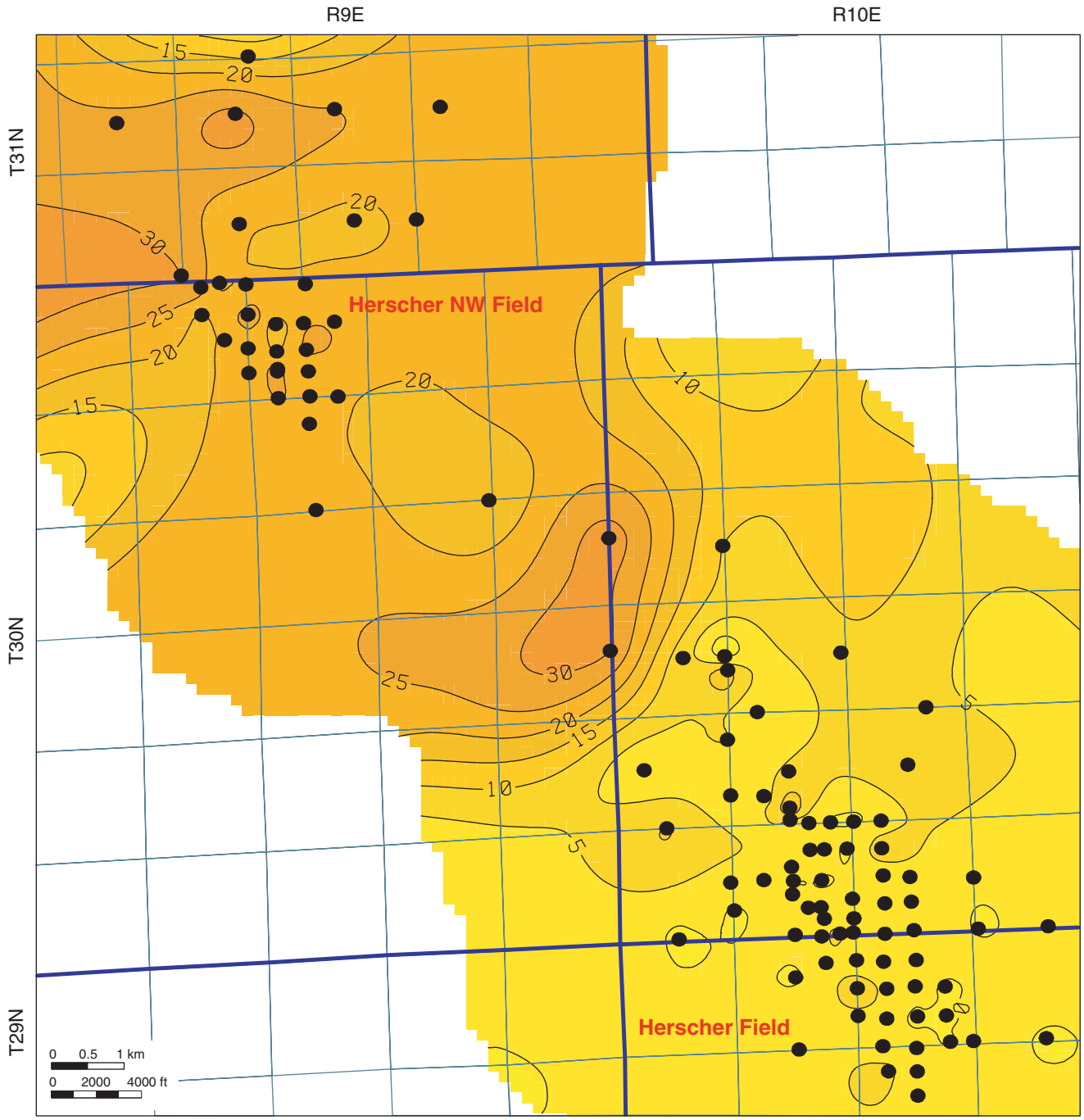

Figure 51 Elmhurst Sandstone isolith shows the thickest Elmhurst Sandstone to occur in the Herscher NW Field. Almost no sandstone is present in the southeastern part of the mapping area in Herscher Field. The contour interval is 5 ft (1.5 m).

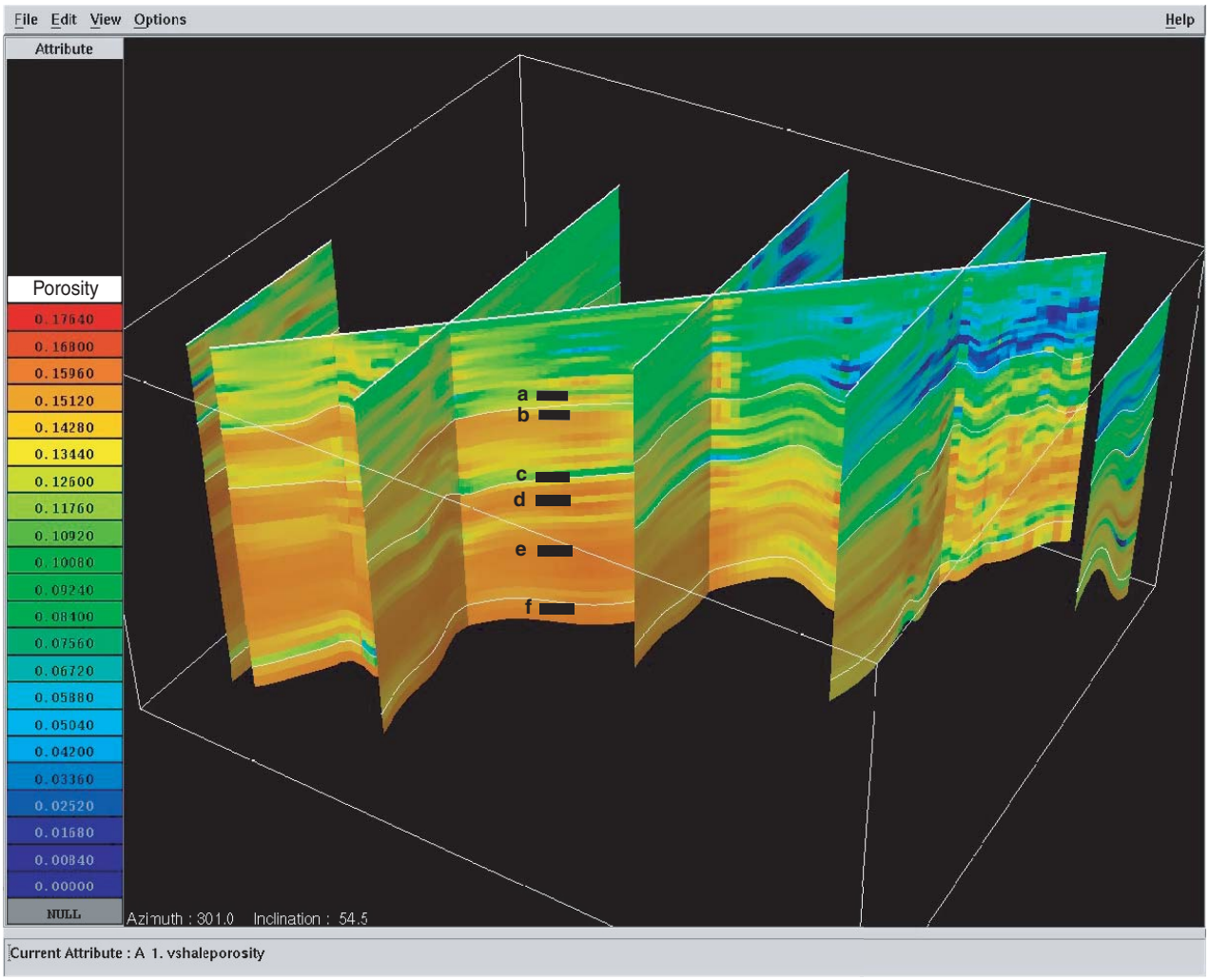

Figure 52 Three-dimensional visualization of the porosity distribution at Herscher Field. The letters on the cross section show the approximate vertical interval from which the stratigraphic slices were derived.

Next, at horizon e (fig. 53E), the porosity slice map illustrates a clean, widespread sandstone halfway between the upper and lower shale markers. This sandstone is a significant gas storage interval in the Herscher Field reservoir. The sandstone appears to have excellent lateral continuity, especially in Herscher NW Field.

Horizon d (fig. 53D) is located just below the upper shale marker bed. This horizon consists of a blanket, high-porosity sandstone at Herscher NW Field. Sandstones have variable, good to excellent porosity and lateral continuity in Herscher Field. Horizon d is also a significant gas storage interval in both fields.

Horizon c (fig. 53C) contains thin, discontinuous shales and sandstones near the top of the Mt. Simon. Some sandstones have acceptable reservoir quality (green) in Herscher Field, but the sandstones with better porosity at this horizon occur in Herscher NW Field. Shale beds are discontinuous and form baffles to gas flow.

The uppermost Mt. Simon (fig. 53B) shows good sandstone continuity and porosity (orange) in the Herscher NW Field area and acceptable porosity (green) in Herscher Field. Gas is stored in this interval in both fields.

The Elmhurst Sandstone is composed of thin, porous sandstone beds in Herscher NW Field that contains gas (fig. 53A). To the southeast, in Herscher Field, this interval consists of low-porosity, fine-grained sandstones, siltstones, and shales that are not used for gas storage.

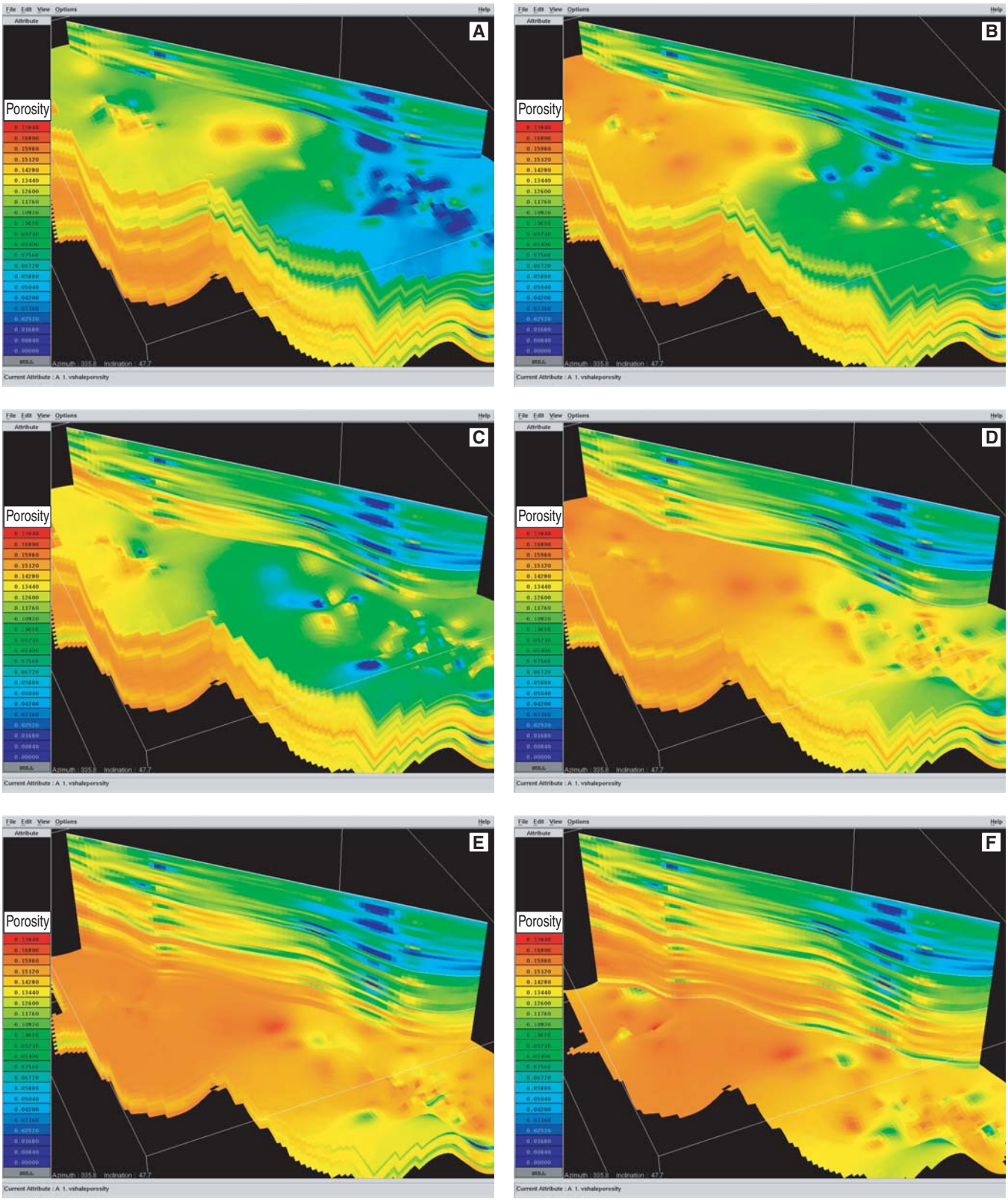

Figure 53 Stratigraphic slices showing the porosity distribution at the Herscher structure.

Conclusions

The main objectives of this project were to compile and map regional Mt. Simon data from all wells in northern Illinois and to complete highly detailed reservoir characterization studies of two Mt. Simon gas storage fields.

Regional Studies

Regional structure maps of the top of the Ordovician Galena Group (also known as the "Trenton limestone"), the St. Peter Sandstone, and the Mt. Simon Sandstone show anticlines that may have potential as new gas storage sites. A regional map of water quality in the upper part of the Mt. Simon Sandstone in northern Illinois indicated a progressive increase in TDS from northern and northwestern Illinois toward the southeast.

Manlove Field

The Manlove Field had abundant core and modern wireline logs that allowed an accurate 3-D porosity model of the Mt. Simon gas storage reservoir. Porosity was calculated using traditional cross plot porosity determination from the neutron and density curves. This calculation was facilitated by abundant core data and many wells with modern compensated porosity logs. Neutron logs from several wells with a "gas effect" could not be used in the modeling.

Reservoir characterization at Manlove Field provided a 3-D visualization showing porous sandstones in a series of stacked tidal channels and bars. The channel sandstones are oriented west to east, approximately 300 m (1,000 ft) wide and typically 2 to 3 m (6 to 10 ft) thick. The bar sandstones are oriented north to south, about 1.6 km (1 mi) wide and up to 6.1 m (20 ft) thick. Natural gas is primarily stored in the bar facies that occur at about 23 m (75 ft) and deeper below the top of the Mt. Simon.

Petrographic studies indicated that the sandstones are cemented primarily with silica overgrowths. The feldspar content increases as sandstone grain size decreases.

Herscher and Herscher NW Fields

Well data from Herscher and Herscher NW Fields consisted primarily of older, uncalibrated, neutron wireline logs, making an accurate model of the porosity distribution difficult to create. Because most wells at Herscher Field were drilled after gas storage had begun, gas affected the field's neutron logs. Conventional methods for calculating porosity values gave anomalously low values in the reservoir intervals.

An innovative methodology using the gamma-ray log was developed to circumvent the problems associated with calculating porosity from the neutron logs in gas-saturated intervals. A transform equation was created using conventionally calculated porosity in off-structure wells, core data, and the Vshale curve that could then be applied to the Vshale curves of wells within the field.

Natural gas is stored in both the overlying Elmhurst Sandstone Member of the Eau Claire Formation and the Mt. Simon in Herscher NW Field, but only in the Mt. Simon at Herscher Field. There were no channels resembling those at Manlove Field. The porosity decreased from northwest to southeast in both reservoir units. Shale beds are thin and discontinuous, forming baffles rather than barriers to gas flow.

Although the variations in data quality made direct comparison difficult between the two gas storage fields in the same formation, an approach using 3-D visualization techniques and different petrophysical methods provided valuable reservoir characterization.

Applications to Other Fields

The Vshale-to-porosity conversions developed for this study can be used to estimate porosities in other fields where no modern wireline logs exist and where gas injection commenced early in the field development. Three-dimensional modeling is the best method for characterizing reservoirs because it highlights reservoir geometries, heterogeneities, seals, and baffles to gas storage. Conformable structure mapping techniques such as from the shallow Galena Group allow shallow stratigraphic tests to be used to delineate the configuration of the Mt. Simon Sandstone, which, in most areas has been penetrated by only a few drill holes.

Acknowledgments

We thank Peoples Energy Corporation and Kinder-Morgan, Inc. for their support of the Mt. Simon gas storage reservoir studies. First Data Services digitized many of our well logs. We thank Tom Davis, Ted Kronas, and Kenneth Hopps for useful discussions and data on the gas storage reservoirs.

This study was prepared with the support of the U.S. Department of Energy under award No. DOE-FG26-99FT40375. Opinions, findings, conclusions, or recommendations expressed in this presentation are those of the authors and do not necessarily reflect the views of the Department of Energy, Kinder-Morgan, Inc., or Peoples Energy Corporation.

We gratefully acknowledge the software support for this research provided by Landmark Graphics via the Landmark University Grant Program.

At the ISGS, Randy Lipking picked many of the log tops for the northern Illinois wells that were used for the regional maps. Andrew Parish assisted with the petrographic analysis. Beverly Seyler prepared the SEM images. Richard Geier and Randy Miller provided assistance with data loading and preliminary field models. William Harrison, Jonathan Goodwin, Dennis Kolata, Rob Finley, and Bev Seyler reviewed the manuscript and provided many helpful suggestions.

References

Adler, F. J., 1987, Mid-continent region: Correlation of Stratigraphic Units of North America (COSUNA) Project: Tulsa, Oklahoma, American Association of Petroleum Geologists.

Anonymous, 1994, Pipeline report, U.S. underground natural gas storage fields: Oil and Gas Journal, Sept. 12, 1994, Special Issue, p. 47.

Atekwana, E.A., 1996, Precambrian basement beneath the central Midcontinent United States as interpreted from potential field imagery *in* B.A. van der Pluijm and P.A. Catacosinos, eds., Basement and basins of eastern North America: Boulder, Colorado, Geological Society of America, Special Paper 308, p. 33–44.

Atherton, E., 1971, Tectonic development of the eastern interior region of the United States, *in* D.C. Bond, Background Materials for Symposium on Future Petroleum Potential of NPC Region 9 (Illinois Basin, Cincinnati Arch, and northern part of Mississippi Embayment): Illinois State Geological Survey, Illinois Petroleum 96, p. 29–43.

Athy, L.F., 1928, Geology and mineral resources of the Herscher Quadrangle: Illinois Geological Survey, Bulletin 55, 120 p.

Bell, A.H., E. Atherton, T.C. Buschbach, and D.H. Swann, 1964, Deep oil possibilities of the Illinois Basin: Illinois State Geological Survey, Circular 368, 38 p.

Bell, A.H., and G.V. Cohee, 1939, Recent development in Illinois with discussion of producing formations below McClosky "Sand": American Association of Petroleum Geologists Bulletin, v. 23, no. 6, p. 807–822.

Benesh, M.E., C.M. Clark, W.R. Clark, E.G. Hammerschmidt, D.L. Katz, J.D. Parent, O.S. Seim, and R.D. Sickafoose, 1956, A study of the Herscher storage reservoir: unpublished report, available from Illinois State Geological Survey library, 74 p.

Bickford, M.E., W.R. Van Schmus, and I. Zietz, 1986, Proterozoic history of the mid-continent region of North America: Geology, v. 14, p. 492–496.

Bradbury, J.C., and E. Atherton, 1965, The Precambrian basement of Illinois: Illinois State Geological Survey, Circular 382, 13 p.

Brown, A., and B. Bowers, 1957, The relationship between neutron log deflection and porosity: Canadian Well Log Society, Canadian Symposium Papers 1, no. 39, p. 39–43.

Buschbach, T.C., 1964, Cambrian and Ordovician strata of northeastern Illinois: Illinois State Geological Survey, Report of Investigations 218, 90 p.

Buschbach, T.C., 1975, Cambrian System, *in* Handbook of Illinois Stratigraphy: Illinois State Geological Survey, Bulletin 95, p. 34–46.

Buschbach, T.C., and D.C. Bond, 1974, Underground storage of natural gas in Illinois—1973: Illinois State Geological Survey, Illinois Petroleum 101, 71 p.

Byers, C.W., 1978, Depositional environments of fine-grained upper Cambrian lithofacies, *in* E. Odom, ed., Lithostratigraphy, petrology, and sedimentation of Late Cambrian-Early Ordovician rocks near Madison, Wisconsin: Society of Economic Paleontologists and Mineralogists, Great Lakes Section, Field Trip Guidebook No. 3, p. 67–82.

Clavier, C., G. Coates, and J. Dumanoir, 1977, The theoretical and experimental bases for the "dual water" model for the interpretation of shaley sands: Society of Petroleum Engineers, Preprint No. 6859, 52nd Annual Meeting, 18 p.

Driese, S.G., C.W. Byers, and R.H. Dott, Jr., 1981, Tidal deposition in the basal Upper Cambrian Mt. Simon Formation in Wisconsin: Journal of Sedimentary Petrology, v. 51, no. 2, p. 367–381.

Droste, J.B., and R.H. Shaver, 1983, Atlas of early and middle Paleozoic paleogeography of the southern Great Lakes area: Indiana Department of Natural Resources, Indiana Geological Survey, Special Report 32, 32 p.

Dull, D.W., 1991, Calibrating old, new logs to cores needed for planning CO_2 flood: Oil and Gas Journal, p. 58–64.

Houseknecht, D.W., and F.G. Ethridge, 1978, Depositional history of the Lamotte Sandstone of southeast Missouri: Journal of Sedimentary Petrography, v. 48, p. 575–586.

Huber, M.E., 1975, A paleoenvironmental interpretation of the Upper Cambrian Eau Claire Formation of west-central Wisconsin: Madison, University of Wisconsin-Madison, M.S. thesis, 110 p.

Kolata, D.R., 1991, Illinois basin geometry, *in* M.W. Leighton, D.R. Kolata, D.F. Oltz, and J.J. Eidel, eds., Interior cratonic basins: American Association of Petroleum Geologists, Memoir 51, p. 197.

Kolata, D.R, W.J. Nelson, C.G. Treworgy, C.P. Weibel, R.D. Norby, Z. Lasemi, R.J. Jacobson, C.S. McGarry, and A.K. Hansel, compilers, 2005, Bedrock geology of Illinois: Illinois State Geological Survey, Illinois Map 14, 2 sheets, 1:500,000.

McBride, J.H., D.R. Kolata, and T.G. Hildenbrand, 2003, Geophysical constraints on understanding the origin of the Illinois basin and its underlying crust: Tectonophysics, v. 363, p. 45–78.

Nelson, W.J., 1995, Structural features in Illinois: Illinois State Geological Survey, Bulletin 100, 144 p.

Sargent, M.L., 1991, Sauk Sequence, Cambrian System through Lower Ordovician Series, *in* M.W. Leighton, D.R. Kolata, D.F. Oltz, and J.J. Eidel, eds., Interior cratonic basins: American Association of Petroleum Geologists, Memoir 51, p. 75–85.

Sargent, M.L., and Z. Lasemi, 1993, Tidally dominated depositional environment for the Mt. Simon Sandstone in central Illinois: Great Lakes Section, Geological Society of America, Abstracts and Programs, v. 25, no. 3, p. 78.

Seilacher, A., 1967, Bathymetry of trace fossils: Marine Geology, v. 5, p. 413–429.

Shaver, R.H., 1985, Midwest basins and arches: Correlation of stratigraphic units of North America (COSUNA) Project: Tulsa, Oklahoma, American Association of Petroleum Geologists.

Sloss, L.L., 1963, Sequences in the cratonic interior of North America: Geological Society of America Bulletin, v. 74, p. 93–114.

Swann, D.H., and H.B. Willman, 1961, Megagroups in Illinois: American Association of Petroleum Geologists Bulletin, v. 45, no. 4, p. 471–483.

Swulius, T.M., 1986, Porosity calibration of neutron logs, Sacroc Unit: Journal of Petroleum Technology, no. 4, p. 468–476.

Templeton, J.S., 1950, The Mt. Simon Sandstone of northern Illinois: Illinois Academy of Science Transactions, v. 43, p. 151–159.

Twenhofel, W.H., G.O Raasch, and F.T. Thwaites, 1935, Cambrian strata of Wisconsin: Geological Society of America Bulletin, v. 46, p. 1687–1744.

Walcott, C.A., 1914, Cambrian geology and paleontology: Smithsonian Misc. Coll., v. 57, p. 345–412.

Willman, H.B., E. Atherton, T.C. Buschbach, C. Collinson, J.C. Frye, M.E. Hopkins, J.A. Lineback, and J.A. Simon, 1975, Handbook of Illinois Stratigraphy: Illinois State Geological Survey, Bulletin 95, 261 p.

Workman, L.E., and A.H. Bell, 1948, Deep drilling and deeper oil possibilities in Illinois: American Association of Petroleum Geologists Bulletin, v. 32, no. 11, p. 2041–2062.

APPENDICES

Appendix 1 Northern Illinois Upper Mt. Simon Sandstone water salinity data.

API number	Company	Farm name	Farm number	Sec	T	R	TDS (mg/L)	Cl (mg/L)
120973414200	USGS	Illinois Beach State Park	1	14	46N	12E	2,570	370
120973414200	USGS	Illinois Beach State Park	LKE 46N12E-14.6g	14	46N	12E	1,600	140
120850034700	Varner Well Drlg.	Galena	JDV 28N1W-24.2b	24	28N	1W	235	
120430101300	American Potash & Chemical Waste Disposal		1	9	39N	9E	620	
120910040000	Hughes Oil Co.	Parish	1	24	31N	13E	38,655	23,224
120070034300		Belvidere	2	25	44N	3E	684	
120070029200	J.P. Miller Artesian Well Co.	Belvidere	3	25	44N	3E	738	
120150000200	Mileager Well Co.	Mt. Carroll	3	2	23N	5E	376	
120310384500	S.B. Geiger	Mt. Prospect Village	5	34	42N	11E	453	
120850041300	C.W. Varner	East Dubuque	1	20	29N	2W	272	
120890066600	Layne-Western Co.	Aurora	12a	15	38N	8E	780	
120890060500	J.P. Miller Artesian Well Co.	Batavia	3	22	39N	8E	459	
120890078200	C.W. Varner	City of Elgin-Schuler St	5	14	41N	8E	395	
120970237200	Cliff Neely	Lake Bluff Village	3	20	44N	12E	510	
121110078200	W.L. Thorre & Co.	Crystal Lake Village	2	5	43N	8E	280	
121410068400	J.B. Miller Well Co.	Polo City	1	9	23N	8E	337	
122010030400	Varner Well Drlg.	Rockford City	Unit 4	34	44N	1E	624	
121550010400	Jones & Laughlin Steel	Waste Disposal Well	1	3	32N	2W	60,000	
120910015100	NGPLA	Knittel	M3	32	30N	10E	17,707	10,000
120910014700	Natural Gas Storage Co.	Kilpatrick	M1	29	30N	10E	16,440	9,500
120910007300	NGPLA	Schwark	M1	32	30N	10E	17,313	12,000
120910007600	NGPLA	Bartlett	M1	33	30N	10E	17,402	10,500
120910009700	NGPLA	Knittel	M1	32	30N	10E	17,201	11,000
120410079900	Ohio Oil Co.	Shaw	1	36	16N	8E	102,700	60,997
121970127400	M.L. Livengood	Herrin	1	23	36N	9E	1,210	400
121090071600	CIPS	Silas Hainline	S-34	31	7N	3W	22,710	10,650
121090071700	CIPS	Proctor Endowment	SM-3	20	7N	3W	20,039	12,400
121090076500	CIPS	J.C. Proctor Endowment	SM-5	20	7N	3W	18,978	
120310242200	Western Springs City	City	1	6.3a	38N	12E	932	
120192171400	Peoples Gas & Coke	O. Bidner	2	15	21N	7E	83,600	48,750
120192197200	Peoples Gas & Coke	V. Sloan	1	5	21N	7E	82,700	47,700
120190075200	Peoples Gas & Coke	F. Hazen	1	20	21N	7E	83,700	49,200

120192254700	Peoples Gas & Coke	Kamerer	3	26	21N	7E	85,500	49,985
120190133700	Peoples Gas & Coke	W. Leischner	3	10	21N	7E	90,400	52,400
121130071700	Nigas	Bates	2	2	24N	2E	77,450	44,000
121130071900	Nigas	Hoopers	1	7	24N	3E	76,200	43,600
121130065600	Nigas	Grimes	1	1	24N	2E	77,450	43,000
121130061600	Nigas	Carden	1	15	24N	2E	81,650	45,100
121130074200	Nigas	Payne	1	14	25N	3E	67,790	40,750
121130074100	Nigas	E.W. Cooke	1	14	25N	3E	65,460	39,250
121130074300	Nigas	Cooke	3	14	25N	3E	66,000	40,000
121130052800	Nigas	J. Anderson	1	31	26N	3E	59,650	36,600
121130056200	Nigas	Furrow	2	31	26N	3E	59,750	34,500
121130056200	Nigas	Furrow	2	31	26N	3E	59,920	34,250
121050026600	Nigas	Fordyce	1	33	30N	3E	17,901	10,200
121050027200	Nigas	Fehr	1	27	30N	3E	25,800	11,230
121050027600	Nigas	Fordyce	4	33	30N	3E	21,400	10,290
121050027600	Nigas	Fordyce	4	33	30N	3E	19,804	10,300
120712035100	Nigas	J. Brook	1	18	9N	4W	14,620	5,600
120712036800	Nigas	Heap	1	16	9N	4W	14,275	5,400
120710031400	Nigas	L. Oliver	1	7	9N	4W	12,950	5,300
120712034900	Nigas	L. Oliver	3	7	9N	4W	18,180	5,250
120710031700	Nigas	Lillard	1	14	9N	5W	14,790	5,200
121050074100	Nigas	Feinhold	2	22	28N	6E	51,700	31,000
121050078300	Nigas	Clevenger	1	17	28N	6E	40,700	23,500
121050074200	Nigas	Dodson	1	5	27N	6E	53,300	29,500
121050074000	Nigas	Mackinson	1	22	28N	6E	50,200	29,000
121050078900	Nigas	Feinhold	5	33	28N	6E	47,100	28,900

Appendix 2 Core description, Peoples Gas Light & Coke, J. Williams #4 well.

Sec. 16, T21N, R7E
Champaign Co., Illinois
Logged by David G. Morse, July 16, 2001
API Number: 120192389600

Top of core: 3,980.0 ft

Thickness (ft.)	Top (ft.)	Bottom (ft.)	Description
4.9	3,980.0	3,984.9	Coarse sandstone, cross-bedded, hematite-mottled parallel to bedding, a few very coarse sandstone grains in local thin beds, 8- to 12-inch-high cross-bed sets. Millimeter-scale mudstone drapes at base; good porosity (9%).
1.9	3,984.9	3,986.8	Buff with pale greenish interbedded coarse sandstone and medium sandstone. Low porosity; somewhat mottled to structureless. Only fair sorting. Vague horizontal bedding with faint vertical burrows (?).
1.8	3,986.8	3,988.6	Medium to coarse sandstone with red and green mudstone laminations; crinkly bedding generally tight, ¼-inch circular horizontal burrows. Medium sandstone interclasts in thin-bedded coarse sandstone.
2.5	3,988.6	3,991.1	Coarse to medium sandstone interbeds, coarse, porous, medium sandstone, non-porous, vertical mottling at top, buff-colored with coarser, green-tinged sandstone.
0.1	3,991.1	3,991.2	Interbedded medium sandstone and dark gray shale and shale intraclasts.
0.8	3,991.2	3,992.0	Coarse sandstone with gray-green mudstone drape and greenish colored sandstone.
1.4	3,992.0	3,993.4	Interbedded dark gray shale laminae, bioturbated or mud cracks (sand filled) and medium and coarse sandstone; thin beds. Delicate horizontal, laminated shale partings.
3.1	3,993.4	3,996.5	Mottled, buff to pale greenish white, coarse sandstone, non-porous.
0.6	3,996.5	3,997.1	Interbedded medium sandstone and very fine dark gray shale laminations.
5.8	3,997.1	4,002.9	Generally homogeneous medium and coarse light buff sandstone. Vertical mottling locally, a few thin green-gray shale intraclasts. One thin interval of cross-bedding at 4,001.5 ft. Fairly tight. Coarsest sandstone has a pale greenish cast. Sandstone is stylolitic at 3,997.5 ft.
0.8	4,002.9	4,003.7	Cross-bedded coarse sandstone.
0.7	4,003.7	4,004.4	Brecciated sandstone.
0.8	4,004.4	4,005.2	Cross-bedded coarse sandstone.
0.3	4,005.2	4,005.5	Medium sandstone with brown shale laminations, sandstone brown to buff and another greenish brown. Non-porous.
2.5	4,005.5	4,008.0	Mottled poorly sorted medium to very coarse sandstone with vertical burrows, thin laminae, 1-inch mudstone at 4,006.5 ft.
1.2	4,008.0	4,009.2	Cross-bedded, coarse sandstone.
8.0	4,009.2	4,017.2	Mottled coarse sandstone and some medium sandstone with vertical disruptions, locally cross-bedding remnants, especially in coarse sandstone intervals.
1.1	4,017.2	4,018.3	Interbedded brownish and dark greenish gray siltstone with rounded horizontal burrows and thin beds of buff to pale orange very fine and medium sandstones.
3.2	4,018.3	4,021.5	Coarse sandstone, faint horizontal bedding, disrupted and mottled, cross-bedded below; becomes medium sandstone toward base. One half inch dark gray shale at 4,019.5 ft.
3.1	4,021.5	4,024.6	Interbedded fine to medium buff sandstone with black wispy shale fine laminations, sands commonly horizontal-burrowed; 4,023.0 ft has vertical burrows.
9.4	4,024.6	4,034.0	Coarse to very coarse light buff sandstone, commonly cross-bedded with thin beds of medium to fine sandstone. Cross-sets typically only a few inches high. Locally contains vertical burrows. Some more poorly stratified beds contain granules to 2 mm.
1.5	4,034.0	4,035.5	Interlaminated medium to fine sandstone and thinly laminated black shale. Abundant burrows; sand-filled, horizontal shale laminae may be rhythmic with short intervals of thin-bedded sandstone and then very thin laminations of sandstone and shale.
4.9	4,035.5	4,040.4	Missing.
0.5	4,040.4	4,040.9	Cross-bedded coarse sandstone.

5.1	4,040.9	4,046.0	Weakly bedded coarse sandstone with vertical burrowed intervals.
1.3	4,046.0	4,047.3	Mostly medium to coarse buff sandstone with stylolites, weakly bedded.
0.2	4,047.3	4,047.5	Horizontally bedded coarse sandstone.
2.0	4,047.5	4,049.5	Highly burrowed and stylotized medium sandstone, weakly bedded.
0.7	4,049.5	4,050.2	Bedded and cross-bedded coarse sandstone.
1.6	4,050.2	4,051.8	Interbedded fine, medium, and coarse sandstone with abundant vertical burrows.
1.1	4,051.8	4,052.9	Interbedded fine and medium sandstone with shale stringers (microlaminated black shale) in burrows or v-shaped cracks.
4.7	4,052.9	4,057.6	Cross-bedded, poorly sorted coarse sandstone with fine matrix and 2-mm grains of quartz; top is mottled; top of main gas storage reservoir; 1 inch pyrite nodule at 4,056.5 ft.
1.9	4,057.6	4,059.5	Fine to medium sandstone with vertical burrows, fluid escape (?) structures.
12.0	4,059.5	4,071.5	Cross-bedded coarse sandstone, very thin black shale stringers at 4,064.6 ft and 4,065.9 ft. Sandstone includes medium sandstone laminae and foresets, floating very coarse grains to 3 mm, and local shale intraclasts.
1.6	4,071.5	4,073.1	Mostly medium sandstone with wispy black shale whiskers.
3.7	4,073.1	4,076.8	Coarse sandstone with 2 inches of very coarse sandstone at base, mostly cross-bedded with a few local stylolites.
1.9	4,076.8	4,078.7	Fine to medium sandstone with burrowed black shale interbeds 1 to 3 inches thick. Sandstone is bioturbated; shales are finely laminated and crinkly.
1.9	4,078.7	4,080.6	Cross-bedded coarse sandstone.
1.1	4,080.6	4,081.7	Fine, medium, and coarse sandstone with a few shale whiskers at top.
3.5	4,081.7	4,085.2	Coarse cross-bedded sandstone with quartz granules.
0.7	4,085.2	4,085.9	Bioturbated medium to fine sandstone with some floating coarse sandstone grains; very fine shale whiskers at top.
2.5	4,085.9	4,088.4	Coarse cross-bedded sandstone; granules to 4 mm at base. Weakly bedded, very bioturbated locally; some stylolites.
1.6	4,088.4	4,090.0	Fine to medium buff sandstone with coarse sandstone thin beds. Some fine sandstone with floating granules and stylolites.
14.9	4,090.0	4,104.9	Coarse, cross-bedded sandstone, fair sorting; local granule layers ½ inch thick. Sandstone with fine black shale whiskers at 4,096.9 ft; gray shale intraclasts at 4,095.8 ft. Possibly over-steepened cross sets at 4,100 ft to 4,101 ft. In general, cross sets appear to be only a few inches high: 93 ft to 95 ft = 1 set 24 inches high. One fourth-inch black shale laminated at 4,103.9 ft.
0.4	4,104.9	4,105.3	Interbedded, fine sandstone and laminated black shale.
2.5	4,105.3	4,107.8	Coarse sandstone; weak bedding at top and cross-bedded at base with granules.
3.7	4,107.8	4,111.5	Medium sandstone with whisker shale interbeds at 4,108.9 ft, 4,110.1 ft, and 4,111.0 ft. Clastic dike (escape structures?) at 4,110.9 ft with some granules to 3 mm; sandstone is bioturbated at base.
4.0	4,111.5	4,115.5	Cross-bedded coarse sandstone with some granules.
0.9	4,115.5	4,116.4	Fine to medium sandstone with black shale fine lamination. Sandstone is homogeneous with some ripples.
2.0	4,116.4	4,118.4	Medium to coarse cross-bedded sandstone, black shale intraclasts at 4,117.0 ft.
1.8	4,118.4	4,120.2	Interlaminated black shale and fine to medium sandstone. One inch of shale at 4,118.5 ft. Two shale beds at 4,119.3 ft to 4,119.7 ft. Bioturbated shale with sand filling.
6.9	4,120.2	4,127.1	Cross-bedded and ripple bedded, fair-sorted medium to coarse sandstone, a few granule trains along bed bases. Some soft sediment deformation (over steep beds at 4,121.7 ft). Shale clasts at base, granules sprinkled throughout.
2.0	4,127.1	4,129.1	Cross-bedded fair sorted coarse sandstone with ripples.
1.7	4,129.1	4,130.8	Medium to coarse sandstone becoming coarse and homogeneous cross-bedded at base.
3.6	4,130.8	4,134.4	Coarse sandstone with local beds of very coarse sandstone, cross-bedded.
1.0	4,134.4	4,135.4	Medium sandstone, planar and ripple bedded, shale chips at top.

3.6	4,135.4	4,139.0	Coarse cross-bedded sandstone with scattered granules.
0.1	4,139.0	4,139.1	Black shale and fine sandstone laminations, bioturbated; sand filled.
1.9	4,139.1	4,141.0	Cross-bedded coarse sandstone; finer at top with more diffuse bedding.
0.8	4,141.0	4,141.8	Medium sandstone with grains of coarse sandstone, weakly ripple bedded.
0.7	4,141.8	4,142.5	Interbedded medium to coarse sandstone and bioturbated black shale-sandstone, cross-bedded.
0.4	4,142.5	4,142.9	Coarse cross-bedded sandstone.
4.2	4,142.9	4,147.1	Interbedded fine, medium, and coarse sandstone with black shale whiskers and laminations. Soft sediment deformation at 4,146.5 ft. Coarser sands are rippled and cross-bedded. Fine sands are nearly structureless, although they may have coarse sandstone grains in a lamination.
1.6	4,147.1	4,148.7	Medium to coarse sandstone cross-bedded to soft sediment deformed.
2.5	4,148.7	4,151.2	Ripple bedded coarse sandstone; ¼-inch thick black shale at base.
4.8	4,151.2	4,156.0	Cross-bedded coarse sandstone; local granules to 4 mm.
0.5	4,156.0	4,156.5	Missing.
0.3	4,156.5	4,156.8	Medium to coarse sandstone with bioturbated black shale.
7.0	4,156.8	4,163.8	Cross-bedded coarse to very coarse sandstone, includes thin intervals of coarse and then medium sandstone.
1.1	4,163.8	4,164.9	Medium sandstone, thin beds with black shale whisker laminations, slight bioturbation.
12.9	4,164.9	4,177.8	Medium and coarse cross-bedded sandstone.
0.1	4,177.8	4,177.9	Laminated green-gray shale.
0.3	4,177.9	4,178.2	Very coarse sandstone, cross-bedded, well cemented.
1.3	4,178.2	4,179.5	Vertical burrows in medium sandstone interbedded with dark green-gray shale which is finely laminated. Burrows up to ¼-inch wide and 1-inch high.
3.1	4,179.5	4,182.6	Medium sandstone, with some coarse grains; ¼-inch-thick granule lags.
0.1	4,182.6	4,182.7	Blackish green laminated shale.
1.0	4,182.7	4,183.7	Rippled medium to coarse sandstone.
0.7	4,183.7	4,184.4	Coarse sandstone, cross-bedded, granules at base.
4.4	4,184.4	4,188.8	Medium to coarse sandstone with ½-inch-thick zone at top with whiskers of black shale.
0.3	4,188.8	4,189.1	Interbedded, bioturbated black shale and medium sandstone; shale is finely laminated.
1.9	4,189.1	4,191.0	Fine to medium sandstone; vertical burrows $\frac{3}{16}$ inch in diameter and 1-inch high.
4.6	4,191.0	4,195.6	Interlaminated black and dark greenish black shale and fine to medium sandstone. Shale has irregular circular horizontal burrows about ¼ inch in diameter. Sandstone has vertical burrows as above.
1.9	4,195.6	4,197.5	Cross-bedded medium to coarse sandstone. Fine pyrite balls $\frac{1}{64}$ inch in diameter at 4,187 ft.
0.1	4,197.5	4,197.6	Black laminated shale.
3.6	4,197.6	4,201.2	Coarse cross-bedded sandstone.
1.6	4,201.2	4,202.8	Medium sandstone with coarse sandstone grains, ¼-inch green shale at 4,201.5 ft becomes reddish toward base.
2.2	4,202.8	4,205.0	Medium sandstone pale pink at top and more reddish downward; sandstone planar bedded and rippled.
0.2	4,205.0	4,205.2	Dark green shale with sandstone blebs (burrows) and red-brown mudstone.
12.6	4,205.2	4,217.8	Red-stained, cross-bedded coarse sandstone. Local granule lag at 4,214.4 ft. Swirly deformation at 4,206.6 to 4,210.5 ft.
0.6	4,217.8	4,218.4	Medium sandstone, mottled pink and pale pink, cross-bedded, sandstone with 3 inches of thick dark green shale and brownish mudstone, bioturbated.
5.2	4,218.4	4,223.6	Cross-bedded, coarse sandstone with local granule laminations.
0.4	4,223.6	4,224.0	Laminated shale and mudstone, dark green and red-brown.
2.5	4,224.0	4,226.5	Reddish, coarse, horizontal thin-bedded rippled (?) sandstone.

Base of core: 4,226.5 ft

Appendix 3 Graphic core description, Peoples Gas, Light & Coke, J. Williams #4 well.

Sec. 16, T21N, R7E
Champaign Co., Illinois

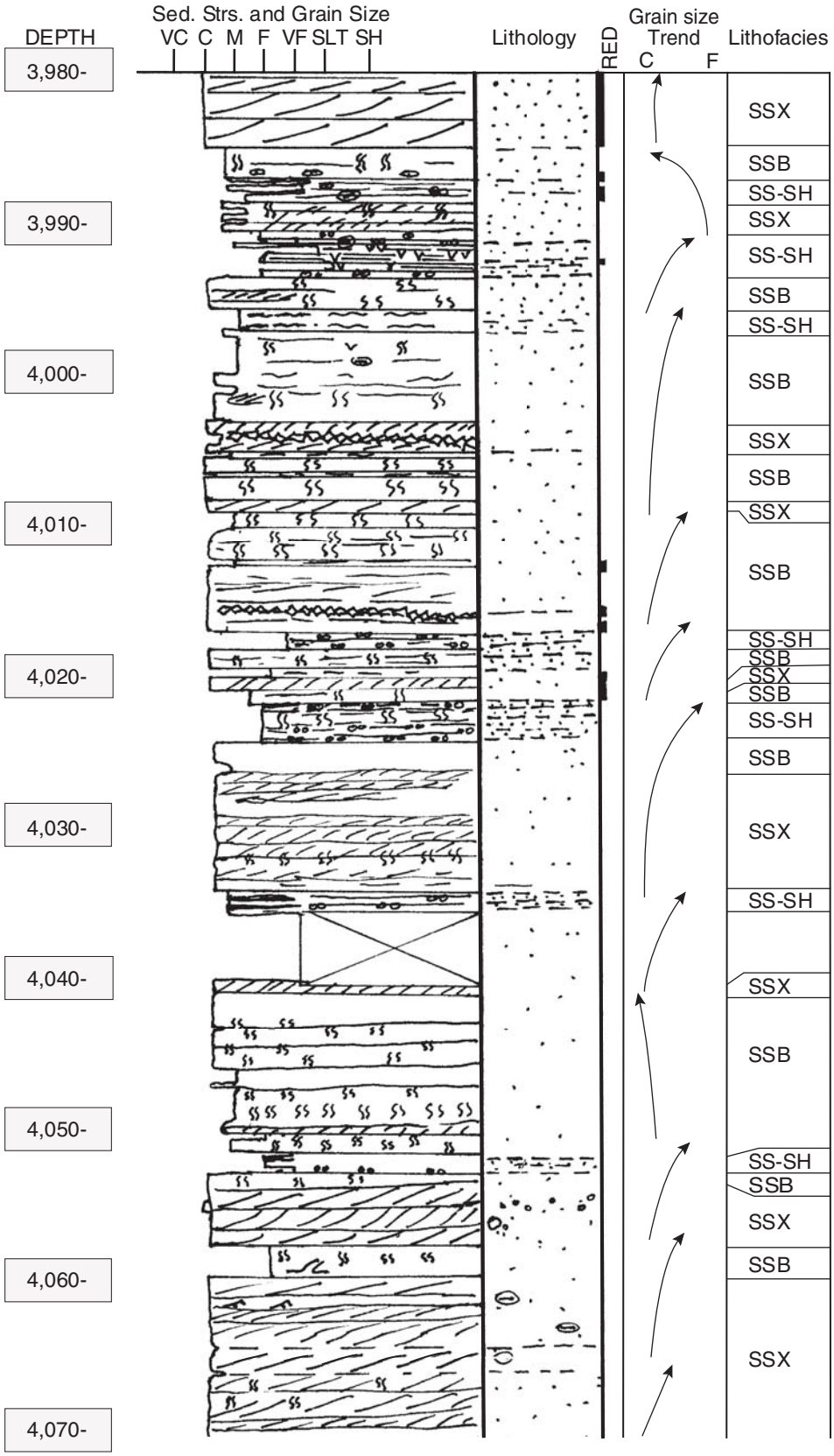

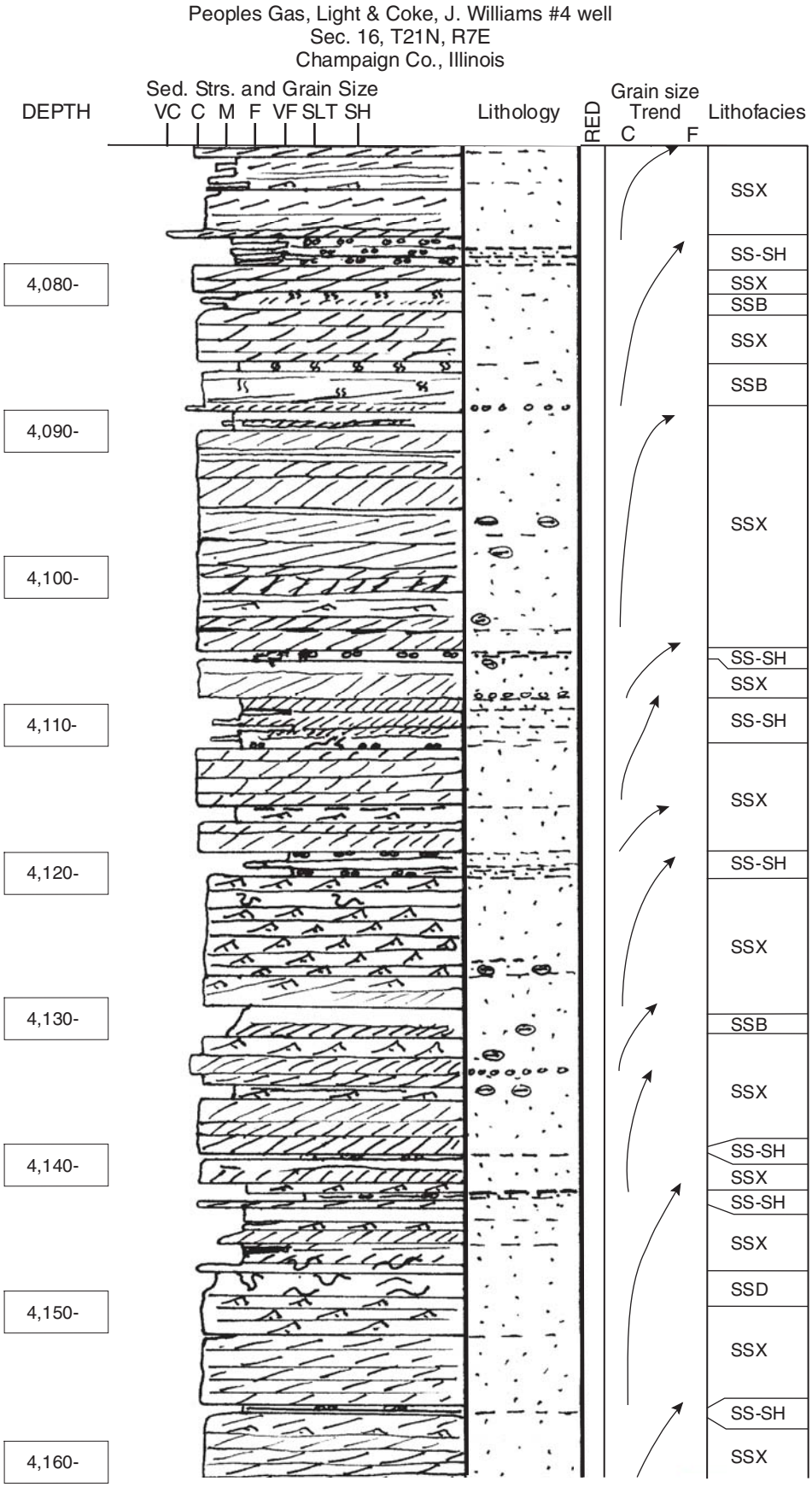
Peoples Gas, Light & Coke, J. Williams #4 well
Sec. 16, T21N, R7E
Champaign Co., Illinois
DEPTH
Sed. Strs. and Grain Size
VC C M F VF SLT SH
Lithology
RED
Grain size Trend
C F
Lithofacies
4,080-
4,090-
4,100-
4,110-
4,120-
4,130-
4,140-
4,150-
4,160-
SSX
SS-SH
SSX
SSB
SSX
SSB
SSX
SS-SH
SSX
SS-SH
SSX
SS-SH
SSX
SSB
SSX
SS-SH
SSX
SS-SH
SSX
SSD
SSX
SS-SH
SSX

Peoples Gas, Light & Coke, J. Williams #4 well
Sec. 16, T21N, R7E
Champaign Co., Illinois

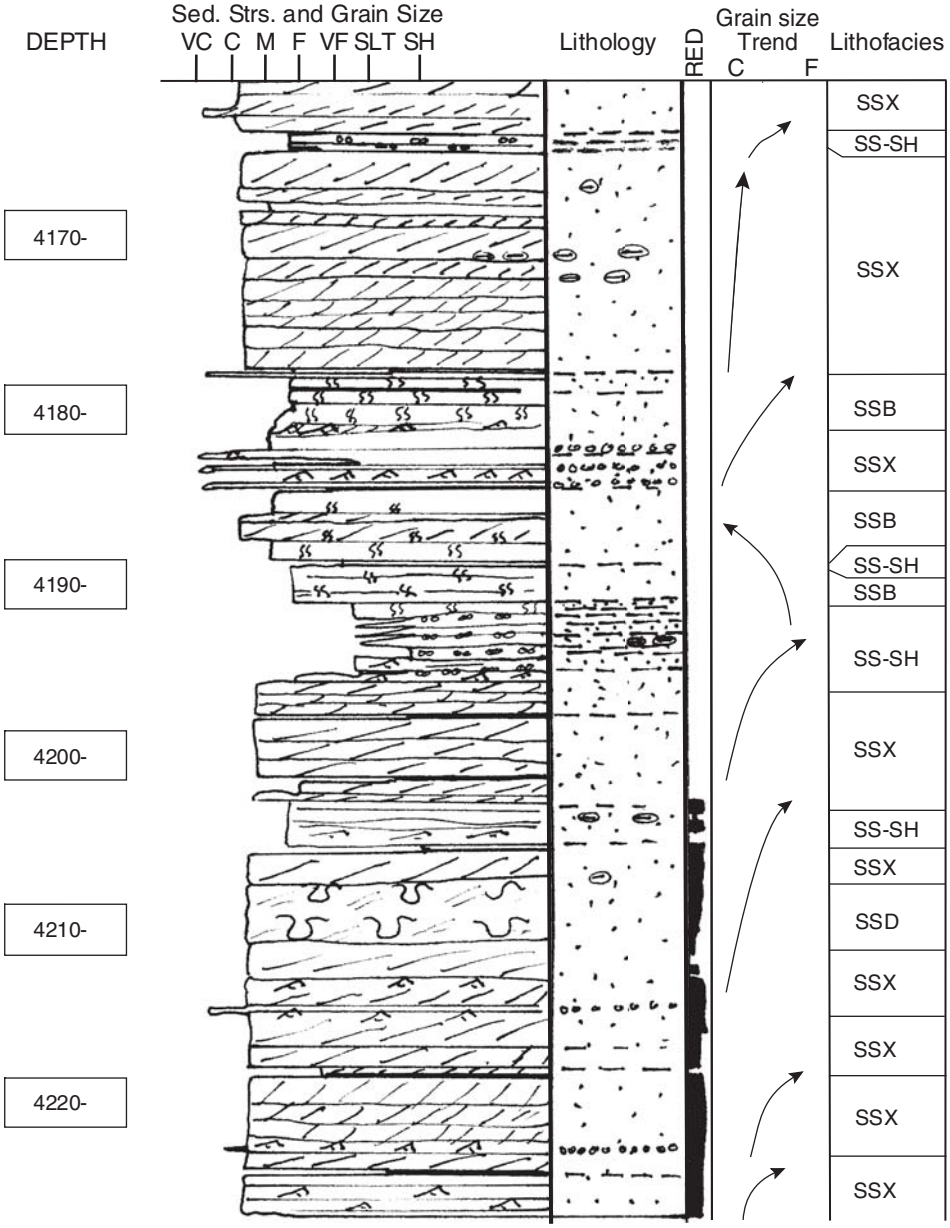

Cross-bedded
Rippled
Mud cracks
Skolithos burrows
Rippled wavy beds
Flasers
Lenticular bedding
Brecciated
Planolites burrows
Shale intraclasts
Thin-section sample

Planar beds
Soft sediment distortion
Root traces
Pyrite concretion
Granules
Sandstone
Siltstone (SLT)
Shale (SH)
Fractured core
Missing core
Fluid escape structure

SSX Cross-bedded medium to coarse sandstone
SSB Bioturbated medium to coarse sandstone
SS-SH Interbedded very fine to medium sandstone and shale
SSD Soft sediment deformed sandstone

Grain size: VC, very coarse; C, coarse; M, medium; F, fine; VF, very fine

Appendix 4 Core description, Peoples Gas, Light & Coke, Hazen #5 well.

Sec. 27, T21N, R7E
Champaign Co., Illinois
Logged by David G. Morse, April 25, 2002
C-15056
API Number: 120192181400

Top of core: 3,985.0 ft

MANLOVE FIELD
Mt. Simon Formation

Thickness (ft)	Top (ft)	Bottom (ft)	Description
1.0	3,985.0	3,986.0	Interbedded pinkish very fine sandstone with internal fine clay laminae and ¼-inch diameter, round horizontal burrows; coarse to medium sandstone with *Skolithos* burrows.
4.8	3,986.0	3,990.8	Interlaminated fine to very fine sandstone and dark gray to black shale. Finer laminated v-shaped, sand-filled mud cracks and horizontal round burrows. Some sands medium size; other bioturbation types also. Wide grazing forms ¾-inch high.
2.0	3,990.8	3,992.8	Interbedded pinkish very fine and medium-coarse sandstone with inclined bedding, faintly bioturbated; traces of greenish gray shale bed remnants. Some fine black dots: pyrite?
1.2	3,992.8	3,994.0	Interbedded very fine pink sandstone and medium-coarse sandstone as above but with some fine gray shale; fine laminations.
1.5	3,994.0	3,995.5	Finely interlaminated dark gray shale and very fine sandstone, round bioturbation burrows and v-shaped, sand-filled mud cracks. Shale very finely laminated, crudely rhythmic.
7.3	3,995.5	4,002.8	Interbedded medium and coarse to very coarse sandstone with rare very thin red and dark gray shale drapes. Sandstone is horizontal to cross-bedded, locally light purple color. Medium sandstone has vertical burrows (*Skolithos*).
0.2	4,002.8	4,003.0	Very dark gray micaceous siltstone.
2.5	4,003.0	4,005.5	Interbedded medium-coarse sandstone, pale cream color, unbedded with faint vertical burrows and a reddish and greenish highly bioturbated fine sandstone with silt; vertical and round horizontal burrows.
0.6	4,005.5	4,006.1	Interlaminated very fine sandstone and gray claystone with sand-filled burrows (¼-inch-diameter circular) and large sandstone burrows.
1.9	4,006.1	4,008.0	Medium-coarse, cream-colored sandstone; locally very coarse beds, weak horizontal bedding, some sandstone with dark gray hue (pyrite?), rounded horizontal burrows and trace of greenish gray silt or clay.
0.5	4,008.0	4,008.5	Pinkish very fine sandstone with wispy shale laminations, mud cracks, and bioturbation.
3.2	4,008.5	4,011.7	Interbedded buff medium to coarse sandstone and fine to very fine sandstone; local bioturbation; round horizontal burrows about ¼-inch in diameter, faint cross-bedding, a few gray-green mud chips on cross-beds.
0.2	4,011.7	4,011.9	Interlaminated very fine sandstone and dark gray siltstone or claystone. Round sand-filled burrows and v-shaped cracks.
16.2	4,011.9	4,028.1	Interbedded fine, medium, and coarse sandstone, cream/buff color; commonly with vertical burrows and local stylolitic intervals. Some weakly cross-bedded sandstone remains. One thin bed of very coarse sandstone was very pure, clean sandstone with quartz overgrowths; very porous.
0.4	4,028.1	4,028.5	Interbedded dark gray silty claystone and very fine sandstone; round horizontal burrows.
3.7	4,028.5	4,032.2	Mottled cream and pinkish bioturbated fair to medium-coarse sandstone; vertical burrows and local stylolites; some floating very coarse sandstone grains.
1.6	4,032.2	4,033.8	Interlaminated dark gray clay/siltstone and very fine sandstone; small round horizontal burrows and larger grazing burrows.
0.6	4,033.8	4,034.4	Pinkish, mottled, vertical burrows; medium sandstone, poorly sorted.

2.6	4,034.4	4,037.0	Buff/cream medium, coarse, and very coarse cross-bedded sandstone.
4.0	4,037.0	4,041.0	Light maroon and buff coarse sandstone; horizontal and cross-bedded with vertical burrows locally and local shale interclasts.
1.8	4,041.0	4,042.8	Pinkish maroon medium sandstone and one thin red shale lamination; sandstone is cross-bedded.
0.4	4,042.8	4,043.2	Thin, interbedded, green-gray siltstone and fine sandstone, bioturbated.
2.3	4,043.2	4,045.5	Greenish gray medium sandstone and mottled buff and pinkish medium sandstone with greenish gray swirls.
1.0	4,045.5	4,046.5	Mottled pinkish, buff and gray-green, medium-coarse sandstone.
2.5	4,046.5	4,049.0	Cross-bedded, medium-coarse, buff sandstone; fines upward, curved trough cross-sets.
2.8	4,049.0	4,051.8	Poorly sorted, weakly bedded fair to medium pinkish buff sandstone with wispy green stylolitic(?) zones at 4,049.2 ft and 4,049.7 ft (may also be bioturbated?). Sandstone beds have faint vertical burrows.
1.9	4,051.8	4,053.7	Coarse to very coarse buff sandstone, cross-bedded and rippled.
0.5	4,053.7	4,054.2	Fine sandstone with stylolitic shale whiskers bioturbated.
0.7	4,054.2	4,054.9	Interlaminated black-gray silt and pinkish very fine sandstone, horizontal round, sand-filled burrows and wedge-shaped v-cracks.
7.6	4,054.9	4,062.5	Weakly bedded buff to medium sandstone with floating very coarse sand grains, locally stylolitic with gray-green or black wispy residue. Vague mottling (bioturbation) 4,060 to 4,062.5 ft. Pyrite patch at 4,061.2 ft. Mud chips in basal 3 inches.
0.6	4,062.5	4,063.1	Coarse cross-bedded sandstone with some very coarse sandstone grains.
6.9	4,063.1	4,070.0	Mottled, interbedded medium and fine sandstone with both vertical and round horizontal burrows. Local stylolitic surface; coarse sandstone thin bed.
1.9	4,070.0	4,071.9	Medium to coarse cross-bedded buff-colored sandstone with local coarse lags at the base of sets. Mottling between 4,071.5 to 4,071.7 ft.
1.1	4,071.9	4,073.0	Interbedded fine to medium-coarse sandstone; mottled bedding within separate beds; stylolitic surface with black silty whiskers at base.
5.4	4,073.0	4,078.4	Cross-bedded medium-coarse sandstone, buff color, a few stylolitic boundaries.
1.6	4,078.4	4,080.0	Fine to very fine sandstone, pinkish with thin shaley interlaminated fine silt. Sands bioturbated ½-inch diameter to 1/16 inch diameter rounded sand-filled burrows.
0.9	4,080.0	4,080.9	Black to dark gray silt with very fine sand-filled round burrows; finely laminated silt with wiggly contacts.
2.3	4,080.9	4,083.2	Fine to medium buff-colored sandstone, bioturbated and cross-bedded.
3.3	4,083.2	4,086.5	Medium to coarse cross-bedded sandstone.
2.5	4,086.5	4,089.0	No sample.
3.7	4,089.0	4,092.7	Medium to coarse cross-bedded sandstone.
0.8	4,092.7	4,093.5	Weakly interbedded fine and medium sandstone, buff; faint horizontal bedding.
2.0	4,093.5	4,095.5	No sample.
1.4	4,095.5	4,096.9	Weakly interbedded fine and medium sandstone, buff; faint horizontal bedding. Whole core analysis sample reference: #114.
2.1	4,096.9	4,099.0	No sample.
1.0	4,099.0	4,100.0	Weakly interbedded fine and medium sandstone as above. Whole core analysis sample reference: #115.
0.7	4,100.0	4,100.7	Cross-bedded medium to coarse sandstone with granule floaters, buff. Whole core analysis sample reference: #116.
2.3	4,100.7	4,103.0	Bioturbated fine to medium sandstone with coarse sandstone and granule floaters; *Skolithos* and local stylolites; two black shale partings.
1.0	4,103.0	4,104.0	Cross-bedded medium to coarse sandstone, buff, porous; shale chips (½ inch long) on cross-beds.
0.8	4,104.0	4,104.8	Bioturbated fine and medium to coarse sandstone interbeds. *Skolithos*.

14.5	4,104.8	4,119.3	Cross-bedded medium, coarse, and very coarse sandstone, tabular foresets, porous, buff to very slight pink tinge in color; grain size sorted along successive foreset laminations, 6 inches to 24 inches set heights.
3.4	4,119.3	4,122.7	No sample.
2.1	4,122.7	4,124.8	Cross-bedded medium and coarse sandstone as above.
1.2	4,124.8	4,126.0	Fine to medium sandstone, structureless, with floating granules and one stylolite with black silt/shale at 4,125.5 ft.
1.4	4,126.0	4,127.4	Cross-bedded coarse to very coarse sandstone with some granules at base of cross-bedded set. Very sharp base over shale.
1.3	4,127.4	4,128.7	Dark gray to black laminated silt with fine sand-filled cracks and burrows toward base.
1.1	4,128.7	4,129.8	No sample.
0.2	4,129.8	4,130.0	Structureless sandstone, fine- to medium-grained with floating granules. Whole core analysis sample reference: #145.
2.0	4,130.0	4,132.0	No sample.
0.5	4,132.0	4,132.5	Cross-bedded medium to coarse sandstone.
0.5	4,132.5	4,133.0	Fine to medium sandstone with possible flame structure with fine sandstone flowing up into coarser sandstone.
1.0	4,133.0	4,134.0	No sample.
0.4	4,134.0	4,134.4	Cross-bedded medium sandstone. Whole core analysis sample reference: #149.
1.4	4,134.4	4,135.8	No sample.
0.7	4,135.8	4,136.5	Cross-bedded medium to coarse sandstone. Whole core analysis sample reference: #151.
3.7	4,136.5	4,140.2	No sample.
7.8	4,140.2	4,148.0	Cross-bedded medium to coarse sandstone. Whole core analysis sample reference: #155 at top and #162 at base. Very heterogeneous size grains on cross-bedded sets. Well sorted within individual laminae.
3.3	4,148.0	4,151.3	No sample.
5.9	4,151.3	4,157.2	Cross-bedded medium to coarse sandstone, sets up to three feet high; mostly medium sandstone, few very coarse grains, a few ½-inch-long mud chips and granules at base.
1.0	4,157.2	4,158.2	Medium to fine sandstone with floating coarse sandstone grains and rare mud chips.
0.1	4,158.2	4,158.3	Finely interlaminated black siltstone and very fine buff sandstone that consists of burrow fills.
6.3	4,158.3	4,164.6	Cross-bedded buff to pinkish medium and coarse sandstone with local zones of stylolites and thin mud chip clasts.
3.4	4,164.6	4,168.0	No sample.
6.3	4,168.0	4,174.3	Cross-bedded buff fine to medium sandstone as above.
2.1	4,174.3	4,176.4	Fine pinkish cream-colored sandstone with stylolites and vertical burrows.
0.1	4,176.4	4,176.5	Interlaminated dark gray-black siltstone and very fine sandstone, burrowed, wavy fine laminations.
1.3	4,176.5	4,177.8	No sample.
0.2	4,177.8	4,178.0	Weakly cross-bedded medium sandstone with floating coarse sandstone grains.
0.4	4,178.0	4,178.4	Laminated dark grayish black siltstone, micaceous.
0.3	4,178.4	4,178.7	Bioturbated very fine sandstone and dark gray black silt. Dense horizontal sand filled burrows. Whole core analysis sample reference: #193.
4.0	4,178.7	4,182.7	Interbedded and interlaminated medium, fine, and very fine sandstone with finely laminated dark gray/black siltstone with sand-filled horizontal burrows (4,180.2 to 4,181.8 ft missing).
0.8	4,182.7	4,183.5	Cross-bedded medium sandstone with fine to coarse sandstone grains.
1.2	4,183.5	4,184.7	Missing.
0.3	4,184.7	4,185.0	Cross-bedded medium sandstone with fine to coarse sandstone grains.
2.0	4,185.0	4,187.0	Very dark gray/black clayey siltstone, laminated with local pinkish very fine sandstone burrow fills, especially near top.

4.6	4,187.0	4,191.6	Medium sandstone with coarser interbeds, cross-bedded, local mud chips in cross-bedded sandstone. One-inch interval at 4,189.0 ft with thin green-gray silty clay wisps; some stylolites between 4,189.0 and 4,190.0 ft.
4.4	4,191.6	4,196.0	Missing.
2.8	4,196.0	4,198.8	Interbedded fine and medium sandstone with some coarser interbeds; weakly cross-bedded and *Skolithos*.
2.7	4,198.8	4,201.5	Fine to medium cross-bedded and weak horizontally bedded sandstone, 1-inch zone with shaley interclasts; flakes at 4,200.8 ft; *Skolithos* at 4,200.0 ft.

Base of core: 4,201.5 ft

Appendix 5 Graphic core description, Peoples Gas, Light & Coke, Hazen #5 well.

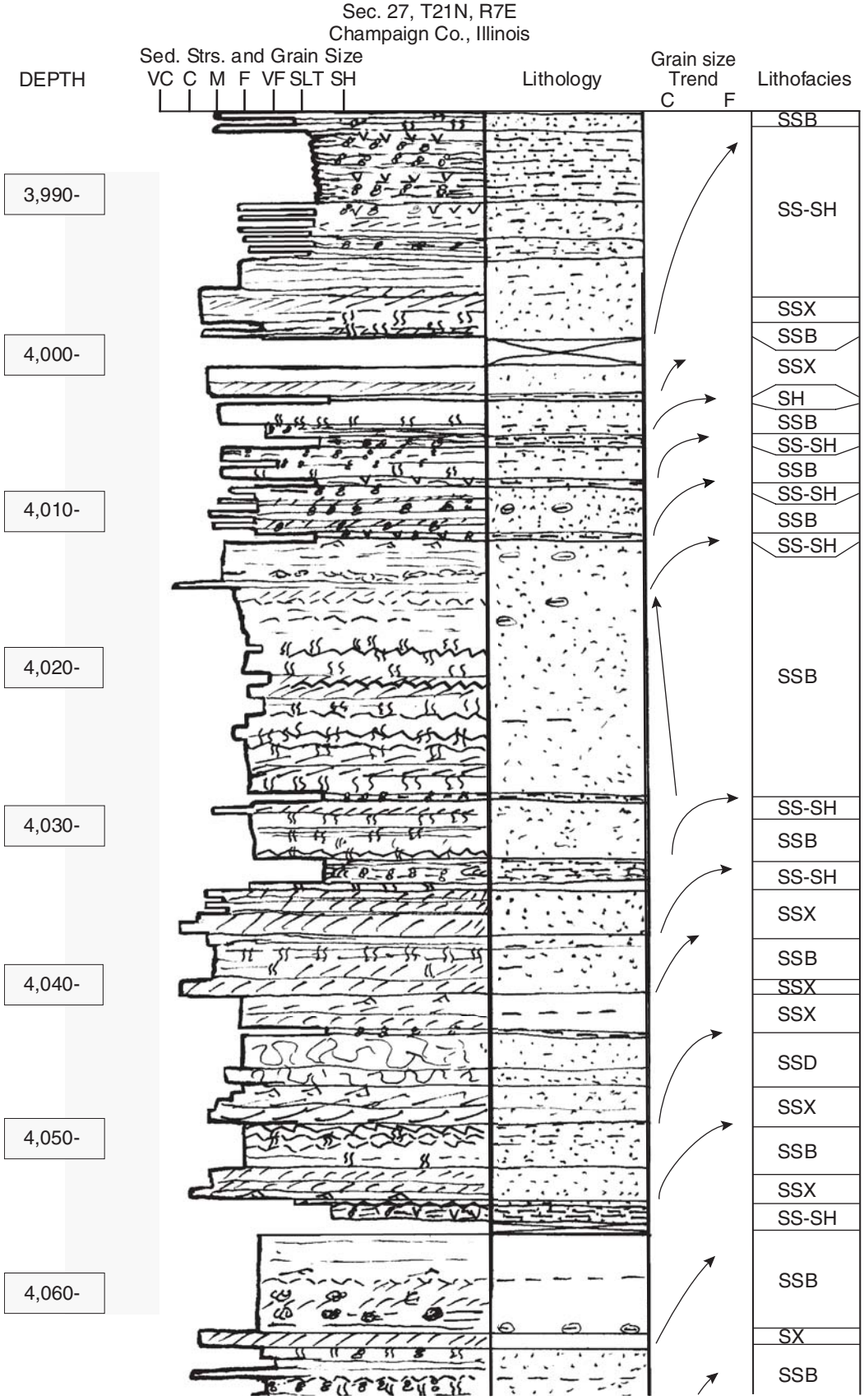

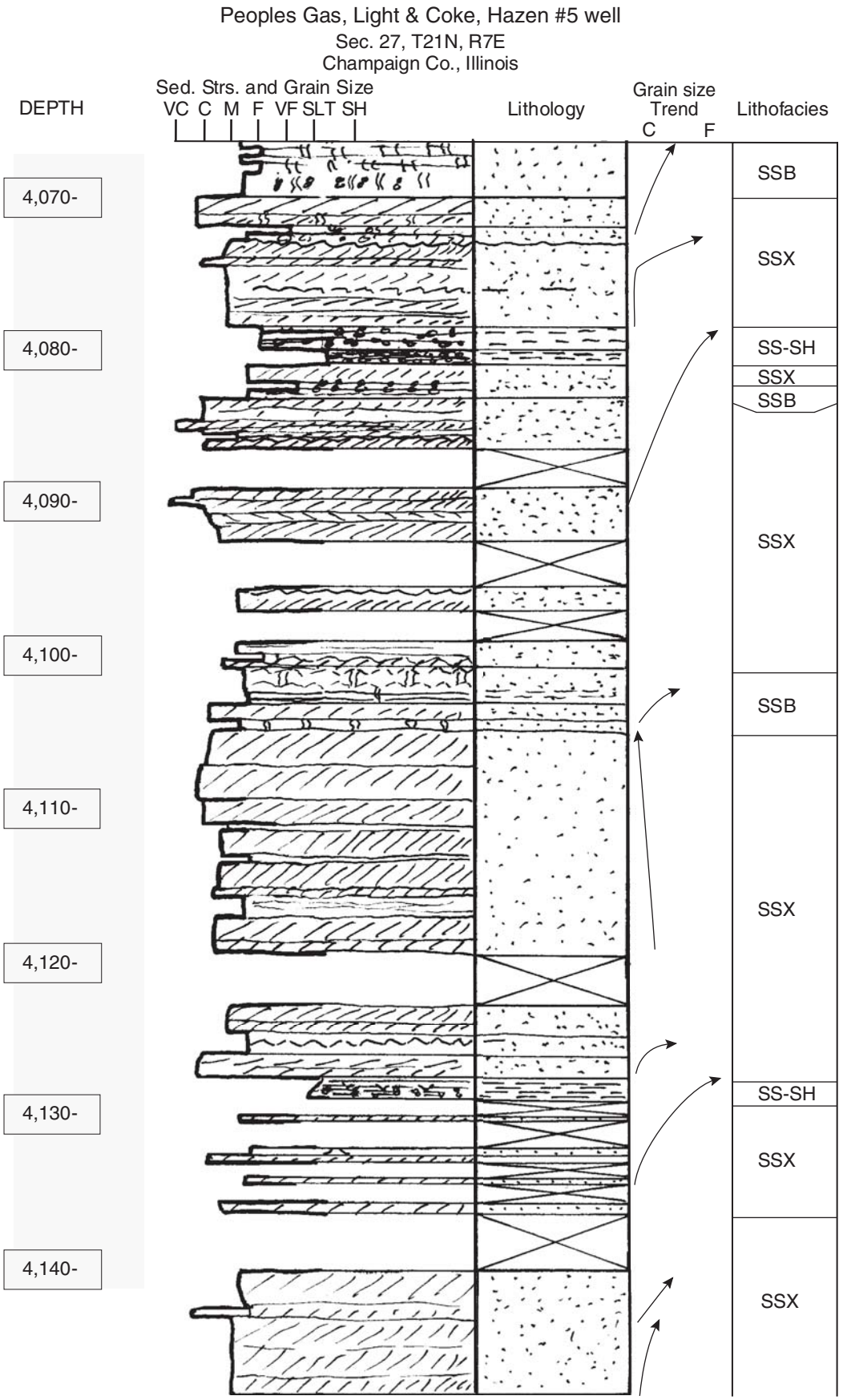
Peoples Gas, Light & Coke, Hazen #5 well
Sec. 27, T21N, R7E
Champaign Co., Illinois
DEPTH
Sed. Strs. and Grain Size
VC C M F VF SLT SH
Lithology
Grain size Trend
C F
Lithofacies
4,070-
4,080-
4,090-
4,100-
4,110-
4,120-
4,130-
4,140-
SSB
SSX
SS-SH
SSX
SSB
SSX
SSB
SSX
SS-SH
SSX
SSX

Peoples Gas, Light & Coke, Hazen #5 well
Sec. 27, T21N, R7E
Champaign Co., Illinois

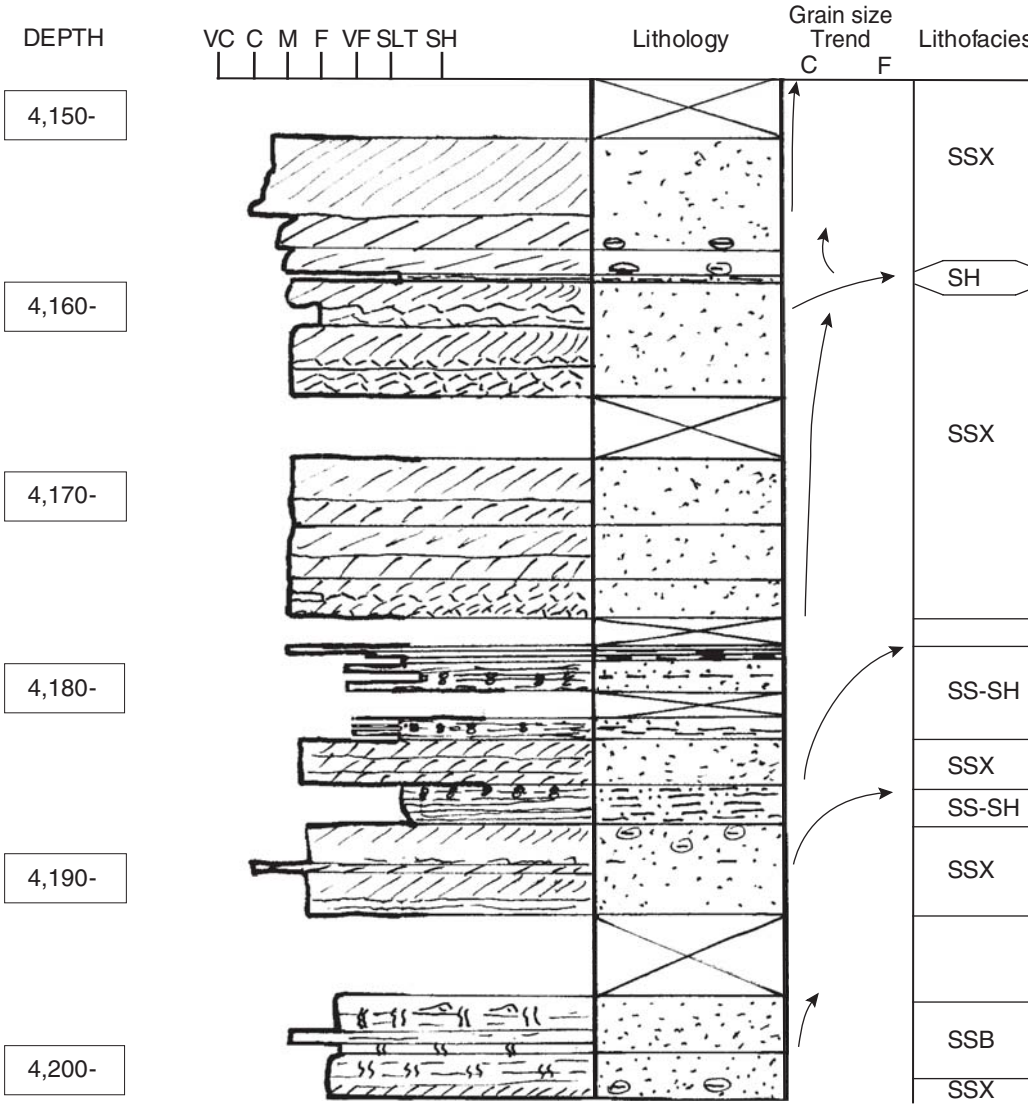

Cross-bedded
Rippled
Mud cracks
Skolithos burrows
Rippled wavy beds
Flasers
Lenticular bedding
Brecciated
Planolites burrows
Shale intraclasts
Thin-section sample

Planar beds
Soft sediment distortion
Root traces
Pyrite concretion
Granules
Sandstone
Siltstone (SLT)
Shale (SH)
Fractured core
Missing core
Fluid escape structure

SSX Cross-bedded medium to coarse sandstone
SSB Bioturbated medium to coarse sandstone
SS-SH Interbedded very fine to medium sandstone and shale
SSD Soft sediment deformed sandstone
SH Shale

Grain size: VC, very coarse; C, coarse; M, medium; F, fine; VF, very fine

Appendix 6 Modal analyses of Manlove Field, J. Williams #4 well.[1]

Depth (ft)	Quartz grains (%)	Poly quartz (%)	K-feld-spar (%)	Detrital clay (%)	Quartz cement (%)	Macro-porosity (%)	Authi-genic clay (%)	Mus-covite (%)	Lithology	Facies[2]	Core porosity (%)	Core perme-ability (mD)
3,981.1	80.3	0.3	1.7	0.0	12.0	5.7	0.0	0.0	coarse Ss	SSX	9.98	309
4,000.1	81.7	1.6	4.9	2.3	5.6	3.9	0.0	0.0	coarse Ss	SSB	5.59	7.13
4,004.9	85.7	1.7	0.3	0.0	7.0	5.3	0.0	0.0	coarse Ss	SSX	6.53	56
4,025.1	77.0	1.3	7.0	0.0	6.3	8.3	0.0	0.0	med ss with granules	SSB	10.19	23.2
4,026.5	81.0	2.0	0.7	0.0	7.7	8.7	0.0	0.0	coarse Ss	SSX	9.33	127
4,034.1	74.3	0.3	15.0	10.0	0.3	0.0	0.0	0.0	med-fine Ss	SS-SH	4.95	0.083
4,049.1	77.3	2.0	11.7	0.0	1.3	7.7	0.0	0.0	med-coarse Ss	SSB	10.48	8.44
4,051.0	75.6	9.6	1.3	0.3	7.1	6.1	0.0	0.0	coarse Ss	SSB	7.48	48
4,052.5	78.7	1.3	14.0	0.0	0.3	5.3	0.3	0.0	med Ss	SS-SH	10.98	0.632
4,058.3	76.7	0.0	8.3	0.0	0.3	14.7	0.0	0.0	med Ss	SSB	17	148
4,059.8	84.0	6.7	1.0	0.0	1.3	7.0	0.0	0.0	coarse Ss	SSX	11.83	325
4,062.8	84.3	0.0	1.3	0.0	2.3	12.0	0.0	0.0	coarse Ss	SSX	12.15	441
4,068.5	92.0	4.7	0.3	0.0	2.0	1.0	0.0	0.0	coarse Ss	SSB	5.76	60
4,077.1	73.7	0.0	16.3	1.3	0.7	8.0	0.0	0.0	med Ss	SSB	12.95	7.12
4,093.2	83.3	0.3	5.3	0.0	2.0	9.0	0.0	0.0	med-coarse Ss	SSX	11.25	94
4,102.0	84.3	0.0	5.7	0.0	4.7	5.3	0.0	0.0	coarse Ss	SSX	8.07	7.7
4,109.1	76.3	0.0	9.7	0.0	2.7	11.3	0.0	0.0	med Ss	SSX/SSB	12.73	32.9
4,124.3	80.3	0.0	4.7	0.0	3.3	11.7	0.0	0.0	coarse Ss	SSX	12.06	137
4,132.0	79.3	0.0	4.0	0.0	5.3	11.0	0.3	0.0	med Ss	SSX	13.38	140
4,135.0	85.0	0.3	4.0	0.0	1.7	8.7	0.3	0.0	med Ss	SSX	11.66	57
4,149.0	88.7	4.3	2.3	0.7	3.3	0.7	0.0	0.0	coarse Ss	SSX	5.81	17.6
4,159.8	78.0	0.0	7.0	0.0	2.0	13.0	0.0	0.0	med Ss	SSX	12.4	78
4,178.1	80.0	7.3	5.0	0.3	4.7	2.7	0.0	0.0	very coarse Ss	SSX	4.86	1.3
4,180.0	80.0	0.0	1.0	0.0	16.0	3.0	0.0	0.0	med-coarse Ss	SSX	6.52	0.363
4,185.1	82.7	0.0	1.3	0.0	12.3	3.7	0.0	0.0	med Ss	SSX	5.3	6.17
4,191.0	67.7	0.0	16.3	10.7	0.3	3.3	1.7	0.0	med-fine Ss	SS-SH	10.17	0.103
4,195.2	66.0	0.0	21.3	7.0	4.3	0.7	0.0	0.7	fine Ss with shale lams	SS-SH	6.28	0.034
4,197.0	81.0	0.3	0.7	0.0	15.0	0.7	2.3	0.0	med Ss	SSX	5.14	0.117
4,207.1	78.3	0.0	5.0	0.0	7.0	9.7	0.0	0.0	coarse Ss	SSX	10.28	60
4,209.1	83.0	1.3	2.3	0.0	3.0	10.3	0.0	0.0	coarse Ss	SSD	12.59	151
4,217.4	79.3	3.7	1.3	0.0	13.0	2.7	0.0	0.0	coarse Ss	SSX	5.9	3.25

[1]Based on 300 points per thin section.

[2]SSX, cross-bedded sandstone; SSB, bioturbated sandstone; SS-SH, interlaminated fine sandstone and shale; SSD, soft sediment deformed sandstone.